To the Graduate Council:

I am submitting herewith a thesis written by Dattatreya Panse entitled "Structure Property Relationship in Irradiated Polymer Blend Films". I have examined the final copy of this thesis for form and content and recommend that it be accepted in partial fulfillment of the requirements for the degree of Master of Science, with a major in Polymer Engineering.

Paul J. Phillips, Major Professor

We have read this thesis

and recommend its acceptance:

Accepted for the Council:

Associate Vice Chancellor and

Dean of The Graduate School

STRUCTURE PROPERTY RELATIONSHIP IN IRRADIATED POLYMER BLEND FILMS

A Thesis

Presented For The

Master Of Science

Degree

The University Of Tennessee, Knoxville

Dattatreya Panse

December 1998

ACKNOWLEDGEMENTS

I would like to thank my major professor, Dr. Paul Phillips for his guidance, encouragement and support during the course of this work. Sincere thanks are due to Dr. Roberto Benson and Dr. Kevin Kit for their efforts and suggestions.

I wish to thank the Materials Science and Engineering department for providing financial support for the first two years. I am grateful to the Department of Physics at University of Sofia, Bulgaria, for supplying the irradiated blend films. I highly appreciate Dr. John Dunlap for his help in microscopy work. I would like to thank Frank Holiway and Randy for their help in obtaining supplies.

I appreciate my fellow students Anita Dimeska, Gyanendra Dutt, Imad Qashou, John Wagner, Rosanne Smith, Samir Abu Iqyas and Stein Schreiber for their friendship and help. I would like to extend special thanks to Bhushan, Mani and Suvrat for their friendship and support. I am indebted to my parents and sister for their love and continued support.

Abstract

Films prepared from blends of polypropylene, ethylene vinyl acetate and, propylene-ethylene copolymer have been irradiated with fast electrons in the dose range of 5-16 Mrad. The effect of irradiation has been investigated by solvent extraction, DSC, DMA and X-ray diffraction techniques. Gel fractions range from 22 percent to 80 percent. The upper limit of the molecular weight between crosslinks has been found out to be 2000g/mol. X-ray diffraction studies show no appreciable distortion of the crystal lattice up to 16 Mrad. A considerable drop in the crystallinity index is obtained only at high dose level. Nonisothermal crystallization studies show that the crystallization temperature decreases with radiation dose. The melting temperatures decrease with dose and the drop is more prominent in samples containing high percentage of polypropylene. Multiple melting peaks are observed for irradiated samples. The enthalpies of melting of EVA increase up to 5 Mrad and then decrease in samples containing high percent of polypropylene. Enthalpies of PP remain constant or slightly decrease with dose. The dynamic mechanical analysis show separate transition peaks for PP and EVA. High storage modulus at high temperature is seen only in case of samples containing high percent of EVA and irradiated with high dose level.

Table Of Contents

List Of Figures

List Of Tables

1 Introduction

The effect of high-energy radiation on polymeric materials is an area of rapidly growing interest. Irradiation of polymeric materials is widespread in many fields for numerous applications such as micro-lithography in electronics industry, sterilization in medical and pharmaceutical field, shrink-tubing in cable and insulation industry, heat-shrink films in packaging industry and many others. Interaction of high-energy radiation with polymeric materials produces several physical and chemical changes in these materials. The two most significant radiation-induced events taking place in polymers are crosslinking and chain scission. Even small amount of crosslinks or chain scission sites per molecule can dramatically affect properties such as maximum service temperature, solubility, modulus etc. These changes, in turn, will determine the suitability of a particular polymer for a particular application. Depending on the chemical structure, a polymer may predominantly undergo scission or crosslinking. With judicious selection of materials, properties of an irradiated system can be tailor-made to suit a particular application. To prepare materials with tailor-made properties, the polymer industry has practiced mixing or blending two polymers for a long time. Polymer blends fill the deficiency in price to performance ratio of existing homopolymers with relatively minor capital investment. Depending on the nature of constituent polymers, irradiated polymer blends can produce properties, which are valuable than those of the parent homopolymer. If the constituent polymers are

predominantly crosslinking, the irradiated blend will have excellent solvent resistance and high temperature strength but poor impact strength. If the polymers are prone to scission, degradation of properties will result. By selecting one predominantly crosslinking and other predominantly scissioning component, the final properties of an irradiated blend can be controlled by changing the blend composition and radiation level. The structure property relationship in irradiated blends consisting of polypropylene homopolymer and copolymer, and ethylene vinyl acetate copolymer has been investigated in this study.

Polypropylene is one of the leading commodity plastics and due to its high crystallinity and high strength to stiffness ratio, it is also preferred in many engineering applications. The ease of orientation makes it suitable for fiber and film applications. This polymer undergoes excessive scission at low radiation doses while at high doses it starts crosslinking. To improve optical and low temperature impact properties, propylene is copolymerized with small amounts of comonomer such as ethylene. The copolymers have lower crystallinity, higher flexibility, lower melting temperature but almost unchanged chemical resistance, taste and odor contribution.

Ethylene vinyl acetate (EVA) is a random copolymer of ethylene and vinyl acetate. It is recognized for its flexibility and toughness (even at low temperatures). The properties of EVA copolymers depend on vinyl acetate content. Increasing vinyl acetate content reduces the crystallinity, improves clarity and improves low temperature flexibility, while decreases melting temperature and permeability. These

copolymers are widely used for packaging films. The responsiveness of EVA copolymers to radiation-induced crosslinking is better than polyethylene, so they are widely used in crosslinked cable insulation materials.

A thorough fundamental understanding of the structure-property relationship in irradiated blends is critical in designing for a specific application. The focus of this research is to understand the effect of radiation dose and blend composition on gel formation, melting and crystallization temperatures, heat of fusion, crystal structure and dynamic mechanical properties of the irradiated blends.

2 Theoretical background and literature review

2.1 Polymers and their properties

Polypropylene homopolymer, polypropylene copolymer and ethylene vinyl acetate copolymer are widely used thermoplastics. A brief synopsis of their structures and properties is presented here.

2.1.1 Polypropylene Homopolymer

Polypropylene, which entered commercial production in 1957, was the first of a group of stereoregular polymers. Even today, it remains the fastest growing major thermoplastic, having worldwide production of about 26.3 million tonnes per year as of 1997 (Modern Plastics 1998). PP is polymerized from propylene monomer under controlled conditions in presence of stereoregular catalysts. Depending on the conditions and catalyst used, the resulting polymer consists of three different types of stereochemical configurations in varying amounts. Among these, isotactic polypropylene is the most important and common commercial form. In isotactic PP, the methyl groups are on the same side of the polymer backbone, providing a structure, which is readily able to crystallize. Isotactic PP has lower densities, higher melting temperatures compared to polyethylenes. Other advantages of isotactic PP include high strength to stiffness ratio, ease of orientation, higher heat resistance, high crystallinity and good flow properties. The disadvantages include low resistance to

oxidation, poor impact strength at low temperatures and excessive degradation even at low radiation doses.

Crystal structure of polypropylene

Isotactic polypropylene is a head-to-tail polymer with a high stereoregularity. The high stereoregularity permits easy crystallization. Upon stretching an isotactic polypropylene along the main chain as a planar trans zigzag conformation on the x, y plane, all of the methyl side chains attached at the asymmetric carbon atoms, are in the same direction normal to the plane as shown in Figure 1 (Natta 1960). In crystalline state, isotactic polypropylene prefers an alternate trans and gauche conformation with respect to the main chain carbon atoms, rather than the trans zigzag conformation as in case of crystalline polyethylene. This conformation results in threefold (3_1) symmetry of helix with a chain repetition of 6.50 Å as shown in Figure 2. Several types of crystalline modifications have been reported resulting from distinct packing modes and lattice framework (Natta 1960). These modifications, which show characteristic x-ray diffraction patterns are described below.

Monoclinic structure: This modification was first referred as monoclinic and later termed as α form (Natta *et al.* 1956, 1960), characterized by five strong and two moderate x-ray diffraction peaks with d-spacings of 6.25Å, 5.25Å, 4.75Å, 4.20Å, 4.05Å, 3.48Å and 3.13Å. Since the monoclinic crystal structure has dimensions of a = 6.65Å, b = 20.96Å, c = 6.50 Å and β = 99°20', the corresponding crystal density is equal to 0.94 g/cc. This is found to be the most stable and common form under the

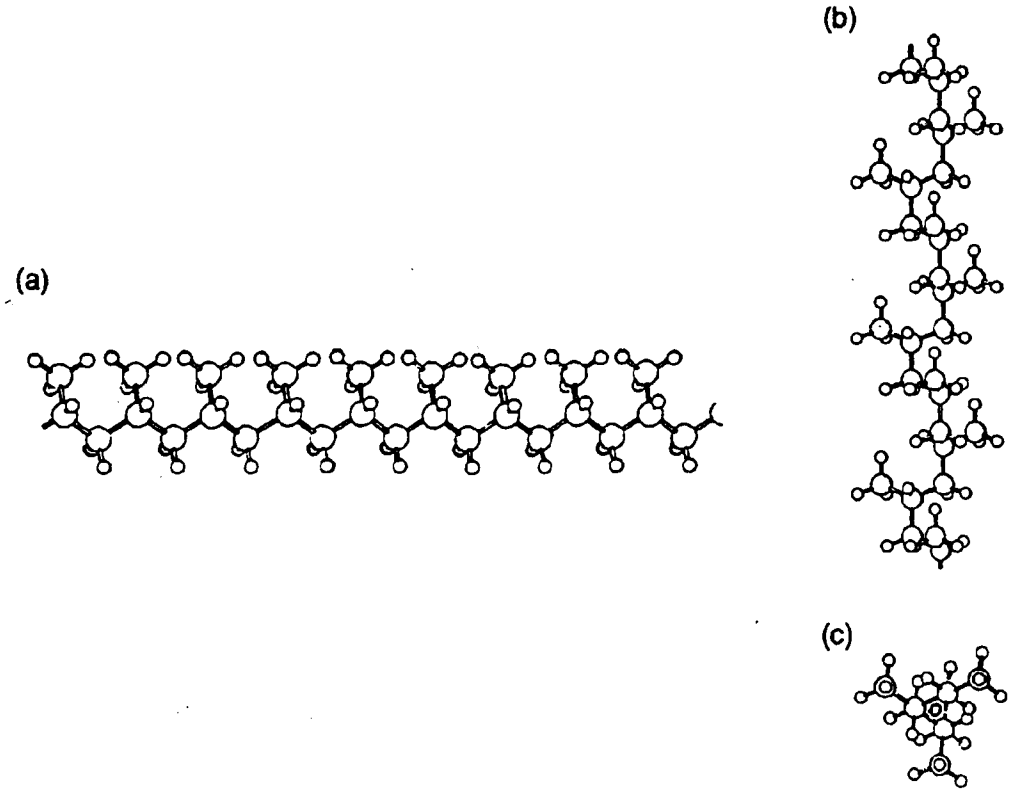

Figure 1.(a) Planar trans zigzag and (b) 3_1 helical conformation of isotactic polypropylene. (c) Top view of the helix (Natta 1960)

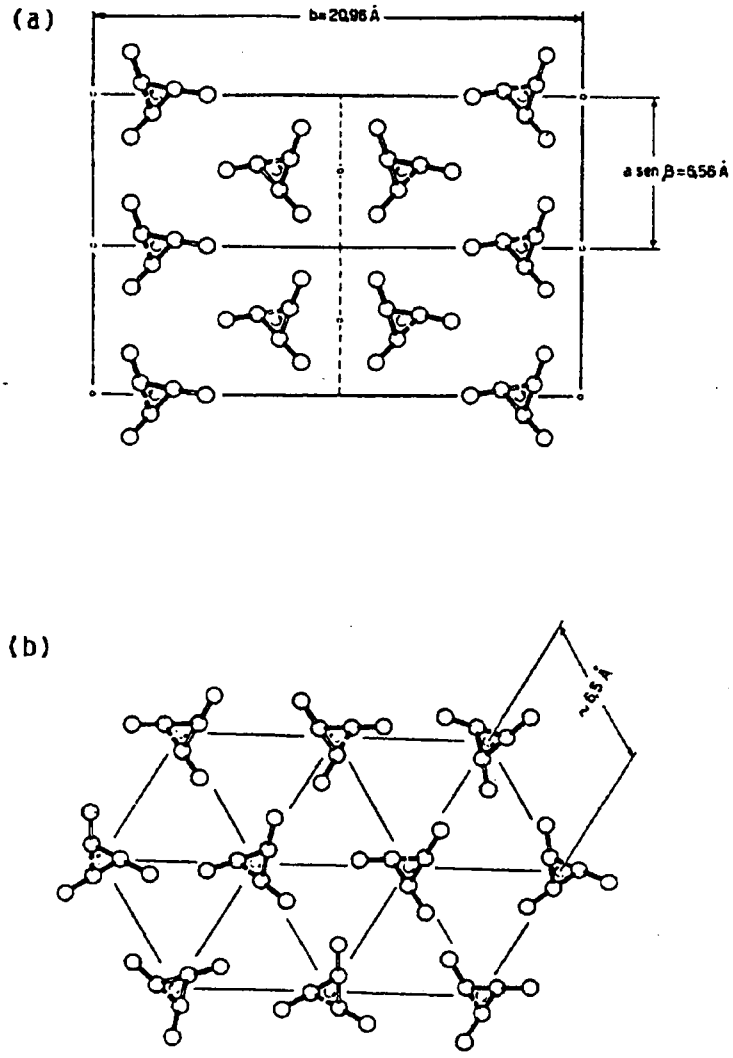

Figure 2.Schematic packings of right and left handed helices in (a) monoclinic and (b) smectic crystalline modification of isotactic polypropylene (Natta 1960)

normal polymer processing conditions.

β -Modification: Isotactic polypropylene with a higher degree of isotacticity and consequently higher crystallinity may occasionally produce a β crystalline form. The structure of this form has been investigated by Lovinger *et al.* (1994) using x-ray diffraction, electron diffraction and packing energy calculations. Since the structure was extensively disordered, they concluded that two models could be visualized satisfying a pseudo hexagonal lattice. It can be a simple trigonal with a = b = 11.03 Å and c = 6.49 Å or a new achiral orthorhombic lattice with a = 11.03 Å, b = 19.10 Å and c = 6.49 Å.

γ-Modification: This modification occurs rarely and only under certain conditions. Morrow and Newman (1968) proposed a triclinic structure of γ-phase of isotactic PP, with a = 6.54 Å, b = 21.4 Å, c = 6.5 Å, β = 99.6° and γ = 99°. More recently, Meille and Bruckner (1991) extensively studied crystal structure using x-ray diffraction and electron diffraction and proposed a pseudo triclinic cell. This pseudo triclinic cell can be transformed into a face centered orthorhombic cell with a = 8.54 Å, b = 9.93 Å and c = 42.41 Å.

Smectic modification: A rapid quenching of isotactic polypropylene melt may produce a paracrystalline of lower order, which is referred as smectic modification (Natta 1959, Gezovich *et al.* 1968, Hendra *et al.* 1984). This form shows a broadened x-ray diffraction pattern. Because of a disorder in the packing, the smectic modification has a density of 0.88 g/cc, lower than that of monoclinic modification.

2.1.2 Polypropylene copolymer

In polypropylene random copolymers, the basic structure of the polymer chain has been changed by the incorporation of a different monomer molecule. Ethylene is the most common monomer incorporated in these copolymers. Random copolymers contain typically 1-10 wt.% ethylene and the ethylene molecules are inserted randomly between the propylene molecules along the polymer chains. The copolymers differ from the homopolymers because the ethylene molecules randomly inserted into the polymer backbone hinder the crystalline arrangement. A reduction in copolymer crystallinity results in reduced stiffness, moderately higher impact strength, lower melting temperature and better clarity than homopolymers. Random copolymers are mainly used in films where high clarity and impact strength is required.

2.1.3 Ethylene vinyl acetate copolymer

Ethylene vinyl acetate (EVA) copolymers include a wide range of thermoplastics containing 5 to 50 wt.% of vinyl acetate. EVAs are made by the copolymerization of ethylene and vinyl acetate. As vinyl acetate and ethylene have very similar reactivity ratios, the pendant acetoxy groups in the resulting copolymer are randomly distributed throughout the polymer backbone. Increase in vinyl acetate content results in lowering of crystallinity, improvement of clarity, low temperature flexibility and stress crack resistance. The main markets for EVAs are packaging, wire and cable

insulation, adhesives and coatings. EVA packaging films are used in meat and poultry wrap, stretch films, produce bags, ice bags and heavy duty bags. The wide use in cable and wire insulation originates from the ability of EVA to undergo crosslinking easily and at low energies than homopolymers. The crystal structure of EVA is same as polyethylene with orthorhombic cell having lattice parameters of a = 7.41 Å, b = 4.94 Å and c = 2.54 Å.

2.2 Polymer blends

Two polymers may be mixed in search of novel properties, of particular combination of properties or of intermediate properties. A major driving force for the growth of polymer blend sector is the relative ease of mixing and blending. The development of a new blend from existing materials is faster and economic than development of a new polymer. Given successful development of a product, scale up is also cheaper since the basic process is of mixing. On the other hand, polymer synthesis on a large scale usually involves a large investment. So from an industrial point of view, polymer blends fill the deficiency in price to performance ratio of existing homopolymers with a relatively minor capital investment.

In the field of polymer blends, the word compatibility and miscibility, although being fundamentally different are used synonymously. The term compatibility will be used here to describe mechanically processable blends that resist large-scale phase segregation and/or give desirable properties. A compatible blend may consist of two

or more phases. The term miscibility will be used strictly in thermodynamic sense i.e.; a blend is called miscible if the free energy of mixing for the blend is negative. Under microscopic investigation, a miscible polymer blend consists of a single phase. On the molecular level, molecules of one polymer intermingle with molecules of another polymer as shown in Figure 3. The blends that are miscible at some temperatures and phase separate at other temperatures are referred as partially miscible. According to the above definition polymer blends can be divided into three basic categories.

* Miscible blends: PS - poly (2,6-dimethyl 1,4-phenylene oxide) (Cizek 1968), PMMA – PVDF (Nishi *et al.* 1975).
* Partially miscible blends: PS - poly (vinyl methyl ether) (Bank *et al.* 1971), Phenoxy resin - polyethersulphone (Singh *et al.* 1986)
* Immiscible blends: PE - PP, PP - PS and many others (Paul *et al.* 1978).

Most of the commercial blends fall into the third category as in case of polymer blends, immiscibility is the rule and miscibility is an exception. These blends often show a phase-separated structure. As the dynamics of interdiffusion of polymers are very slow due to the long chain nature of the molecules, the growth of these phase domains is very slow and this restricts the size of domains in 0.1 to 100-μm. range. The polymer present in lower concentration usually forms a discontinuous phase whereas the polymer present in the higher concentration forms a continuous phase. It

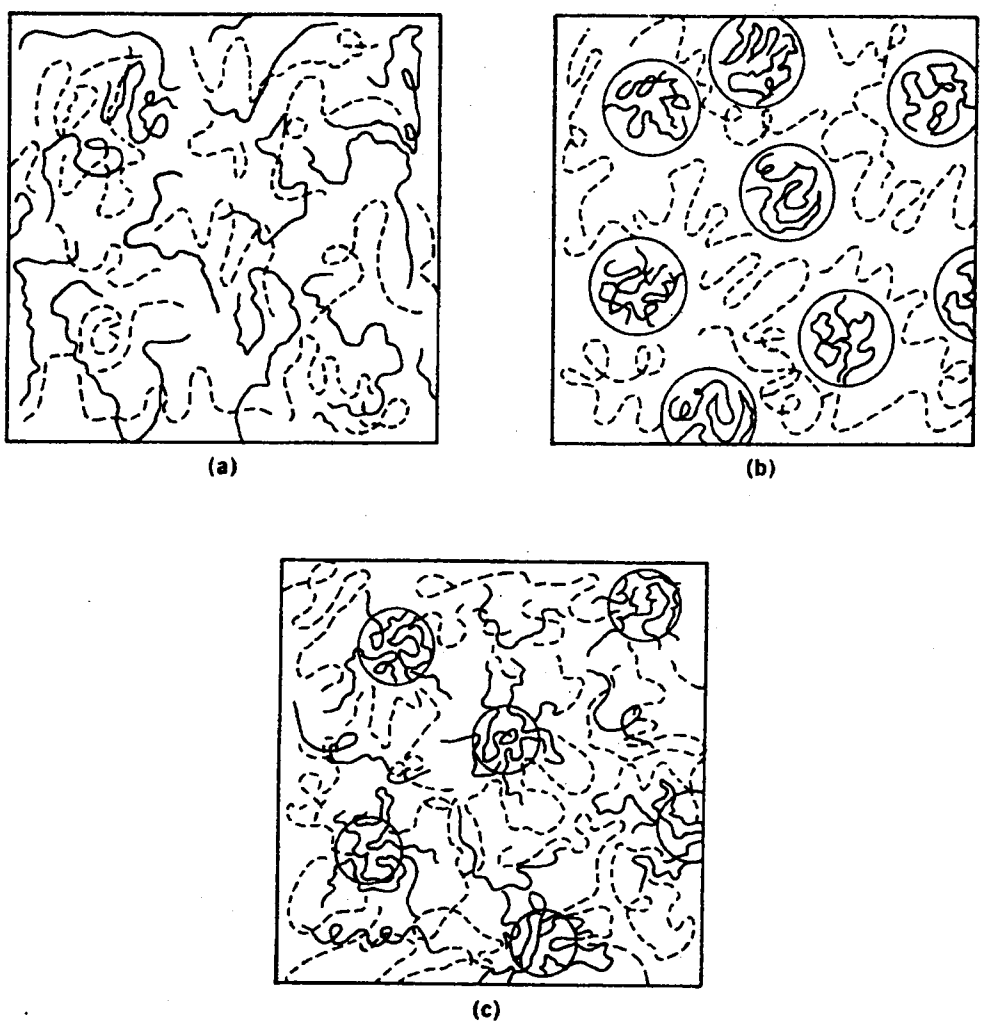

Figure 3.Morphologies of a blend of polymer A (solid lines) and polymer B (dashed lines); (a) Miscible; (b) Immiscible; (c) Partially miscible. (Paul 1988)

is worth mentioning that the miscibility is not always necessary to get superior properties. In fact, most of the time synergetic properties in blends are obtained due to two-phase nature of the blend (Paul *et al.* 1988, Bucknall 1977). Over the years, various researchers have studied the effect of blend miscibility on properties and these studies show that miscibility affects mechanical, optical and transport properties of blends. There are various methods employed to study miscibility and many authors have extensively reviewed this topic (Paul 1978, Olabisi *et al.* 1979, Walsh *et al.* 1985). The most widely used methods are listed below.

2.2.1 Methods to study miscibility in blends

Glass transition temperature: This is the most widely used method to study miscibility in polymer blends. Glass transition (T_g) occurs when certain motions of a polymer chain become active. The ability of a polymer chain to display such motion depends on the energy that it has and the amount of available space. As the space available is a function of the local environment of the chains, these motions are on the scale of a few nanometers. Thus T_g of a blend can be different from the constituent polymers only if they are mixed on a molecular scale. If the mixing is not on a molecular scale, the blend components will show T_g characteristic of each constituent. Thus, a blend with a single T_g is said to be miscible while a blend showing multiple T_gs is said to be immiscible. The glass transition temperature is normally measured by DSC or DMA. For ideal systems, which are miscible and amorphous over the entire composition

range, the T_g can often be predicted by using simple equations. The Gordon-Taylor expression (Gordon *et al.* 1952) and the Fox equation (Fox 1956) are widely used to predict T_g values. The two expressions are presented below.

Gordon-Taylor: $$T_g = W_a \cdot T_{ga} + W_b \cdot T_{gb} \qquad \text{(Eq. 1)}$$

Fox expression: $$\frac{1}{T_g} = \frac{W_a}{T_{ga}} + \frac{W_b}{T_{gb}} \qquad \text{(Eq. 2)}$$

where W_a, W_b are weight fractions of polymers A and B in the blend and T_{ga} and T_{gb} are their respective T_gs. The use of T_g for studying blend miscibility has its own limitations. If both components have the same or very close T_g(s) or when a small quantity of polymer is present in the mixture some difficulties may be experienced in resolving the T_g(s). Furthermore T_g is associated with a domain size of at least 100 Å. Phase separated domains below this value can not be easily detected by this technique.

Interaction parameter: The Flory interaction parameter (χ) may be used to predict miscibility in polymer blends. A negative value of interaction parameter indicates miscibility while a positive interaction parameter indicates immiscibility (Flory 1953). The interaction parameter may be determined by neutron scattering or from the experimental spinodal and bimodal curves.

Scattering: Scattering techniques provide a sensitive method for determining whether blends are miscible or immiscible. Light scattering in case of polymers differing in refractive indices can be employed to determine miscibility (Datta and Lohse1996).

Small angle neutron scattering has emerged as a powerful tool in study of blend miscibility. It can be used to obtain interaction energies for miscible blends and conformational information about the components.

Spectroscopy: A variety of spectroscopic techniques have been used to obtain information about blend phase structure and underlying molecular interactions (Shaw 1985). FTIR has been most widely used, especially for systems involving hydrogen bond formation.

Microscopy: As the size of blend phases indicates the amount of interaction between the blend components, a study of phase size and distribution may give some idea about miscibility (Sawyer and Grub 1995). Blends having large phase domains may be studied by optical microscopy while for smaller domains electron microscopy is imperative. In electron microscopy, image contrast is obtained as a result of variation in electron density among the structures present. But most of the polymers have low atomic number elements such as carbon, hydrogen, and oxygen in their main chain. As a result they do not exhibit sufficient difference in electron density to distinguish between the phases present in a blend. To improve contrast, heavy metal shadowing or staining by addition of high atomic number element in specific structures has been widely used. Some other methods to distinguish phases include solvent extraction and cryo-fracture.

2.2.2 Thermodynamics of polymer-polymer miscibility

The physical properties of polymer blends depend critically on morphology. The development of morphologies is to a great extent determined by the thermodynamic of mixing. Current understanding of these interactions is based on two theoretical developments viz. Flory-Huggins theory (Flory 1941, 1953) and random phase approximation theory by de Gennes. The mixing of macromolecules is a fundamentally different process from mixing of small molecules. In the mixing of macromolecules, the entropy of mixing is small compared to that of small molecules. Most of the high molecular weight polymers are immiscible because the change in enthalpy of mixing is greater than zero and exist as a phase separated domains. In the Flory-Huggins theory, the free energy density of mixing of two polymers labeled 1 and 2 is given by

$$\frac{\Delta G_m}{kT} = \frac{\Phi \cdot \ln \Phi}{\vartheta_1 \cdot N_1} + \frac{(1-\Phi)\cdot \ln(1-\Phi)}{\vartheta_2 \cdot N_2} + \frac{\chi \cdot \Phi \cdot (1-\Phi)}{\vartheta} \qquad \text{(Eq.3)}$$

where N_i is the number of monomers in chain *i*, and ϑ_i is the volume of each monomer in chain *i*, Φ is the volume fraction of component 1 in the mixture, ϑ is the arbitrary reference volume, χ is the Flory-Huggins interaction parameter, ΔG_m is the free energy change on mixing per unit volume, k is the Boltzmann constant and T is the absolute temperature. The first two terms on the right hand side represent combinatorial contribution to ΔG_m that arises due to the increase in the number of distinguishable states in the mixture, relative to the pure components. The third term

represents of non-combinatorial contribution to ΔG_m. The interaction parameter is the measure of random, pair-wise contact between monomers. It depends on temperature, monomer architecture, specific interaction and finite compressibility. Classical thermodynamics may be used to predict phase diagrams on the basis of equation 3. If χ is only function of T, the spinodal curve, and i.e. a curve enclosing the region within which a homogeneous mixture is thermodynamically unstable is given by

$$\chi(T) = \frac{\upsilon}{2}\left[\frac{1}{N_1 \upsilon_1 \Phi} + \frac{1}{N_2 \upsilon_2 (1-\Phi)}\right] \qquad \text{(Eq.4)}$$

The binodal curve, which is the locus of compositions of the two phases in thermodynamic equilibrium with each other, can be obtained by solving two simultaneous equations:

$$\ln\left[\frac{\Phi^1}{\Phi^2}\right] + (\Phi^2 - \Phi^1)(1 - N_1\upsilon_1 / N_2\upsilon_2) + \frac{\chi(T) N_1 \upsilon_1}{\upsilon}\left[(1-\Phi^1)^2 - (1-\Phi^2)^2\right] = 0 \qquad \text{(Eq.5)}$$

$$\ln\left[\frac{1-\Phi^1}{1-\Phi^2}\right] + (\Phi^1 - \Phi^2)(1 - N_2\upsilon_2 / N_1\upsilon_1) + \frac{\chi(T) N_2 \upsilon_2}{\upsilon}\left[(\Phi^1)^2 - (\Phi^2)^2\right] = 0 \qquad \text{(Eq.6)}$$

where ϕ^1 and ϕ^2 are the volume fractions of polymer 1 in the coexisting phases.

The binodal and spinodal curves meet at the critical point and the volume fraction of component 1 at the critical point is given by the following equation.

$$\Phi_C = \frac{1}{1 + (N_1\upsilon_1 / N_2\upsilon_2)^{1/2}} \qquad \text{(Eq.7)}$$

The Flory-Huggins interaction parameter at the critical point is given by

$$\chi_C = \frac{\upsilon}{2}\left[\frac{1}{(N_1\upsilon_1)^{1/2}} + \frac{1}{(N_2\upsilon_2)^{1/2}}\right]^2 \qquad \text{(Eq.8)}$$

The phase diagram of a polymer blend in T-ϕ space can be determined from the equations and some examples of the phase diagrams are shown in Figure 4.

The Flory-Huggins theory does not take into account for the compressible nature of the mixture or any change in the volume on mixing. Theories allowing for these volumetric issues are called equation of state theories, which have received much attention in recent years (Brannock *et al.* 1990, Sanchez *et al.* 1978 and 1976). In these theories, the terms in the Flory-Huggins theory are expanded by introducing contributions to the enthalpy and entropy of mixing resulting from volume considerations and expressed as reduced pressure, volume and temperature. The resulting equations are quite complicated. Like the simpler Flory-Huggins theory, these theories also determine miscibility by calculating interaction parameter.

2.2.3 Blends containing one or more semicrystalline polymers

The majority of polymer blends used in engineering applications contain some level of crystallinity. The reinforcing action of the crystallites improves mechanical and chemical properties of the blend. In case of an immiscible blend, crystalline melting point and crystallization behavior remains unaffected by addition of an amorphous polymer. On the other hand, addition of amorphous polymer to a semicrystalline

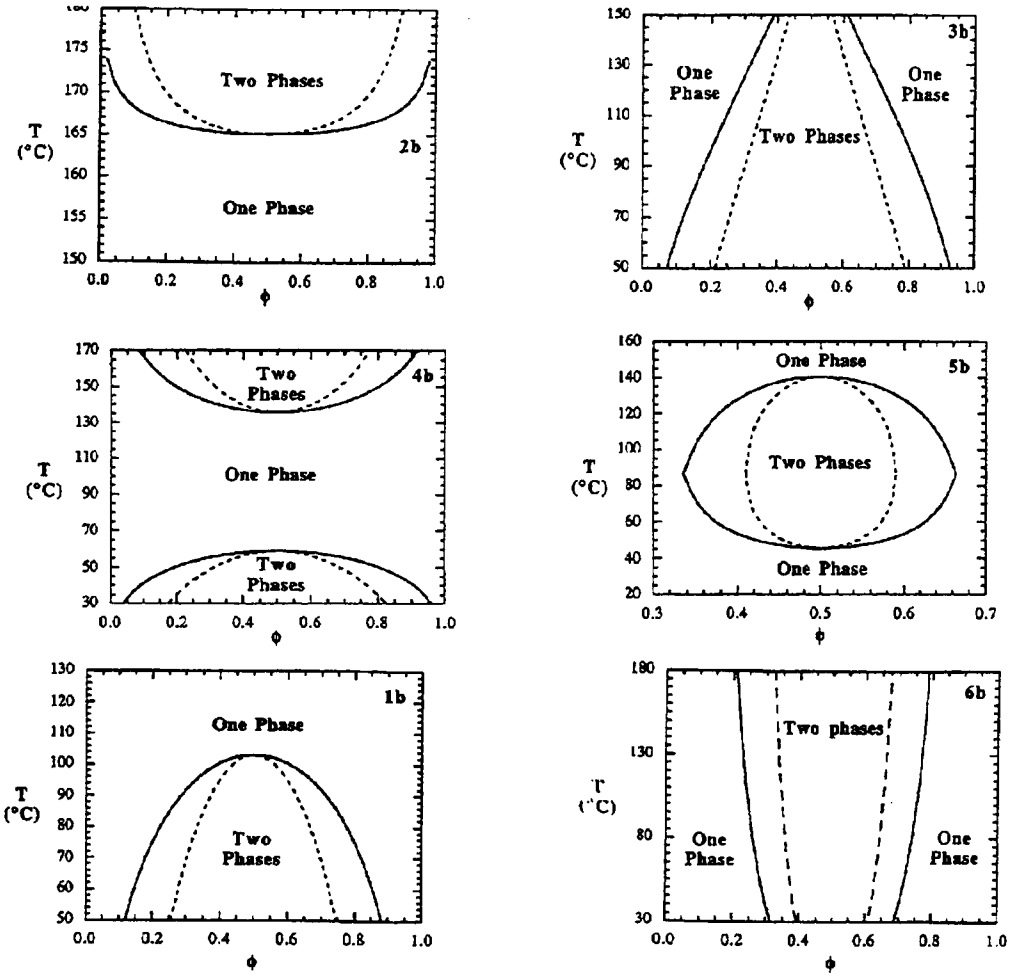

Figure 4.Phase Diagrams for mixtures

polymer, in a miscible blend, affects the crystallization behavior of the semicrystalline component. The reduction in lamellar thickness and the expansion in the interlamellar distances in a semicrystalline polymer to accommodate the chains of amorphous polymer affects the melting and crystallization behavior of the semicrystalline polymer as shown in Figure 5 (Rostami 1990). The surface and lateral free energies are also affected. The depression in melting point in a miscible blend has been reported in the literature for blends of Poly(vinyledenefluoride) with Poly(methylmethacrylate) (Nishi *et al.* 1975), poly(ethylene oxide) with polyethersulphone (Walsh *et al.* 1985) and poly(ethylene oxide) with polycarbonate (Iriante *et al.* 1989).

In case of blends containing only semicrystalline components, the miscibility is dependent on the abilities of their amorphous regions to interact favorably. To form a homogeneous blend, two chemically different chains must have some degree of miscibility and co-crystallization habit. If one or both of the factors are absent, phase separation or two different crystals may be formed. Other factors such as tactcity and difference in crystalline unit cell may also result in immiscibility. The determination of miscibility between two semicrystalline polymers is difficult. The melting temperature of the minor phase becomes undetectable and the depression on the melting temperature of the major phase not always becomes evident.

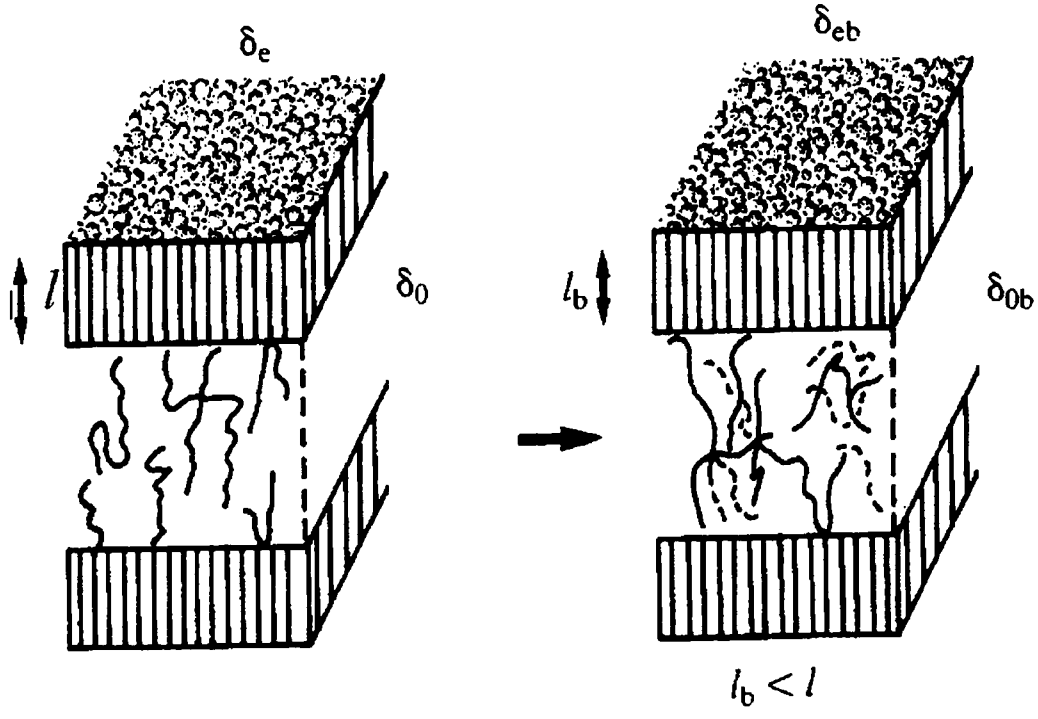

Figure 5.Schematic representation of the crystalline and amorphous regions of a homopolymer with and without the second component (Rostami 1990)

2.2.4 Literature reports on PP/EVA blends

Blom *et al.* (1996) found that the addition of EVA (33 wt.% VA) imparted better impact strength to iPP compared to EVA (28 wt.% VA). Addition of EVA improved the impact properties of PP/HDPE blend by approximately 50% but did not affect the tensile properties to any significant extent. As a compatibilizer, EVA improved the impact strength and elongation at break. Olabisi *et al.* (1979) reported maximum impact strength for 70/30 iPP/EVA, which was attributed to the uniform distribution of 1.75-μm size EVA particles. In another study by Maciel *et al.* (1996) phase inversion was observed for EVA concentrations greater than 70%. Greco *et al.* (1987) studied the effect of composition of polypropylene copolymer on the structure and morphology of iPP/PPC blend. They found that higher the amount of iPP in the copolymer, higher is the nucleating effect of the copolymer on the homopolymer. The melting temperature of crystallized phase in blends was 6-10°K higher than pure iPP. They attributed this behavior to selective extraction of defective molecules from iPP matrix by the copolymer. D'Orazio *et al.* (1994) studied iPP/ Ethylene-propylene rubber blends and observed a smaller crystal size in blend compared to pure iPP. A noticeable depression in the melting temperature was shown by the iPP phase crystallized in presence of cured EPR indicating less perfect and thinner lamellar crystals. In a study by Thomas *et al.* (1992) the mechanical and dynamic properties were found to depend mainly on the particle size in iPP/EVA blend. EVA remained as a dispersed phase up to 50 wt.% EVA and a phase inversion with formation of an

interpenetrating network was observed for a higher concentration, slightly different than that observed by Maciel *et al.* (1996). The average domain size was found to increase with increased concentration of EVA, which was explained on the basis of coalescence. The dynamic mechanical studies of crosslinked blend exhibited peak broadening suggesting promotion of interfacial bonding between the phases by crosslinking.

2.3 Radiation and Polymers

The early studies on the effects of nuclear reactor radiation on polymeric materials initiated the development of radiation processing of polymers. Physical changes in polymers and the mechanisms of crosslinking and chain scission under exposure to radiation energies were first established in the 1950s and 1960 (Davidson *et al.* 1948, Charlesby and co-workers 1953, 1954, 1960, Chapiro 1962). In 1957 radiation-induced crosslinking reactions were used by Raychem Corporation to produce shrink tubing and, W.R. Grace & Co. to produce polyolefin packaging for films and bags. In late 1950s Goodyear investigated radiation to modify rubber substrates for tire applications. Today both Raychem and W.R. Grace employ radiation-induced reactions and, Goodyear and Firestone are among the largest users of radiation cured materials for tire applications. Radiation processing technology is growing rapidly in the United States, Europe, Asia, especially Japan, where approximately 60 electron-processing systems are used in industrial or pilot-plant installations (Snyder 1983).

Radiation processing of polymers generally involves non-particulate radiation such as microwave, infrared, x-rays, gamma rays or particulate radiation such as electrons, protons, deuterons, beta particles etc. The most common commercially used radiation sources are cobalt 60, low and high-energy electron accelerators, light energy and plasma or glow discharge energy sources (McGinniss 1982).

Radioisotope Cobalt 60 produces highly energetic gamma rays with energy in the range of 1.17 to 1.33 MeV and is primarily used for preserving food, sterilization of medical products and crosslinking of high performance monomer-polymer impregnated wood composites for flooring (Dole 1983, Ransohoff 1981, Spinks *et al.* 1964). Cesium-137 also produces gamma radiation, but of lower energy (0.66 MeV). Various sources of energetic electron radiation are available for the industrial application and their energy ranges from 0.3- 4 MeV. Plasma radiation sources fall into three categories. Gas arcs under atmospheric pressure in 5000-50000 °K range produce thermal plasmas. Cold plasmas are produced by glow discharges such as those found in neon signs. Hybrid plasmas are between cold and thermal plasmas and are defined as having numerous small thermal sparks uniformly distributed throughout large volumes of non-ionized gas molecules. Corona and ozone generator discharges are associated with this type of plasma.

The choice of radiation source in the higher energy range depends upon availability, impact on manufacturing processes (product handling, shielding, safety, equipment cost and maintenance), radiation penetration depth required and desired radiation

dose rate. High-energy or low energy electron accelerators are most useful for crosslinking thin samples (< 6mm thickness, i.e. films, laminates etc.) of polymer at high dose rates. The advantages of electron accelerator equipment are the ability to focus a beam or curtain of high-energy electrons and turn it on and off at will with a degree of shielding. The energy absorption in a polymer from electron irradiation occurs through ionization and excitation. Both ions and excited species may be involved in subsequent chemical reactions or they may be neutralized or deactivated. Large dimension polymeric materials require the penetrating power of high-energy x-rays or gamma rays which in turn require high shielding capabilities, large impact on manufacturing operations, and low dose rates with long residence times for production output (Becker *et al.* 1979). The gamma and x-ray radiation transfer energy to substrate molecules by three processes. Very high-energy photon generates an electron and a positron, which undergo annihilation. Most energy is deposited in the substrate by deflection of the incident photon by the electron cloud around the atom. At lower energies, this incident photon is completely absorbed by the substrate atom to produce ionization. Thus the radiation chemistry of gamma and x-rays is mainly due to electrons.

The actual amount of radiation energy produced by the source and the quantity of radiation impinging on the sample is very important. Any quantitative estimates of chemical changes produced by radiation require measurement of energy absorbed in the substrate. Radiation intensity is calibrated with the help of dosimetry, in which a

standard ferrous sulfate solution is exposed to ionizing radiation and oxidized to ferric sulfate (15.6 molecules per 100 eV of energy absorbed). Dosimetry can also be performed using photographic film, polyethylene, Faraday cup, and colored ions in glass and dyes in plastics (Dole 1972). Some common definitions used in radiation chemistry and physics are given below.

Absorbed dose is the amount of energy imparted to matter expressed in grays.

Absorbed dose rate is the absorbed dose per unit time expressed in grays per unit time.

Gray is the unit of the absorbed dose.

1 Gray (Gy) = 1 J /kg = 100 rad

The **G value** is the magnitude of a particular reaction occurring per 100eV of energy absorbed.

The irradiation of polyolefins and subsequent chemical reactions and determination of their physical properties have been extensively investigated (Charlesby 1960, Dole 1983). Even though the monomer structure is simple, other factors such as morphology, branch content, tacticity, impurities and presence of oxygen complicate the mechanism by which the chemical and physical properties change.

The interaction of high-energy radiation with polyolefins can be described as follows:

RH ^^^^^^^^^^->(RH)* (excited state)

$$(RH)^{*} \rightarrow R\ H^{+} \cdot (radical-ion) + e^{-} \text{ (electron ejection)}$$

$$(RH)^{*} \rightarrow R\cdot + H\cdot \text{ (molecular dissociation)}$$

$$RH^{+}\cdot + RH \rightarrow R\cdot + RH_2^{+} \text{ (energy transfer)}$$

$$RH_2^{+} + e^{-} \rightarrow R\cdot + H_2 \text{ (electron capture)}$$

$$RH_2^{+} + e^{-} \rightarrow RH + H\cdot \text{(electron capture)}$$

$$RH + e^{-} \rightarrow RH^{-}\cdot \text{(electron capture)}$$

$$RH^{+}\cdot + RH^{-}\cdot \rightarrow R - R + H_2 \text{ (charge neutralization)}$$

where RH = polyolefin macromolecules.

The main types of radicals produced are alkyl, allyl and polyenyl radicals (Ungar 1981) and their structures are shown below.

Alkyl radical $-CH_2-\dot{C}H-CH_2-$

Allyl radical $-\dot{C}H-CH=CH-$

Polyenyl radical $-\dot{C}H-(CH=CH)_n-$

The decay time for the radicals range from one day for alkyl radicals to several months for allyl radicals at 77K. Polyenyl radicals are very stable even at room temperature (McGinniss 1986). Due to the chemical reactions of these radicals, many structural changes are liable to occur which may affect properties of materials. So it is very important to quantify the effects of high-energy radiation on polymeric materials. During the early studies of the physical and chemical effects of ionizing radiation on materials, the special case of high polymers became clear (Charlesby 1960, Bopp *et al.* 1953, McGinniss 1982). The molecular changes produced in polymers include scission and crosslinking, evolution of small molecular products

such as H_2, C0, $C0_2$ and CH_4, depending on the composition of the polymer, loss and formation of unsaturation. The structural changes include change in crystallinity and on the molecular architecture in the amorphous phase.

The term scission is defined as any event, which results in the breakage of one polymer molecule into two parts. It may occur as a result of ionization of the irradiated polymer molecule and a direct rearrangement of the backbone into two separate entities or the ionized polymer molecule may undergo loss of side-groups and subsequent rearrangement resulting in scission. Many times scission is called degradation since the breakdown of the polymer chains result in loss of structural strength and the physical properties are degraded or diminished. Although these changes are not always undesirable, as in case of PTFE, where radiation-induced scission is used to improve flow properties of the polymer.

Crosslinking occurs when two polymer molecules join to form one large molecule. It may result when hydrogen is abstracted from two neighboring polymer molecules leaving two radicals in close proximity, which may react to form a crosslink. Crosslinking may result in improvement of mechanical properties of a material since the molecular weight increases due to formation of a three dimensional network. Crosslinking has been found to cause reduction in solubility, reduction in heat stability temperature, and increment in chemical resistance and mechanical properties. Table 1 gives a list of polymers that are either prone to scission or crosslinking.

Because of the ability of high-energy radiation to induce large-scale changes in molecules, it is increasingly employed in polymer industry to improve polymer performance. The properties improved by radiation processing include:

- Mechanical strength
- High temperature stability
- Low temperature stress cracking
- Permeability resistance
- Solvent resistance
- Antibacterial properties

Table 1 Types of polymers undergoing either crosslinking or chain scission. (Dawes *et al.* 1996)

Prone to Crosslinking	Prone to Scission
Polyacrylates, PVC, Polysiloxanes, Polyamides, Polystyrene, Polyethylene copolymers such as EVA and EMA, Ethylene propylene elastomers, Polyethylene.	Polyisobutylene, Poly (α-methylstyrene), Polymethacrylates, Poly (vinylidene chloride), Polypropylene ether. Polytetrafluroethylene, Cellulose and derivatives.

The commercial development of radiation-induced modification of polymeric materials applies to several manufacturing areas: wire and cable insulation, heat-shrinkable articles, curing of elastomers, plastics, paints and inks, electron beam lithography, medical sterilization, polymer property control and outer space applications.

2.3.1 Literature reports on irradiated polymers

Various researchers have studied the radiation chemistry of PP. Charlesby (1960); Dole (1973) and Chapiro (1962) have excellently reviewed the main chain scission in isotactic PP. The effect of gamma radiation on PP, PVC, EPR has been described by Seguchi and co-workers (1981, 1982, 1983a, 1983b). A study by Dunn *et al.* (1979) concluded that the ultimate mechanical degradation in an irradiated sample is independent of whether the sample was irradiated in air or vacuum. Tidjani and Watanabe (1996) studied effect of gamma radiation dose on the chemical structure and molecular weight of isotactic polypropylene. The study showed formation of carbonyl, hydroperoxide and hydroxyl groups in irradiated PP, but no formation of any unsaturated group was detected in FTIR spectra. At lower doses, ketones and esters were found in higher concentrations. The weight average molecular weight dropped from 180000 to about 60000 after 5 Mrad dose. In a study by Brooks (1983) MFI, which is an indication of molecular weight was found to increase from 23 g/10min for unirradiated polypropylene to 118 g/10min for polypropylene irradiated

with a dose of 1.5 Mrad. Excessive degradation at low doses has also been reported by (Chappell 1963) and Tidjani (1996). Van Gisbergen *et al.* (1989a, 1989b) reported that the weight average molecular weight dropped from 570,000 to 180,000 after 8.8 Mrad dose. The molecular weight distribution was reported to change from 6.9 for unirradiated sample to 3.7 for sample irradiated with 8.8 Mrad. All these studies show a significant lowering of molecular weight with radiation dose as a result of chain scission in polypropylene. Due to the chain scission reaction in polypropylene, many authors (Nishimoto *et al.* 1991a, 1991b, Charlesby 1959, Yurkevich *et al.* 1973, Williams *et al.* 1977) have reported a lowering of mechanical strength in irradiated polypropylene. The crystalline properties of polypropylene are affected by irradiation and crystalline properties in turn affect the radiation response of polypropylene. In a study by Williams *et al.* (1977) higher chain scission efficiency was reported in samples with higher crystallinity. They attributed this effect to lower mobility of trapped radicals produced in the crystalline regions, which eventually lead to chain scission. The effect of radiation on the degree of crystallinity varies with dose and irradiation conditions. In samples irradiated with 1600 Mrad, the crystallinity was reported to drop by as much as 85% (Tomlinson *et al.* 1967) but these high radiation doses are not of commercial importance. Gielenz *et al.* (1982) demonstrated that the samples irradiated in melt state show significant drop in crystallinity as compared to solid state irradiated samples. The changes produced by radiation in crystalline and amorphous phase influence the thermal behavior of polymers. Krestev *et al.* (1988)

and Minkova *et al.* (1989) have reported a decrease in melting point with increasing radiation dose. The enthalpies of melting and the crystallinity coefficients were found to decrease by about 35% at 2.2 Mrad. All the changes in crystalline phase and amorphous phase have an impact on the permeability of polymers. A study by Kita *et al.* (1988) reported effect of radiation dose on molecular weight and permeability of polypropylene films. The permeability was found to increase due to chain scission. All this may have considerable consequences on the utility of irradiated polymers in packaging applications.

There are very few studies on irradiated propylene copolymers. In a study by Meligi *et al.* (1995), degradation of polypropylene copolymer was found to be much lower than polypropylene homopolymer. The peak of molecular weight distribution for polypropylene copolymer was found to shift progressively to lower values with storage time. The post irradiation degradation in polypropylene copolymer was also found to be lower than the homopolymer. The difference in the behavior has been attributed to polymer morphology prior to irradiation.

In case of EVA copolymers, the basic polymer structure changed by the addition of comonomer often adds to the responsiveness to ionizing radiation treatment (Brooks 1983). If good physical properties are desired at lower radiation doses, then higher % of vinyl acetate in ethylene vinyl acetate is desirable. Sweet (1979), Datta *et al.* (1996a), Minkova *et al.* (1989) studied the radiation behavior of ethylene vinyl acetate and found EVA to be a polymer of crosslinking type. Gel formation in EVA

has been reported to start at 10 Mrad by Thomas *et al.* (1987). Brooks (1983) has reported crosslinking in EVA on the basis of improvement in elastic modulus and reduction in percent elongation. EVA was reported to have far better responsiveness to radiation than polyethylene. The crosslinking in EVA produced by high-energy radiation has been reported (Brooks 1983, Thomas *et al.* 1987, Matsui *et al.* 1992 and 1990, Mannheim *et al.* 1987) to cause several changes in mechanical and crystalline properties and consequently in permeability. Datta *et al.* (1996a) have reported no changes in interplanar spacing or interchain distance on irradiation of trimethylolpropane trimethacrylate (TMPTMA) modified EVA. X-ray crystallinity and heat of fusion has been reported to pass through a peak at 10 Mrad while the melting point was unaffected by dose. In contrast to this study, Matsui *et al.* (1992) reported that electron beam irradiated EVA is a scission type polymer. The melting point and DSC crystallinity was found to decrease with dose.

2.3.2 Irradiated polymer blends

As previously mentioned, polymer blending is a very attractive way of obtaining superior properties. If a blend has to be irradiated, then the reactivities of individual components play very important role in determining the final properties of the irradiated blend. If both components of a blend undergo chain scission, then the irradiated blend will show poor tensile strength, chemical resistance, transport properties etc. If one component is crosslinking type and the other is chain scission

type then the final properties of the irradiated blend can be finely tuned by changing the amount of radiation dose and composition. Irradiation of polymer blends has not been extensively studied and very few papers are available in the literature on this topic. The most investigated blends have been of polyolefins and of polyolefins with engineering thermoplastics. Spadaro *et al.* (1984) and Rizzo *et al.* (1983) studied mechanical and physiochemical properties of LDPE/ iPP blends irradiated under vacuum. They found lack of interaction between the components during irradiation. Van Gisbergen *et al.* (1989a, 1989b) studied effect of electron beam irradiation on PP/Ethylene-propylene-diene monomer blend. They reported less orientation in irradiated blend than unirradiated blends after subsequent processing. The irradiated PP/EPDM blend was reported to exhibit pronounced difference in the rheological behavior compared to irradiated PP. This was explained by hypothesizing formation of graft copolymers from PP onto EPDM rubber particles. Minkova and Nikolova (1989b) studied electron beam irradiated PP/ EVA and PP/LDPE blends. The elongation at break was found to be independent on radiation level. Thomas *et al.* (1987) studied tensile properties of PP/EVA blend and discovered that the blends containing higher proportions of PP (>50%) undergo predominant chain scission at low doses (<50 Mrad) which causes a drastic drop in tensile strength. Minkova *et al.* (1995) studied crystallization behavior of irradiated EVA/ PP blend and reported that EVA and PP crystallize in the same temperature interval. The crystallization

temperature and the DSC crystallinity were reported to decrease with increase in radiation dose. The crystallinity was not determined by WAXD in any of the studies.

2.4 Polymer crystallization

Crystallization of polymers has been a topic of scientific and commercial interest. It is known that some polymers in spite of their long chain nature can crystallize to some extent. Several factors affect the ability of a polymer to crystallize such as structural regularity of main chain, absence of bulky and/or irregularly spaced substituents on the polymer chain and the presence of vibrational and rotational motions in the chain so that different conformations are possible. Polymers crystallized from melt often exhibit a spherulitic morphology. A spherulite consists of chain folded lamellae radiating from a central point as shown in Figure 6 (Fischer 1957). Primary crystallization starts with a single crystal or an inhomogeneous entity and develops through sheaf like morphologies, finally obtaining a spherulitic structure (Figure 7). The structure of polymer crystals and growth of polymer crystals has been extensively reviewed by Phillips (1990, 1992), Bassett (1981), Wunderlich (1976) and Keller (1968). In 1878, Gibbs developed the first theoretical treatment of crystallization based on thermodynamics. Over the years, various new theoretical approaches were developed and the most widely used crystallization theory for polymers is based on nucleation model proposed by Hoffman and Lauritzen (1961).

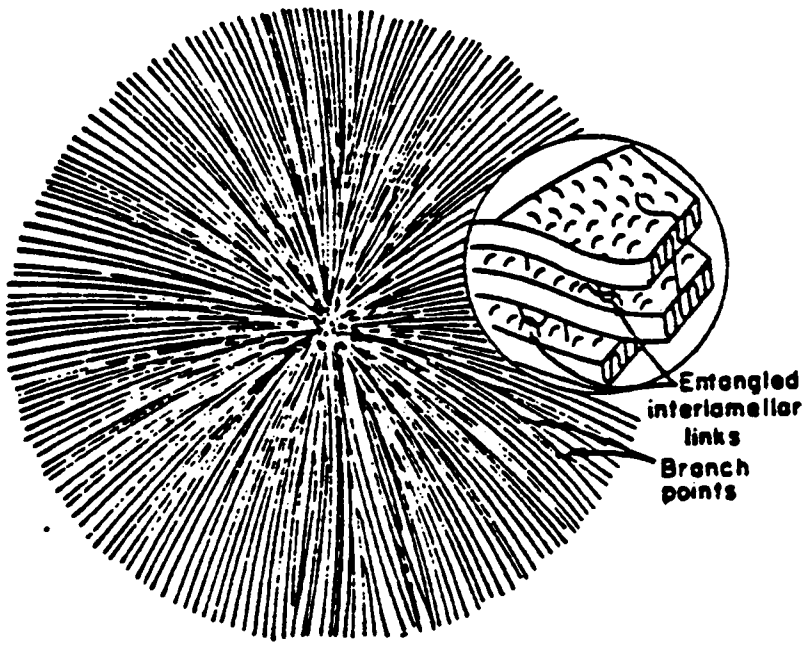

Figure 6.Structure of a polymer spherulite (Hoffman *et al.* 1976)

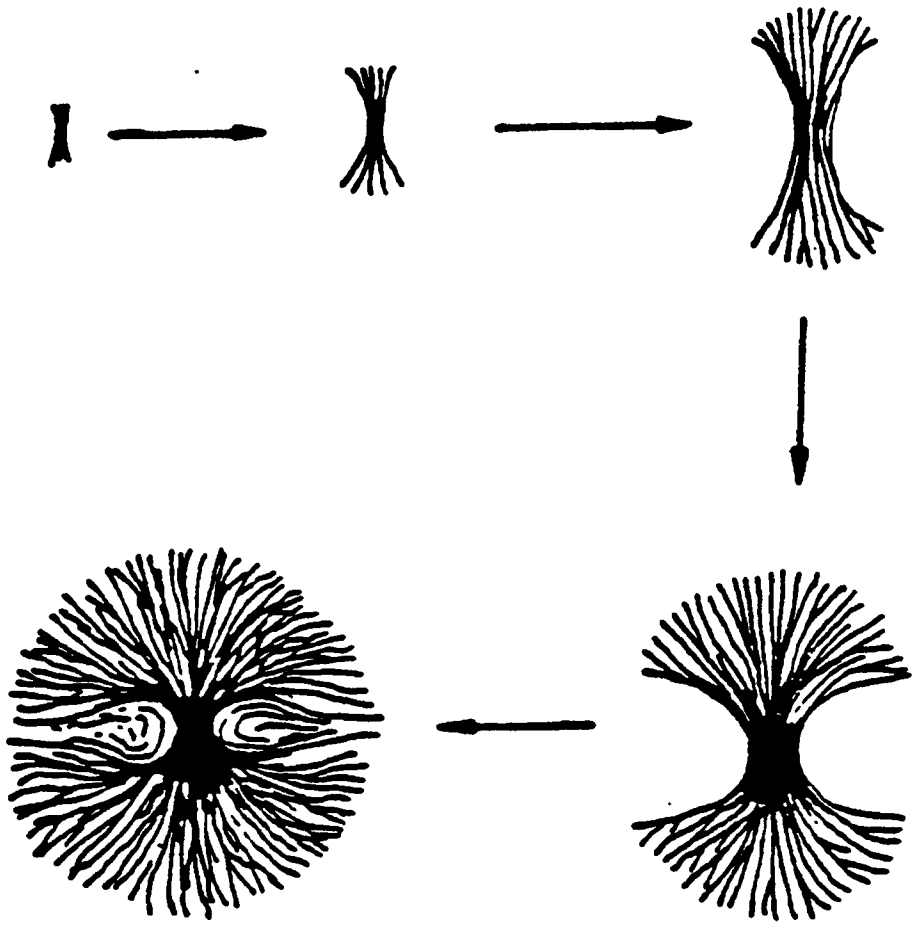

Figure 7.Growth of a spherulite from axiallites (Bassett 1981).

Based on the nucleation theory, various studies have been carried out to study the effect of molecular weight, crosslinking and copolymer content on crystallization process (Phillips and Lambert 1990, Hoffman and Miller 1988, Mezghani and Phillips 1995, Kao and Phillips 1986), but only studies on crosslinked systems will be discussed here. In crosslinked systems, the crystallization temperatures, has been shown to decrease with increasing crosslink density. An increase in the crosslink density results in a decrease in the chain mobility. The constraints imposed by crosslinks shorten the portion of the chain, which is able to crystallize resulting in a lower crystallization temperature. The sol fraction (extractable part) was found to influence the crystallization behavior of the gel fraction (crosslinked part) in the unextracted systems. The crystallization rate was affected by crosslinking and the sol fractions were found to crystallize faster than the gel fractions.

The crystallization in polymer blends is more complex than crystallization in homopolymers. Nishi and Wang (1975) and, Alfonso and Russell (1986) have reviewed the crystallization in miscible blends. The complexity of polymer blend crystallization arises from several factors. Due to the change in the chemical potential of the melt arising from specific interactions between the components, the free energy necessary to form a critical nucleus on the crystal surface and the mobility of both the crystallizable and non-crystallizable components are affected. As the crystallization proceeds, the non-crystallizable component must diffuse away from the growth front. The rate at which the growth front advances reflects a competition between the

inherent capability of the crystal to grow and the transport of the non-crystallizable component in the mixture and the slower of the two processes dictates the kinetics. The concentration of the crystallizable material at the growth front is reduced by an amount proportional to the volume fraction of the crystallizable component. The glass transition temperature of the non-crystallizable component affects the mobility of chains at solid-liquid interface. All these factors make crystallization of miscible blends very complicated. In case of immiscible blends, the crystallization theories of homopolymer can be applied, as there is no interaction between the blend components. The important factor affecting the crystallization in immiscible blends is the crystallization temperature of blend components. If one component is crystallizing before another and if the growth front is excluding non-crystallizable or non-crystallized polymer, a depression in growth rate is observed. If the non-crystallizable polymer is engulfed by the growth front, then the growth rate remains unaffected (Bartczak *et al.* 1986). Crystallites of one component may also act as nucleating agents for other component, which may change the size and number of crystallites (Bartczak *et al.* 1986, Nadkarni *et al.* 1992).

2.5 Melting of polymer crystals

Polymer melting is considered to be a reversible process in which its ordered crystalline regions are converted into a disordered amorphous phase. The behavior of

a lamellar polymer crystal is governed by several factors including lamellar thickness, surface free energy, lattice imperfections and internal stress fields.

In a single lamellar polymer crystal, the free energy of formation may be written as

$$\Delta G = 2(a+b)\cdot l\cdot\sigma + 2ab\sigma_e - a\cdot b\cdot l\cdot\Delta f \qquad \text{(Eq.9)}$$

where, a, b are lateral dimensions, l is the crystal thickness, Δf is the bulk free energy of fusion and σ and σ_e are the lateral and fold surface free energies respectively. Since a>>1 and b>>1, the first term in the equation may be neglected.

When a polymer crystal melts, ΔG becomes zero. Using this condition and above equation,

$$T_m = T_m^0\left[1-\left(\frac{2\cdot\sigma_e}{l\cdot\Delta h_f}\right)\right] \qquad \text{(Eq.10)}$$

where, T^o_m is the equilibrium melting point and Δh_f is the heat of fusion per unit volume of crystal.

Copolymerization results in lower chain regularity, reducing the melting point and the sequence length of the crystallizing component. Crosslinking is shown to have similar effect on crystallization (Andrews *et al.* 1971). Thus both crosslinks and copolymer can be considered as defects which hinder crystallization process. Flory (1955) and Sanchez and Eby (1973, 1975) have developed theories of copolymer crystallization based on the interdependence of melting of crystals, the degree of incorporation of non-crystallizable component in the crystal lattice and its kinetics. Flory's theory is based on the concept of defect exclusion from the crystal lattice while the theory

proposed by Sanchez and Eby is based on inclusion of defects in the crystal lattice. The concept of defect inclusion and exclusion is shown in Figure 8.

Flory's exclusion equation is expressed as

$$\frac{1}{T_m^0} - \frac{1}{T_m} = \frac{R}{\Delta H_f} \ln(1-x) \qquad \text{(Eq.11)}$$

where x is the overall defect content, T_m^0 is the equilibrium melting temperature of homopolymer, ΔHf is the heat of fusion, R is the gas constant.

Sanchez and Eby expressed the change in melting temperature as

$$\frac{1}{T_m^0} - \frac{1}{T_m} = \frac{R}{\Delta H_f}\left[\frac{x_{ce}}{RT_m} + (1-X_c)\ln\left(\frac{1-x_c}{1-x}\right) + X_c \ln\left(\frac{x_c}{x}\right)\right] \qquad \text{(Eq.12)}$$

This equation reduces to Flory's equation of defect exclusion, when $x_c = x$.

In case of miscible polymer blends, where one of the components crystallizes, a depression in melting point of crystallizable polymer is observed reflecting a change in the chemical potential of the amorphous phase due to specific interactions between the blend components. In case of immiscible blends no such depression has been observed. The depression in the melting point can be predicted using Flory-Huggins theory, which predicts that the equilibrium melting point of the blend will be lower than the equilibrium melting point of the pure polymer such that

$$\frac{1}{T_m} = \frac{1}{T_m^0} - \frac{R V_{2u}}{\Delta H_u V_{1u}} \chi (1-\Phi_2)^2 \qquad \text{(Eq.13)}$$

where, T_m^0 and T_m are equilibrium melting temperatures of pure component and

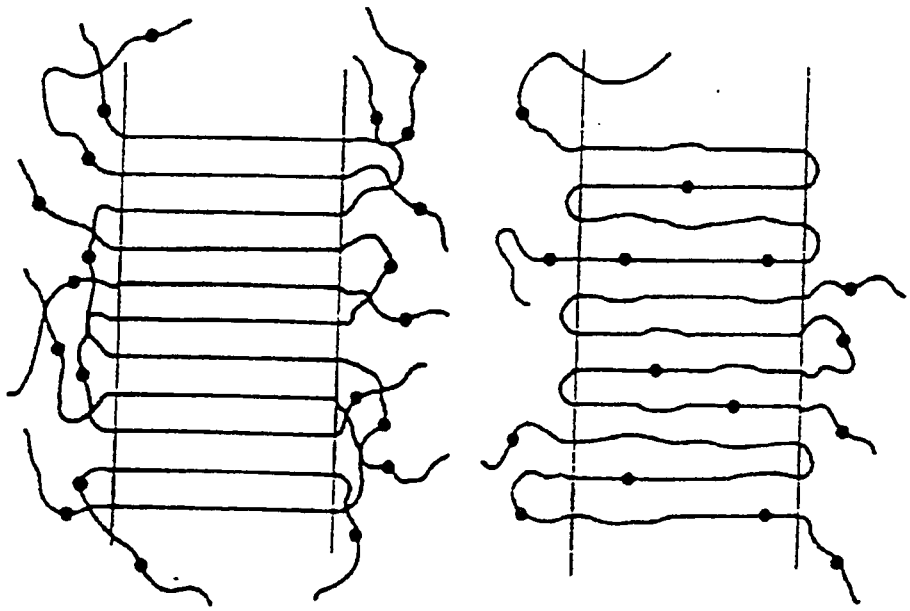

Figure 8.Schematic presentation of defect inclusion (right) and defect exclusion (left) models.

mixture respectively, V_{iu} is the molar volume of component *i* with volume fraction Φ_i This equation has been widely used to calculate the interaction parameter but this approach has been criticized by Alfonso and Russell (1986).

3 Experimental

3.1 Materials

The blends under investigation were made of ethylene vinyl acetate copolymer (EVA), polypropylene homopolymer (PPH) and polypropylene copolymer (PPC). EVA copolymer (MFR 18g/10min) was obtained from BASF. Polypropylene copolymer (MFR 2g/10min) with an ethylene content of up to 10 wt.% was obtained from a Bulgarian company. Polypropylene homopolymer (MFR 2g/10min) was also a Bulgarian product. No information is available about the molecular weight distribution in these polymers.

3.2 Blend preparation and irradiation

The blend compositions investigated here are listed below.

50 wt.% EVA + 50 wt.% PPH

50 wt.% EVA + 25 wt.% PPH + 25 wt.% PPC

40 wt.% EVA + 20 wt.% PPH + 40 wt.% PPC

82 wt.% EVA + 9 wt.% PPH + 9 wt.% PPC

Department of Physics at Sofia University, Bulgaria supplied all the blend samples in film form. According to them, the samples were prepared by melt blending the polymers in a Brabender Plasticorder at 180-225°C. The tubular films were extruded at 190°C and were cooled in air to room temperature. The semicrystalline films were

irradiated in an electron-beam accelerator in air to radiation doses of 5-16 Mrad. The unirradiated blend films with the compositions listed above and films irradiated with doses of 5 Mrad, 8Mrad, 10 Mrad, 11 Mrad and 16 Mrad were studied. Following nomenclature was used to identify samples.

EVA content / PPH content / PPC content / Radiation dose in Mrad. Thus a blend containing, 50 wt.% EVA and 50 wt.% PPH and irradiated with 10 Mrad is written as 50/50/0/10.

3.3 Extraction

Solvent extraction was performed on the as received blend samples using boiling toluene method. The apparatus used for the experiment is shown in Figure 9. The samples were weighed accurately and enclosed in stainless steel wire-mesh baskets. During extraction, there exists a possibility of fragmentation of samples. If all the fragments are not collected after extraction, erroneous results may be obtained. To avoid this stainless steel wire-mesh baskets were used to retain all fragments together after extraction. In order to prevent any oxidation of the samples during extraction, an antioxidant (2,6-Di-*tert*-butyl-4-methylphenol) was added to toluene. The baskets were placed in boiling toluene for 48 hours. After 48 hours, the insoluble portion of the films, known as gel, was removed from boiling toluene and placed in a vacuum oven at 80°C for 5 hours. The vacuum dried gel was weighed accurately to calculate gel and sol fractions using following equations.

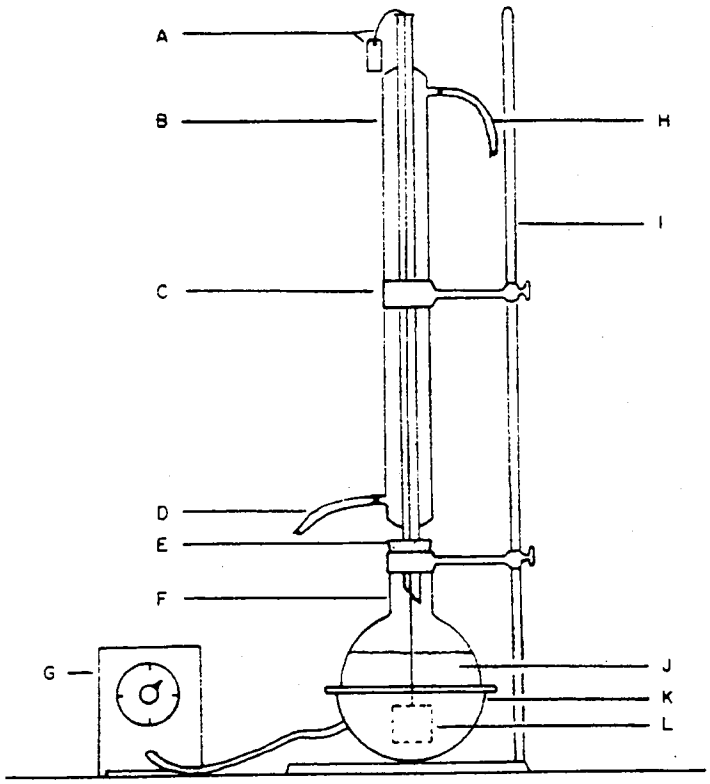

A—Identification tag and fine wire attached to cage.
B—Reflux condenser.
C—Ring stand clamp.
D—Water inlet.
E—Ground-glass or cork joint.
F—Large-mouth round-bottom flask.
G—Variable transformer.
H—Water outlet.
I—Ring stand.
J—Decahydronaphthalene or xylene.
K—Heating mantle.
L—120-mesh wire cage containing the specimen.

Figure 9. Extraction apparatus (from ASTM D 2765)

$$Gelfraction = w_1 / w_0 \quad \text{(Eq.14)}$$

$$Solfraction = 1 - Gelfraction \quad \text{(Eq.15)}$$

where, w_1 is the weight of the samples after extraction and drying, and w_0 is the weight of the sample before extraction.

3.4 Differential scanning calorimetry (DSC)

All samples were tightly enclosed in aluminum DSC sample pans and weighed accurately. The experiments were conducted on a Perkin-Elmer DSC-7 instrument, which was calibrated using melting onset and heat of fusion of pure Indium. The samples (as received) were heated from –45°C to 190°C at 10°C/min. They were held at 190°C for 5 minutes to erase all thermal history and were cooled to –45°C at 10°C/min. The temperatures where DSC scans displayed endothermic peaks, were chosen as apparent melting temperatures and, temperatures where exothermic peaks were displayed, were chosen as apparent crystallization temperatures.

3.5 Dynamic mechanical analysis (DMA)

The dynamic mechanical analysis was performed on an AutoRheovibron Dynamic Viscoelastometer (Imass Inc.) The samples (as received) were cut into 3.5cm x 0.5cm strips and they were tested under a tensile load of 20g. All samples were heated from –100°C to 160°C at 1°C/min. The instrument was cooled to –100°C using liquid

nitrogen. Storage modulus, loss modulus and tanδ were calculated from the experiment. The data was collected at three frequencies (1.1 Hz, 11 Hz and 110 Hz) but only the data collected at 11 Hz was used in the analysis.

3.6 Wide angle x-ray diffraction (WAXD)

WAXD studies were performed on as received samples, to determine the effect of blend composition and radiation dose on crystal lattice. All experiments were conducted on a Rigaku diffractometer using CuKα (λ=1.542Å) radiation. Diffraction patterns were obtained in a reflection mode. Scans were taken from 10° to 40° (2θ). The operating voltage and the current of the tube were kept at 35 kV and 20 mA, respectively. The peaks were indexed to calculate line broadening and lattice parameters. Crystallinity indices were calculated by separating peaks into two parts, crystalline and amorphous and measuring the areas under crystalline peaks and amorphous halos.

4 Results

4.1 Extraction

The gel fraction is a measure of the extent of crosslinking in polymers and it was determined by extracting soluble or uncrosslinked part of the irradiated samples with boiling toluene. This direct extraction method was found more efficient than Soxhlet extraction method as the temperature of boiling toluene solution is much higher than the temperature of toluene condensate used in Soxhlet method. The gel and sol fractions in the samples were calculated from the extraction experiment and the results are presented in Table 2 and Figure 10.

It is clear from Table 2 and Figure 10, that initially the gel fraction increases rapidly with the radiation dose and approaches a plateau after 10 Mrad. This behavior is not observed for 40/20/40 blend, so it may be a feature of blends containing higher amounts of EVA (≥ 50 wt.%). No significant difference can be seen between the blends containing same amount of EVA but differing in the amount of other components. In case of 50/25/25 samples, the presence of 25% PPC along with 25% PPH does not have any significant effect on the radiation response of the blend and the response is almost identical to that of 50/50/0 blend. It suggests that EVA may be the gel content determining factor for these blends. For same dose level gel fraction increases with increase in the amount of EVA in the samples. The data indicates that EVA is a polymer of crosslinking type. Several studies in the literature support this

Table 2 Gel fraction and sol fraction data.

Sample ID	Gel fraction (X)	Sol fraction (S)
50/50/0/0	0.0	1.0
50/50/0/5	0.335	0.665
50/50/0/8	0.406	0.594
50/50/0/10	0.491	0.509
50/50/0/16	0.563	0.437

Sample ID	Gel fraction (X)	Sol fraction (S)
50/25/25/0	0.0	1.0
50/25/25/5	0.285	0.715
50/25/25/8	0.424	0.576
50/25/25/10	0.50	0.50
50/25/25/11	0.508	0.492

Table 2 (continued)

Sample ID	Gel fraction (X)	Sol fraction (S)
40/20/40/0	0.0	1.0
40/20/40/5	0.223	0.777
40/20/40/8	0.316	0.684
40/20/40/10	0.408	0.592
40/20/40/11	0.390	0.610
40/20/40/16	0.581	0.419

Sample ID	Gel fraction (X)	Sol fraction (S)
82/9/9/0	0.0	1.0
82/9/9/5	0.468	0.532
82/9/9/8	0.688	0.312
82/9/9/10	0.693	0.307
82/9/9/16	0.801	0.199

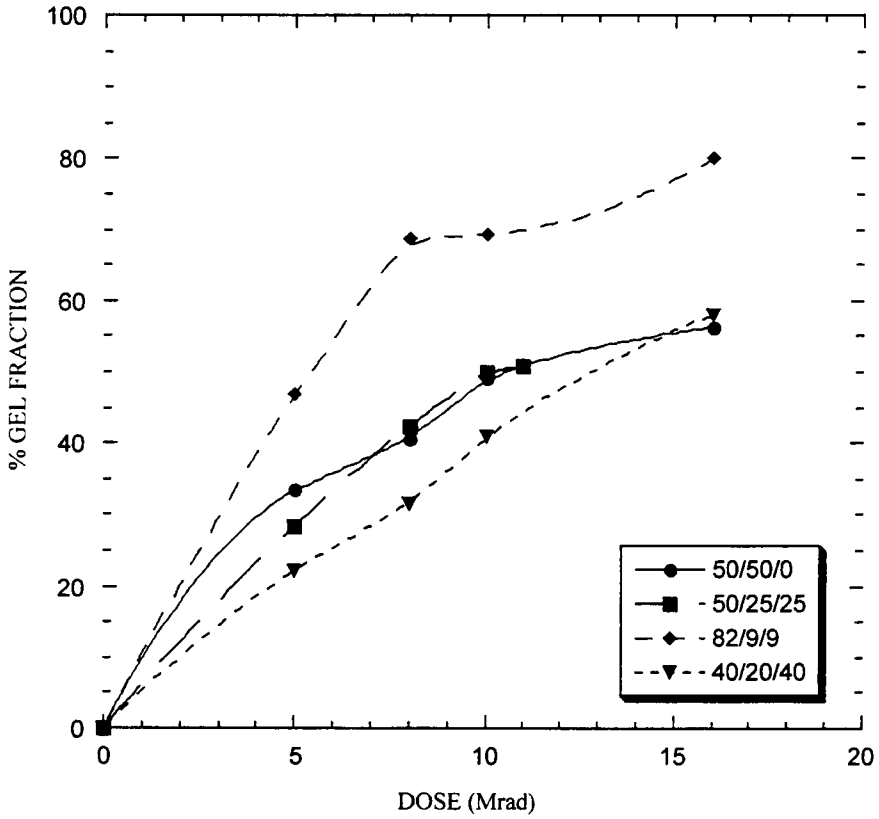

Figure 10.Variation in gel fraction with radiation dose for the blend compositions.

result. Thomas *et al.* (1987) and Matsui *et al.* (1992) found high gel fraction in irradiated EVA. In their study, the gel fraction reached 80% at 15 Mrad. The gel fraction results obtained in the present study are different from those obtained by Minkova *et al.* (1995) for EVA-PPH blend irradiated with same level of radiation doses. They reported gel fractions in the range of 50-60% and independent of radiation dose and blend composition. As the method of determining gel fraction is not described, the discrepancy between the results can not be explained.

4.2 Differential scanning calorimetry study

The melting and re-crystallization behaviors of the samples were studied with DSC. The samples were heated to 190°C and cooled to -45°C at 10°C/min, to study their melting and crystallization behavior.

4.2.1 Melting behavior study

The melting scans of the samples are shown in Figure 11 to Figure 14 and the variation in melting temperatures with radiation dose is presented in Figure 15 and Figure 16 and, Table 3. Two prominent peaks are seen in all samples. The low temperature peak can be attributed to melting of EVA and the high temperature peak can be attributed to melting of PP homopolymer. No distinct melting peak for PPC is seen in any of the samples. It is possible that the incorporation of ethylene in the copolymers is resulting in a very low crystallinity and inconspicuous melting peak.

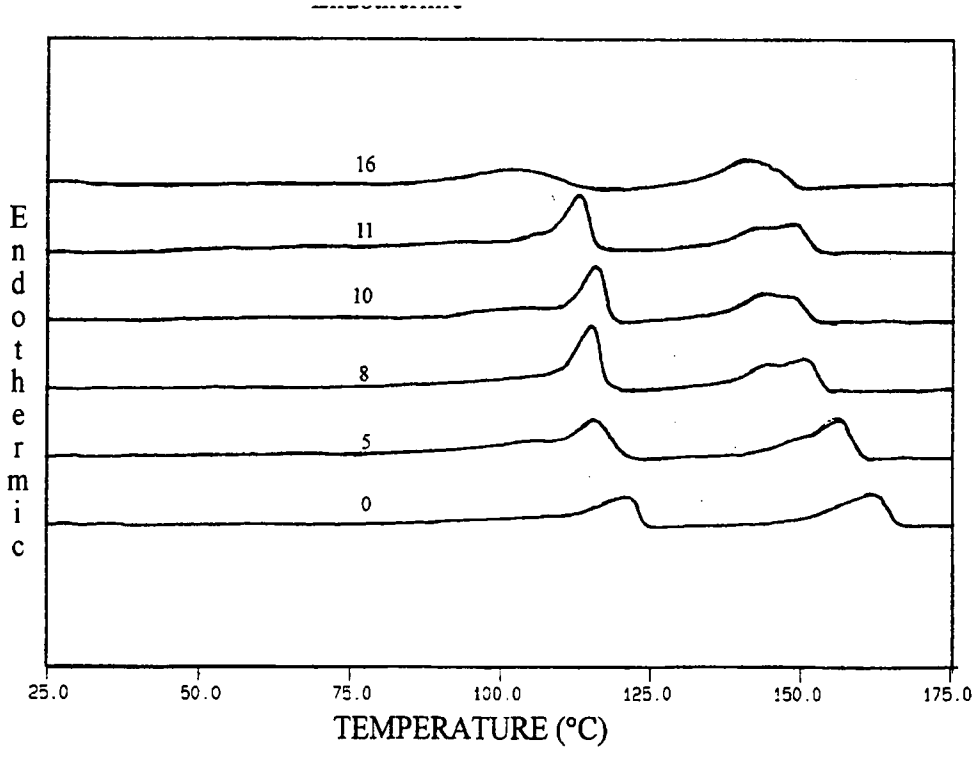

Figure 11. Melting behavior of 50/50/0 blend (numbers on top of curves indicate dose in Mrad)

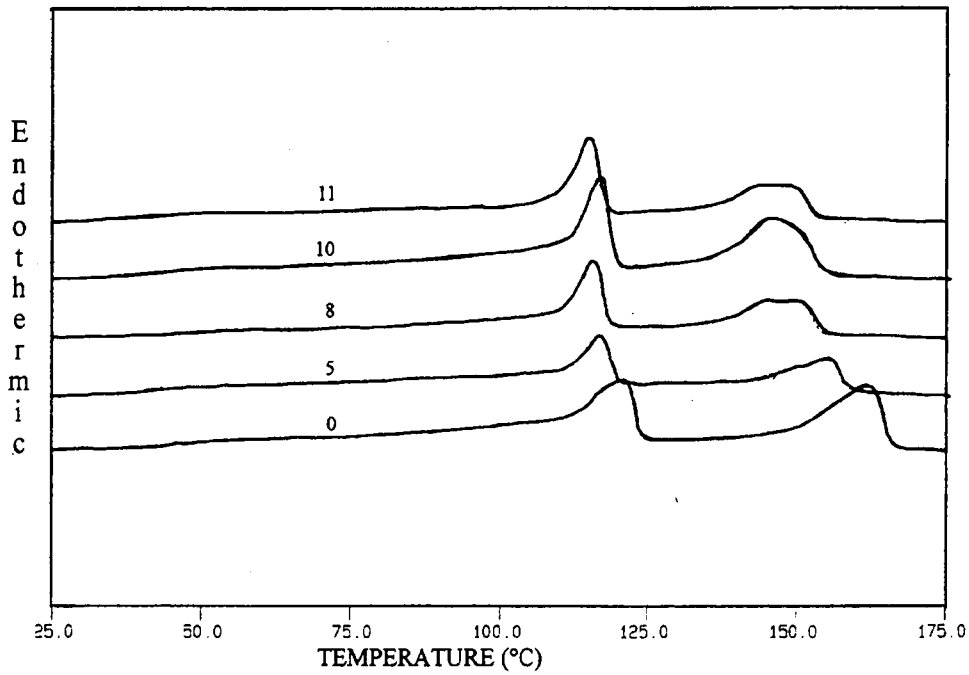

Figure 12. Melting behavior of 50/25/25 blend (numbers on top of curves indicate dose in Mrad)

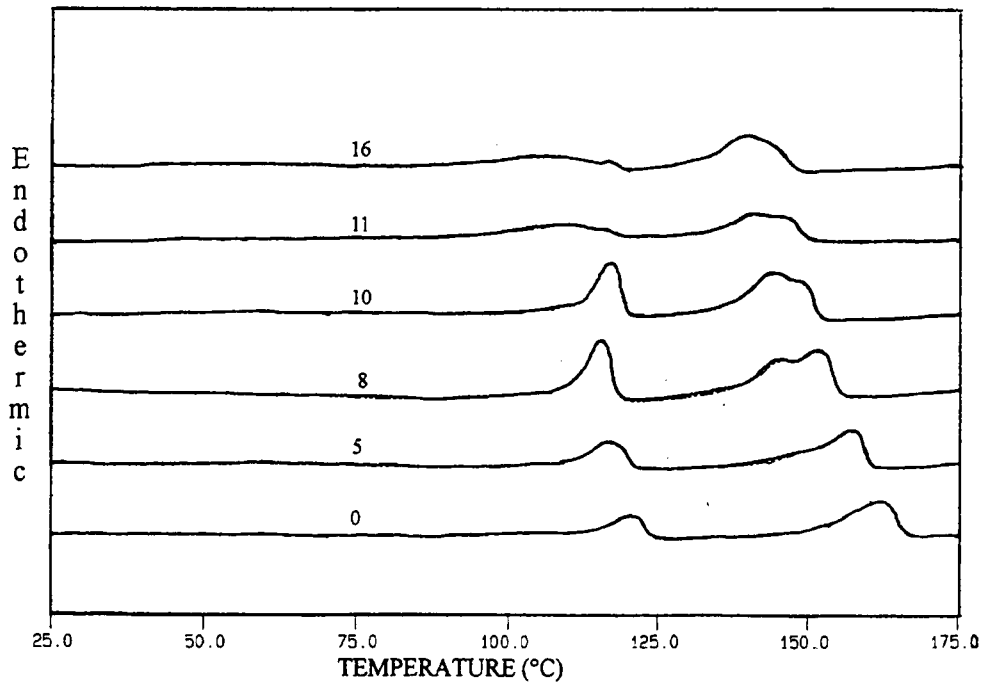

Figure 13. Melting behavior of 40/20/40 blend (numbers on top of curves indicate dose in Mrad)

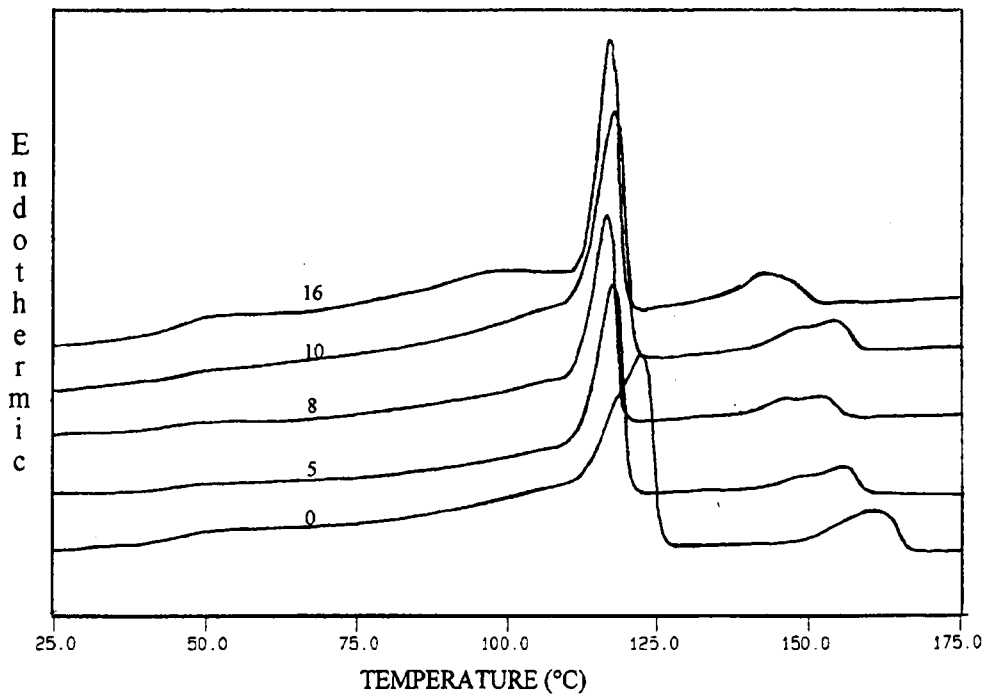

Figure 14. Melting behavior of 82/9/9 blend (numbers on top of curves indicate dose in Mrad)

Table 3 Variation of melting temperature with radiation dose.

T_m^1 = melting temperature of EVA component

T_m^2 = melting temperature of PP component

Sample ID	T_m^1 (°C)	T_m^2 (°C)
50/50/0/0	121.01	161.49
50/50/0/5	115.56	156.26
50/50/0/8	115.06	150.52
50/50/0/10	115.70	144.33
50/50/0/11	113.01	148.35
50/50/0/16	101.07	140.35

Sample ID	T_m^1 (°C)	T_m^2 (°C)
50/25/25/0	120.80	161.77
50/25/25/5	116.88	155.31
50/25/25/8	115.78	149.73
50/25/25/10	117.01	145.63
50/25/25/11	115.47	144.16

Table 3 (continued)

Sample ID	T_m^1 (°C)	T_m^2 (°C)
40/20/40/0	120.41	161.70
40/20/40/5	116.93	157.551
40/20/40/8	115.67	151.884
40/20/40/10	116.86	144.06
40/20/40/11	110.19	141.32
40/20/40/16	107.06	140.13

Sample ID	T_m^1 (°C)	T_m^2 (°C)
82/9/9/0	122.14	160.58
82/9/9/5	117.61	155.64
82/9/9/8	116.70	151.76
82/9/9/10	117.93	149.20
82/9/9/16	117.18	142.60

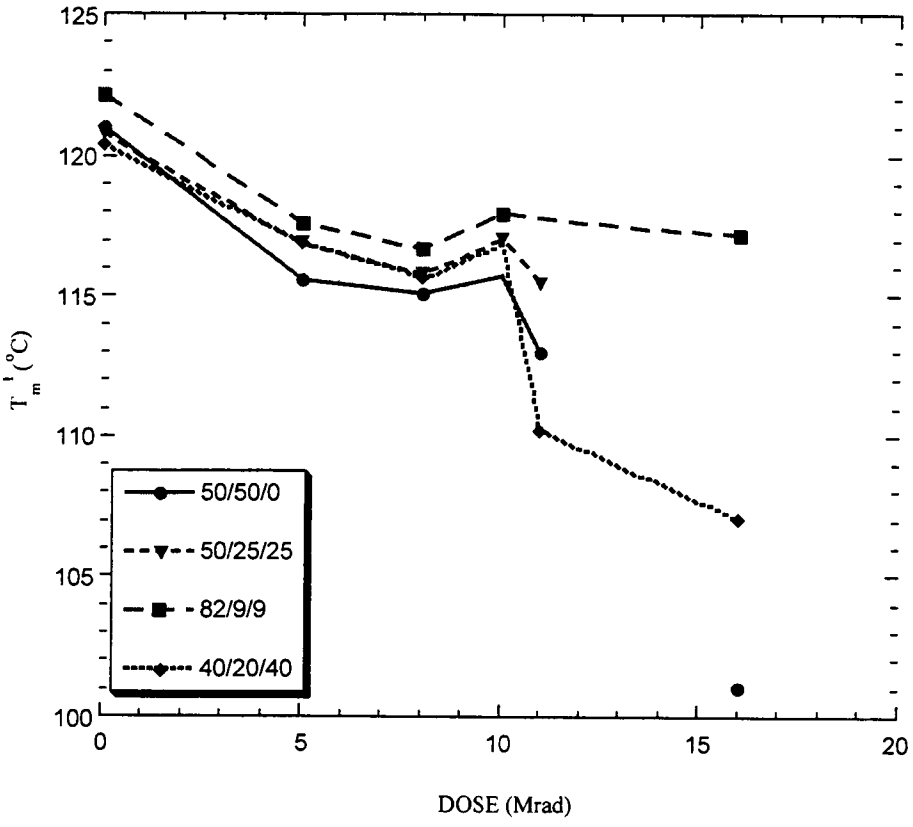

Figure 15. Variation in melting temperatures of EVA component with radiation dose.

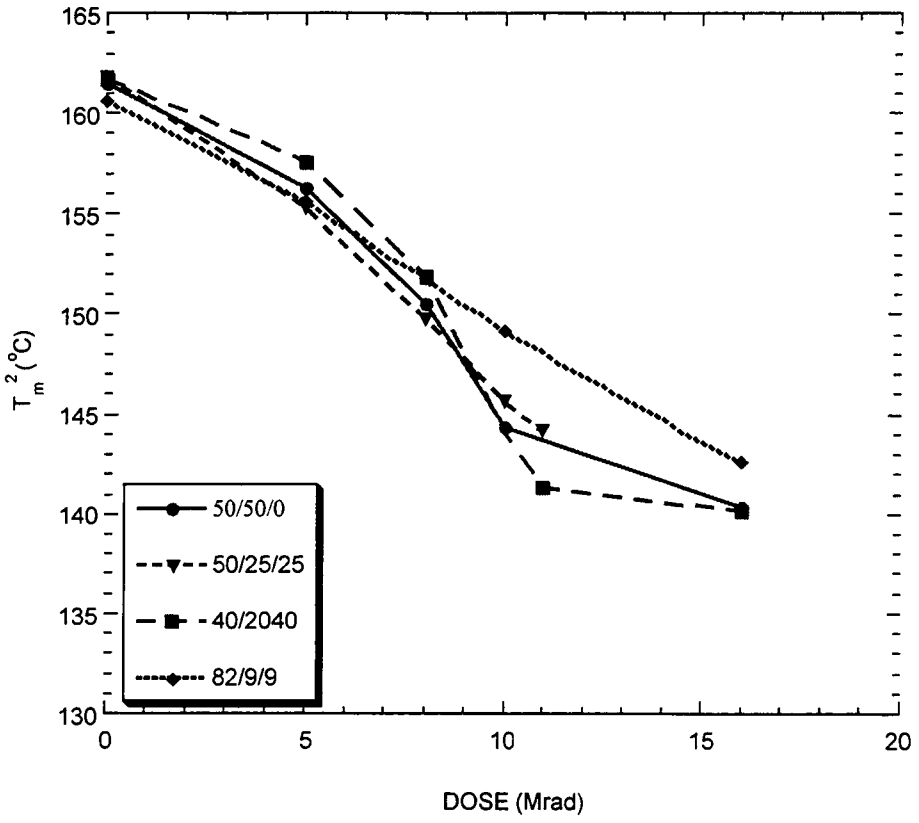

Figure 16. Variation in the melting temperatures of PP component with radiation dose.

The melting of PPC crystallites may also be hidden in the melting range of EVA. The apparent melting temperatures of EVA component and PP component are almost independent of blend composition. This may be an indication of incompatibility between crystallites of blend constituents. This behavior was reported by Minkova *et al.* (1989) for EVA-iPP blend irradiated with doses up to 16 Mrad. All compositions exhibit lowering of melting temperatures with increasing radiation doses. In case of 50/50/0 blend, appearance of a shoulder and broadening of high temperature melting peak is seen for irradiated samples. The sharpness of low temperature peak appears to increase with dose up to 10 Mrad and at 16 Mrad, broadening and lowering of peak temperature is seen. In case of 50/25/25 blend samples, a small shoulder, seen at low doses disappears at high doses. The broadening of melting range with increasing radiation dose is seen in case of melting of PP component. In case of 40/20/40 blends, the intensity of EVA melting peak increases with radiation dose and at the same time the melting temperature decreases with radiation dose. Broadening and multiple melting peaks are seen in case of melting of PP component along with a decrease in melting temperature with radiation dose. The presence of multiple iPP melting peaks has been reported by Busfield *et al.* (1979) and Rabello et al. (1997) in irradiated PP. This may be attributed to the change in molecular weight, molecular weight distribution due to radiation-induced crosslinking and chain scission reactions and reorganization during heating in DSC. The 82/9/9 blends show high intensity, sharp peaks for EVA melting, which may be caused by a higher weight percent of EVA

present in these blends. A moderate decrease in melting temperature with radiation dose is seen these samples. Appearance of a shoulder peak is very noticeable for 82/9/9/16 sample. Broadening and multiple melting peaks are seen for melting of PP and EVA components.

The changes in melting temperatures of EVA and PP with increasing radiation dose are shown in Figure 15 and Figure 16. A significant and continuous drop in melting temperature of PP is seen in all blends. The melting temperature of EVA drops significantly in case of 50/50/0, 50/25/25 and 40/20/40 blends, but in case of 82/9/9 blend, it drops initially and quickly reaches a plateau. The amount of PP present in the blends seems to affect the melting behavior of these blends. The plateau in melting temperature of EVA in 82/9/9 samples may be due to the lower weight fraction of PP present in these samples. As the amount of PP is lower, the number of free radicals in PP, which can degrade EVA crystals is also lower. Another factor may be the presence of sol fraction in these blends. Small amount of sol fractions has been known to result in higher melting temperature (Lambert 1988). There are a few studies in literature about the effect of radiation dose on the melting behavior of EVA and PP. Minkova *et al.* (1989) observed a decrease in melting temperature of EVA with increasing radiation dose. The melting temperatures obtained by them are higher than the melting temperatures obtained in this study. The difference may be attributed to different heating rate used in the experiments and post irradiation period. Datta *et al.* (1996a) reported a constant melting temperature for EVA irradiated with doses up

to 20 Mrad. Broadening of melting peaks is more noticeable for melting of PP component.

4.2.2 Heat of fusion study

Areas under endothermic peaks were used to calculate the heat of fusion of blend samples. The heat of fusion of a polymer depends on crystallinity and crystal perfection. The heats of fusion of EVA component and PP component, for different compositions and radiation doses are tabulated in Table 4 and the variation in heats of fusion of EVA and PP with radiation dose is shown in Figure 17 and Figure 18. In calculating heat of fusion of EVA, it is assumed that the possible contribution of PPC melting to area under EVA melting peak is negligible. The heat of fusion of EVA (ΔH_{EVA}) increases up to 5 Mrad and then decreases in 50/50/0, 50/25/25 and 40/20/40 samples. In case of 82/9/9 samples, ΔH_{EVA} decreases with dose. The heat of fusion of PP component (ΔH_{PP}) shows some variation with dose. But this variation is very small in all the blends. Minkova *et al.* (1989) observed that the enthalpies of EVA melting decrease with radiation dose, in blends containing lower amounts ($\leq$ 50 wt.%) of EVA and for higher EVA contents, enthalpies increase with dose up to 10 Mrad and then decrease. The decrease in the heats of fusion with radiation dose may be attributed to lowering of crystallinity, introduction of defects in the crystal structure by radiation and change in crystalline and amorphous phase enthalpies due to crosslinking and chain scission.

Table 4 Heat of fusion data of blend samples.

Sample ID	ΔH_{EVA} (J/g)	ΔH_{PP} (J/g)
50/50/0/0	49.49	31.62
50/50/0/5	53.01	31.28
50/50/0/8	47.40	31.01
50/50/0/10	44.77	28.12
50/50/0/11	42.71	28.49
50/50/0/16	30.72	27.74

Sample ID	ΔH_{EVA} (J/g)	ΔH_{PP} (J/g)
50/25/25/0	62.59	35.53
50/25/25/5	76.85	33.30
50/25/25/8	58.45	30.55
50/25/25/10	57.37	32.30
50/25/25/11	58.17	30.49

Table 4 (continued)

Sample ID	ΔH_{EVA} (J/g)	ΔH_{PP} (J/g)
40/20/40/0	36.00	41.15
40/20/40/5	40.07	40.08
40/20/40/8	25.20	41.87
40/20/40/10	29.75	38.90
40/20/40/11	27.32	34.06
40/20/40/16	29.50	33.64

Sample ID	ΔH_{EVA} (J/g)	ΔH_{PP} (J/g)
82/9/9/0	102.92	13.49
82/9/9/5	101.01	12.56
82/9/9/8	99.79	12.35
82/9/9/10	102.07	13.13
82/9/9/16	89.46	10.29

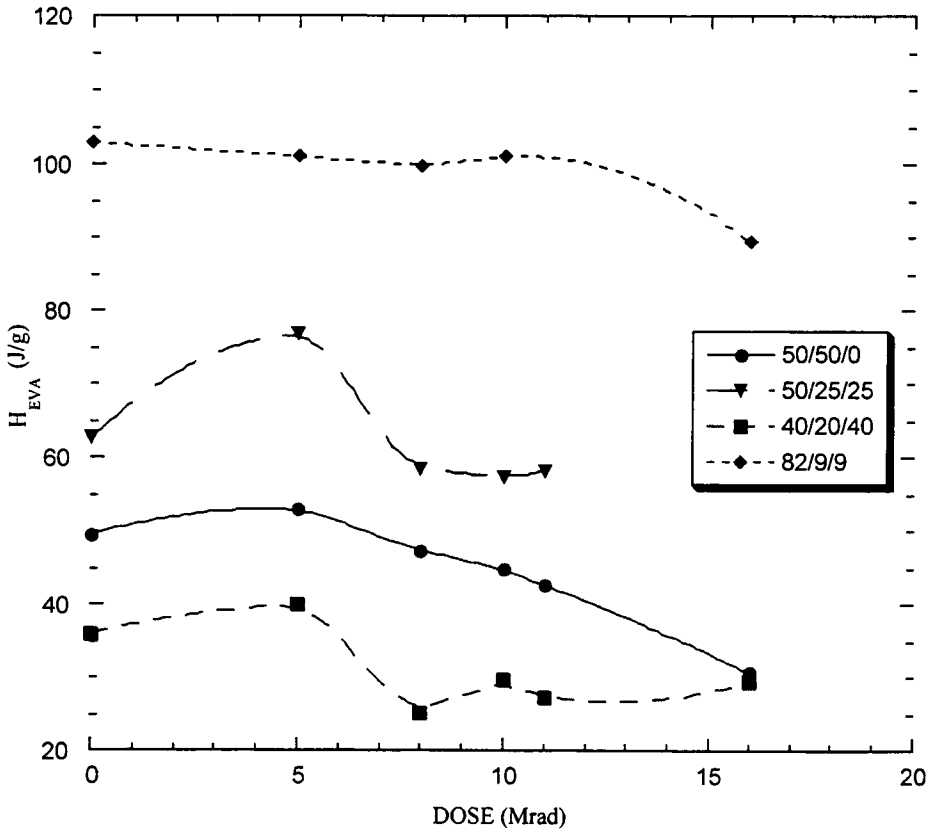

Figure 17. Heat of fusion of EVA component in the blend samples

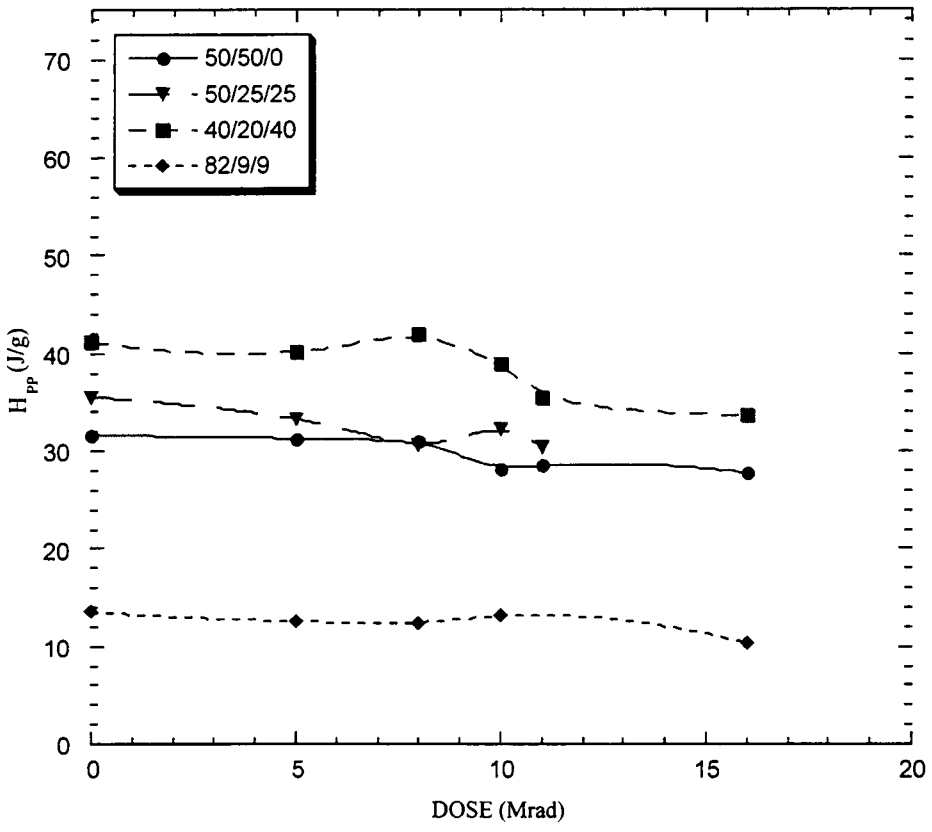

Figure 18. Heat of fusion of PP component in the blend samples

Datta *et al.* (1996a), in their study of irradiated EVA, reported that the enthalpy exhibited a maximum value at 10 Mrad and then decreased with dose. They attributed this behavior to the presence of strong intermolecular interactions up to 10 Mrad and the breakdown of structure and chain slippage at higher radiation doses. The findings in this study are slightly different from the literature reports.

4.2.3 Non-isothermal crystallization behavior

All samples were melted and held at 190°C for 5 minutes to erase thermal history. The Crystallization behavior was studied by cooling the samples from 190°C to –45 °C at 10°C/min. The cooling scans for the blend compositions are presented in Figure 19 to Figure 22 and the crystallization and onset of crystallization temperatures are presented in Table 5. A decrease in crystallization temperature with radiation dose is seen for all samples. In case of 50/50/0/0 sample, a distinctly bimodal crystallization peak is seen, suggesting that EVA and PP components are crystallizing in different temperature intervals. For irradiated samples, a monomodal crystallization peak is seen along with a small low temperature peak. The temperature of the small peak decreases with radiation dose The crystallization onset temperature decreases initially with radiation dose but remains constant at high radiation doses.. In case of 50/25/25 blends, a bimodal crystallization peak is seen for 50/25/25/0 and 50/25/25/5 samples and a monomodal crystallization peak with a small shoulder is seen for 50/25/25/8, 50/25/25/10. The crystallization onset temperature remains almost unchanged for the

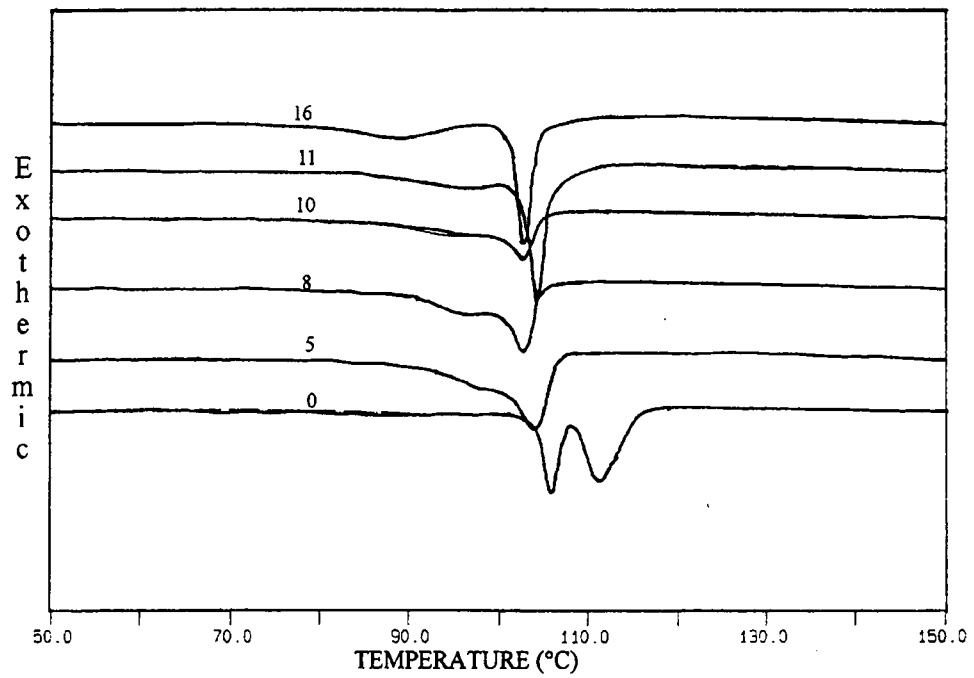

Figure 19. Crystallization behavior of 50/50/0 blend for the radiation doses (in Mrad) shown on the top of the exotherms.

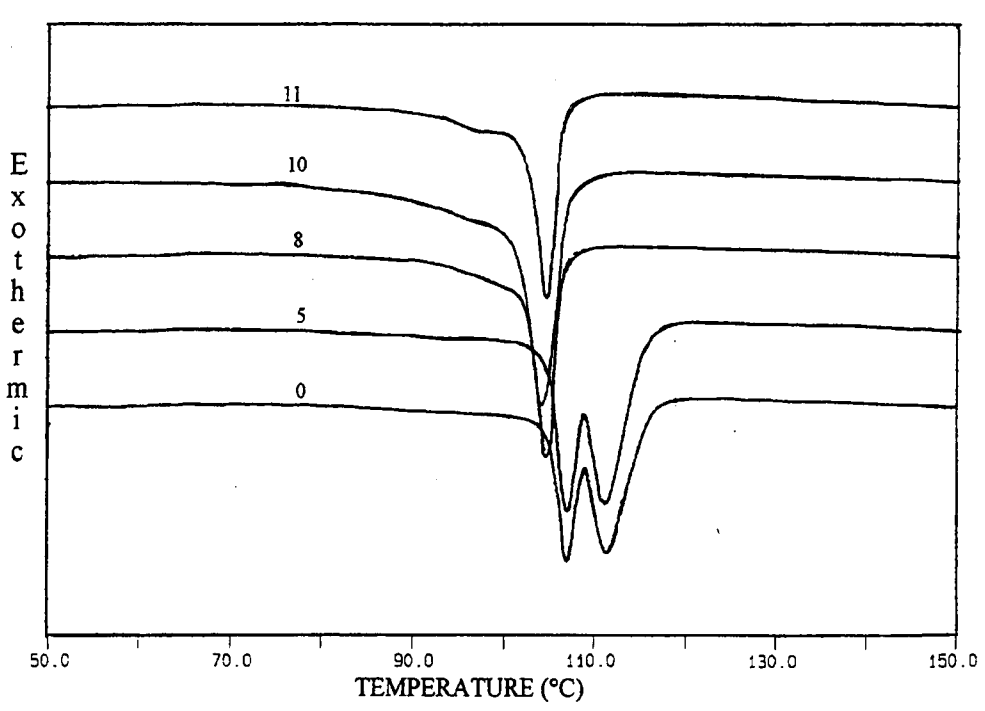

Figure 20. Crystallization behavior of 50/25/25 blend for the radiation doses (in Mrad) shown on the top of the exotherms.

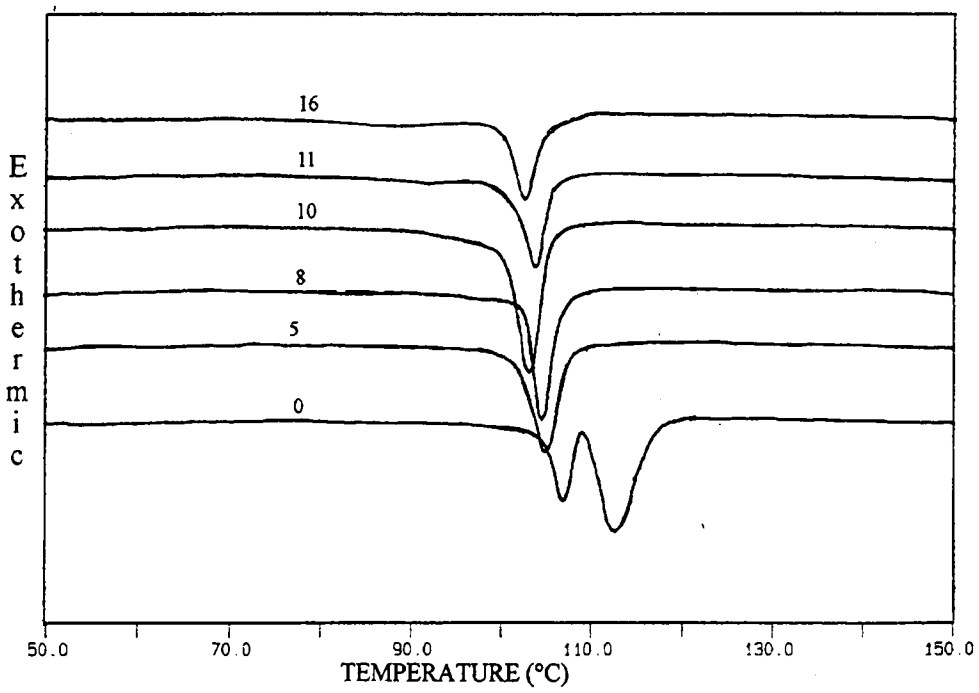

Figure 21. Crystallization behavior of 40/20/40 blend for the radiation doses (in Mrad) shown on the top of the exotherms.

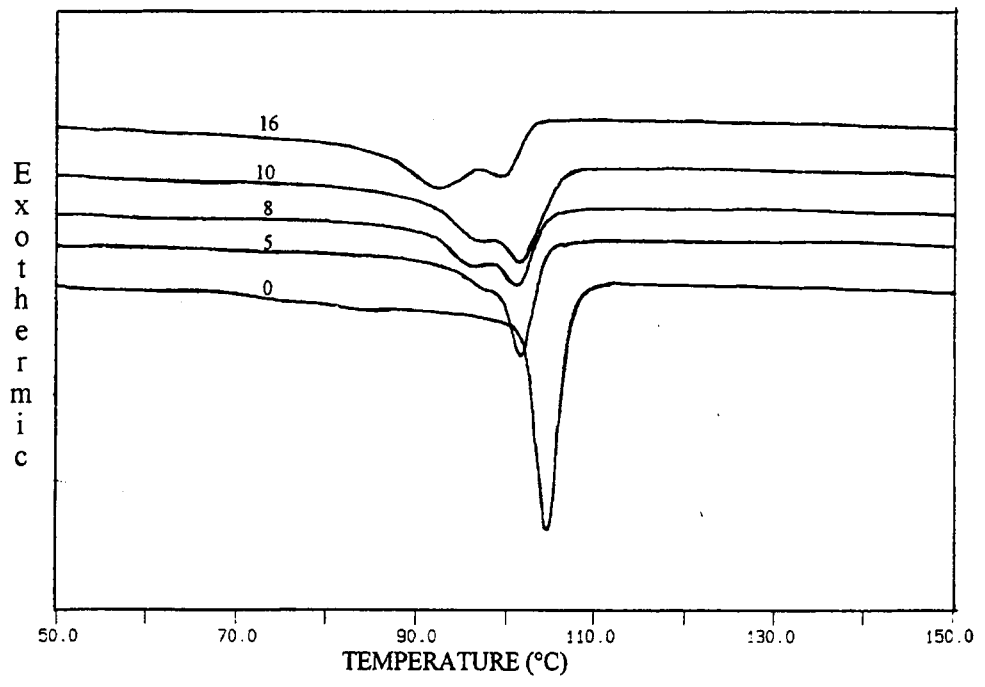

Figure 22. Crystallization behavior of 82/9/9 blend for the radiation doses (in Mrad) shown on the top of the exotherms.

Table 5 Non-isothermal crystallization behavior of blends

H =Higher temperature peak

L = Lower temperature peak

Sample ID	T_c (°C)	T_{onset} (°C)
50/50/0/0	105.90(L)	107.93
50/50/0/5	103.92	106.50
50/50/0/8	102.81	99.52
50/50/0/10	102.69	104.77
50/50/0/11	103.3	104.81
50/50/0/16	102.86 (H)	104.42

Sample ID	T_c (°C)	T_{onset} (°C)
50/25/25/0	111.69 (H)	115.83
50/25/25/5	111.38 (H)	113.97
50/25/25/8	104.86	106.45
50/25/25/10	104.29	107.19
50/25/25/11	104.85	106.46

Table 5 (continued)

Sample ID	T_c (°C)	T_{onset} (°C)
40/20/40/0	112.61(H)	116.99
40/20/40/5	105.05	107.30
40/20/40/8	104.66	106.54
40/20/40/10	103.28	105.34
40/20/40/11	103.29	105.35
40/20/40/16	102.82	105.12

Sample ID	T_c (°C)	T_{onset} (°C)
82/9/9/0	104.70	107.24
82/9/9/5	101.79	104.33
82/9/9/8	101.32 (H)	104.44
82/9/9/10	101.34 (H)	104.04
82/9/9/16	92.60 (L)	102.77

irradiated samples. In case of 40/20/40 blends, a bimodal crystallization peak is observed for 40/20/40/0 sample. The high temperature peak disappears with radiation dose and the temperature at which the low temperature peak occurs, also decreases and the samples irradiated with doses up to 10 Mrad show monomodal crystallization peaks. A small low temperature peak is seen in case of 40/20/40/16 sample. This peak may be resulting from crystallization of gel fraction. The crystallization onset temperature remains almost unchanged for the irradiated samples. The crystallization behavior of 82/9/9 blends is very different from that of other blends. A monomodal crystallization peak, indicating co-crystallization is seen for the unirradiated sample but the irradiated samples show bimodal crystallization peaks. The bimodal peaks suggest different crystallization temperatures for gel and sol fraction present in these blends. In a study by Minkova *et al.* (1995), on non isothermal crystallization behavior of irradiated EVA-iPP blends bimodal peaks were observed for blends with high EVA content (70%-90%) and irradiated with 5 Mrad, 10 Mrad and 16 Mrad. Very distinct double peaks were not observed. unirradiated sample did not show bimodal peaks. This is in good agreement with the behavior of 82/9/9 blends observed in the present study. In their study, monomodal peaks were seen for blends containing 50% EVA and 40% EVA irradiated with 5 Mrad and 10 Mrad, indicating separate crystallization of the two components in the same temperature zone. This is contrary to the behavior of 50/50/0, 50/25/25 and 40/20/40 blends in the present

study. The difference may be attributed to difference in the amounts of crosslinked material in the two studies.

4.2.4 Glass transition temperature study

The glass transition temperature is a very important parameter in study of blend miscibility. DSC scans of blend samples were analyzed to calculate glass transition temperature. No noticeable glass transition is seen for any blend sample. As the blend components are crystallizable, their crystallites may be hindering the motion of chain segments in the amorphous region. The crosslinks introduced by the radiation must be adding to the restriction imposed by crystallites. DMA studies on blend sample may be helpful in resolving transition temperatures.

4.3 Wide Angle X-Ray Diffraction Study

Wide-angle x-ray diffraction study on the blend samples was carried out to study the effect of blend composition and radiation dose on crystal lattice. The diffraction patterns are shown in Figure 23 to Figure 26. In all diffraction patterns, three strong diffraction peaks are seen. The diffraction peak that occurs in 16.4° to 17° 2Θ range is assigned to (040) reflection of monoclinic α-form of PP. The diffraction peak that occurs in 20.9° to 21.8° 2Θ is assigned to (110) reflection of orthorhombic unit cell of EVA and (111) reflection in monoclinic α-form of PP The last major reflection that

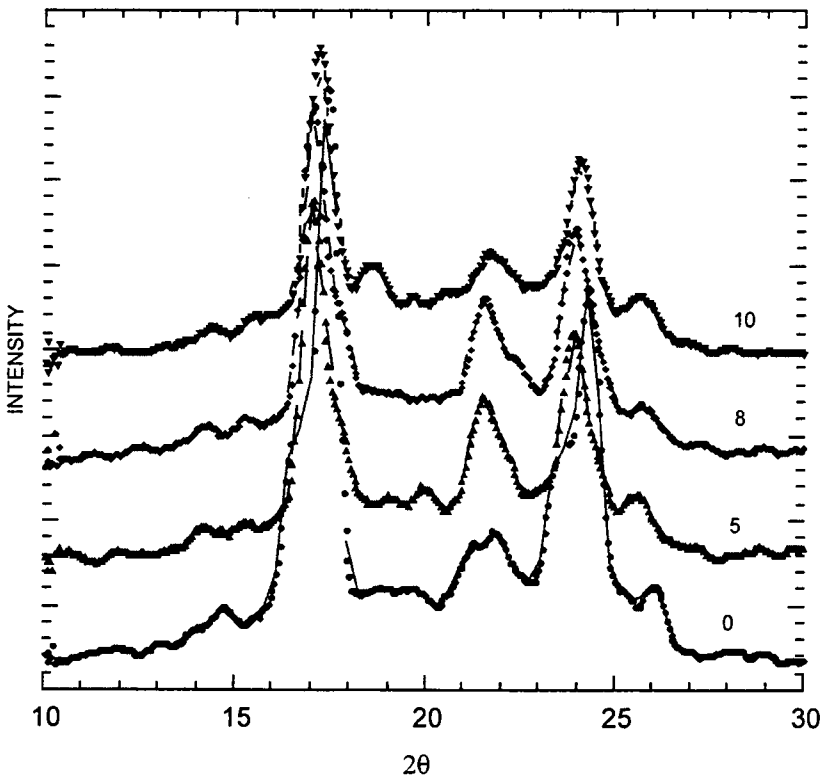

Figure 23. WAXD pattern of 50/50/0 blend (numbers on top of curves indicate dose in Mrad)

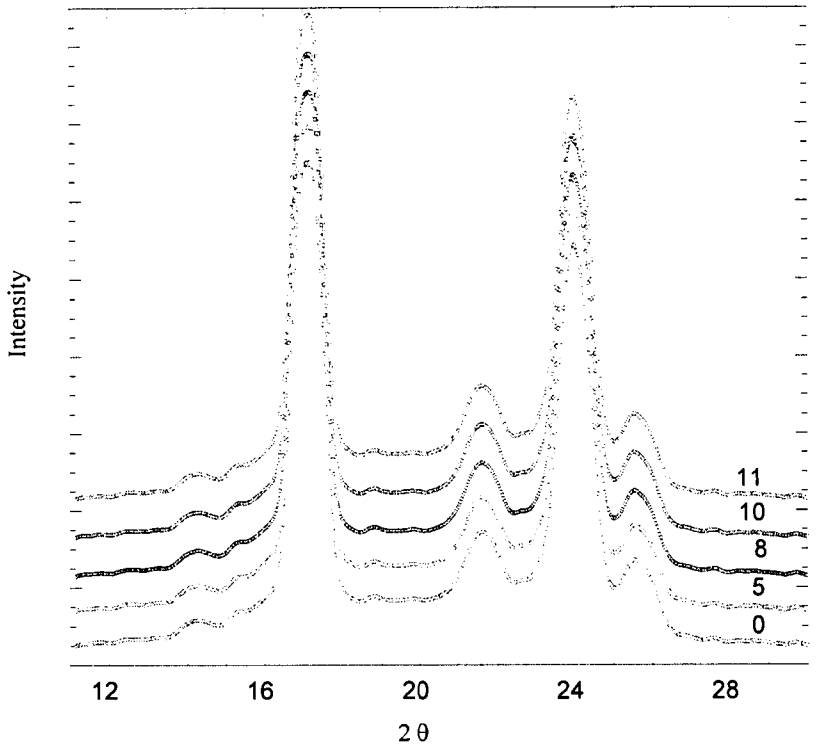

Figure 24. WAXD pattern of 50/25/25 blend (numbers on top of curves indicate dose in Mrad)

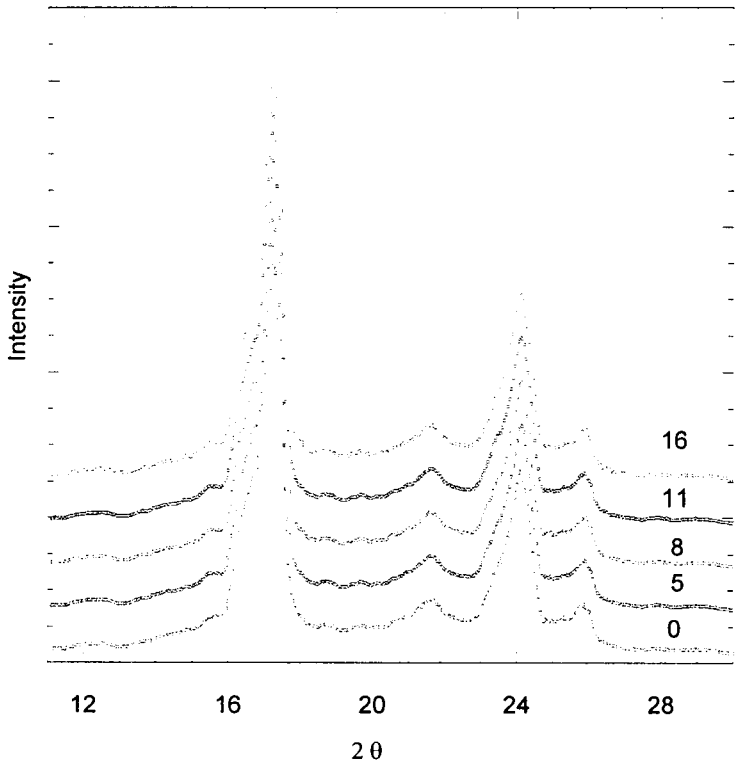

Figure 25. WAXD pattern of 40/20/40 blend (numbers on top of curves indicate dose in Mrad)

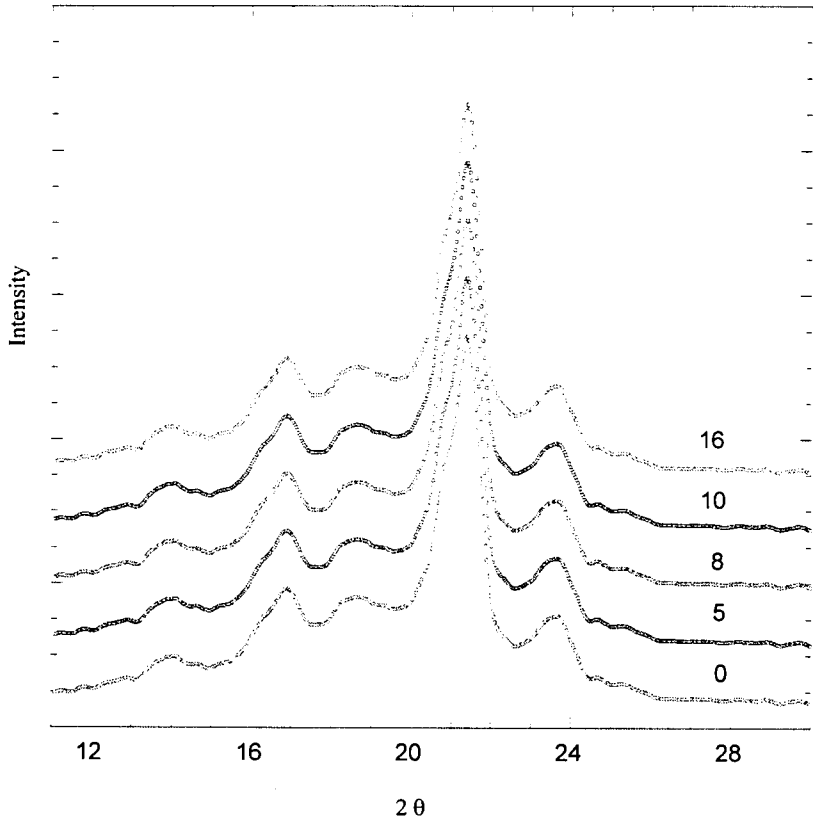

Figure 26. WAXD pattern of 82/9/9 blend (numbers on top of curves indicate dose in Mrad)

occurs in 23.4° to 24° 2Θ is assigned to (200) reflection of orthorhombic unit cell EVA. For some samples, small diffraction peaks are observed at 2Θ = 25° to 25.7°, 2Θ = 13.8°-14.8° and 2Θ = 18.3°-18.5°. Studies by Ray *et al.* (1994) and Datta *et al.* (1996a) on EVA and EVA as a blend component obtained similar results. The (040) reflection is the strongest in 50/50/0, 50/25/25, 40/20/40 blends, while the (110) reflection is the strongest in 82/9/9 blends. The intensity of (200) reflection is stronger than the intensity of (110) in 40/20/40, 50/25/25 and 50/50/0 blends. Thus as the amount of EVA in the blend increases, the intensity of (040) and (200) reflection reduces and the intensity of (110) reflection increases. A change in the orientation of crystallites on blending may be the reason for this behavior.

4.3.1 Crystallinity study

X-ray diffraction scans are analyzed to calculate crystallinity for blend samples. The methods of measuring the degree of crystallinity by x-ray diffraction are based on the principle of total coherent scattering intensity from assemblage of N atoms is independent of their state or aggregation. This is a direct consequence of the law of conservation of energy. If I(s) is the total intensity of coherent x-ray scatter from a specimen at the point S in reciprocal space lattice, the integrals of these intensities over all reciprocal space are

$$\int_0^\infty I(S)\cdot dV = 4\pi \int s^2 \cdot I(s)\cdot dS = Const. \qquad \text{(Eq.16)}$$

where, $|S| = s = 2\sin\theta/\lambda$ is the magnitude of the reciprocal lattice vector S. If the intensity scattered from crystalline phase is Ic and that from the amorphous phase is Ia , then the degree of crystallinity (X_c) is given as

$$X_C = \frac{\int_0^\infty s^2 Ic(s)ds}{\int_0^\infty s^2 I(s)ds} \qquad \text{(Eq.17)}$$

where, I(s) = Ia(s) + Ic(s).

There are a lot of difficulties associated with actual use of this equation to calculate degree of crystallinity. Corrections such as incoherent scattering, Lorentz factor, absorption, number of atoms irradiated, thermal motion, lattice imperfection and air scattering are necessary to calculate the degree of crystallinity. For simplicity, the crystallinity index (which is the degree of crystallinity without making the above mentioned corrections) is calculated for the EVA and PP components and the results are presented in Table 6 and, Figure 27 and Figure 28. The crystallinity indices are obtained by separating peaks for EVA and PP components and assuming that the amorphous region is proportional to weight percent of each component. It can be seen from the table, that there is no drastic change in the crystallinity index with radiation dose. In case of 50/50/0, 50/25/25 and 40/20/40 blends, the crystallinity is almost independent of radiation dose up to 10 Mrad. As the introduction of crosslinks does not drastically affect the crystallinity, there may be possible incorporation of crosslink junctions inside polymer crystal. In case of 82/9/9 blend, crystallinity reaches a peak

Table 6 Crystallinity indices calculated from x-ray diffraction data for blend samples.

Sample ID	Crystallinity index of EVA	Crystallinity index of PP
50/50/0/0	46.66	56.28
50/50/0/5	45.13	55.16
50/50/0/8	43.60	53.91
50/50/0/10	44.90	55.13

Sample ID	Crystallinity index of EVA	Crystallinity index of PP
50/25/25/0	54.03	60.34
50/25/25/8	53.50	56.33
50/25/25/10	52.46	55.61
50/25/25/11	53.07	56.88

Table 6 (continued)

Sample ID	Crystallinity index of EVA	Crystallinity index of PP
40/20/40/0	53.90	62.78
40/20/40/5	52.83	60.10
40/20/40/8	51.38	58.66
40/20/40/11	50.77	58.80
40/20/40/16	43.77	51.18

Sample ID	Crystallinity index of EVA	Crystallinity index of PP
82/9/9/0	39.52	57.78
82/9/9/5	39.62	58.18
82/9/9/8	41.62	60.19
82/9/9/10	35.50	54.54
82/9/9/16	26.58	39.57

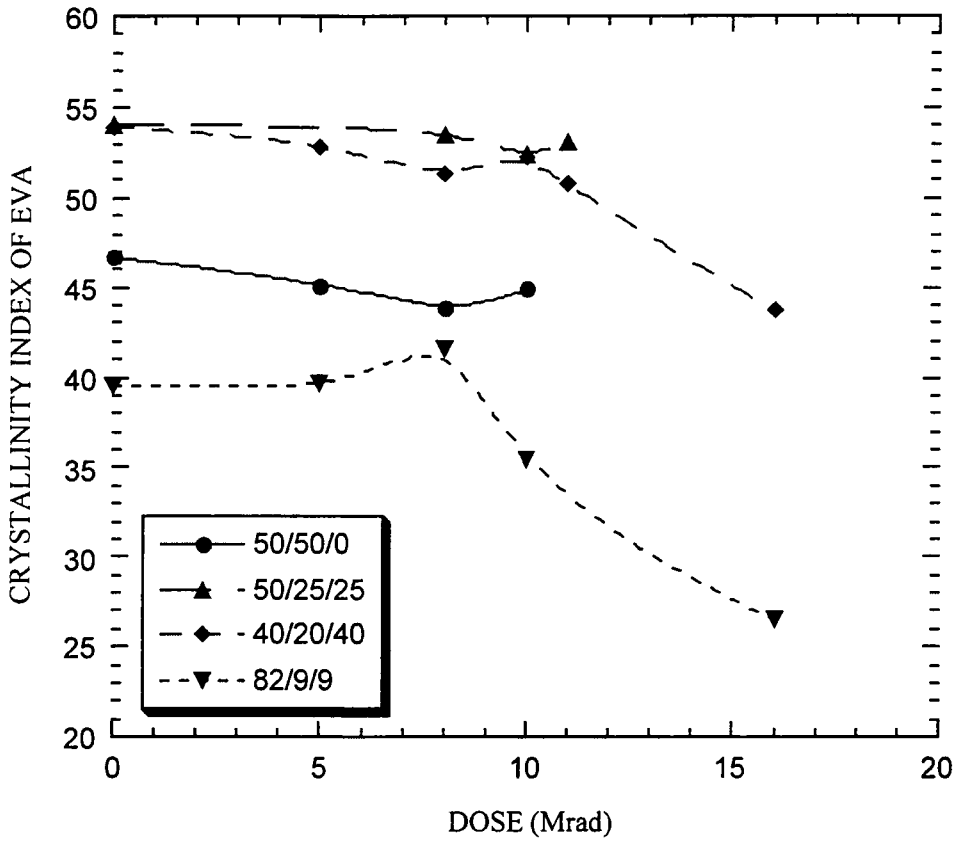

Figure 27. Variation in crystallinity index of EVA component with radiation dose.

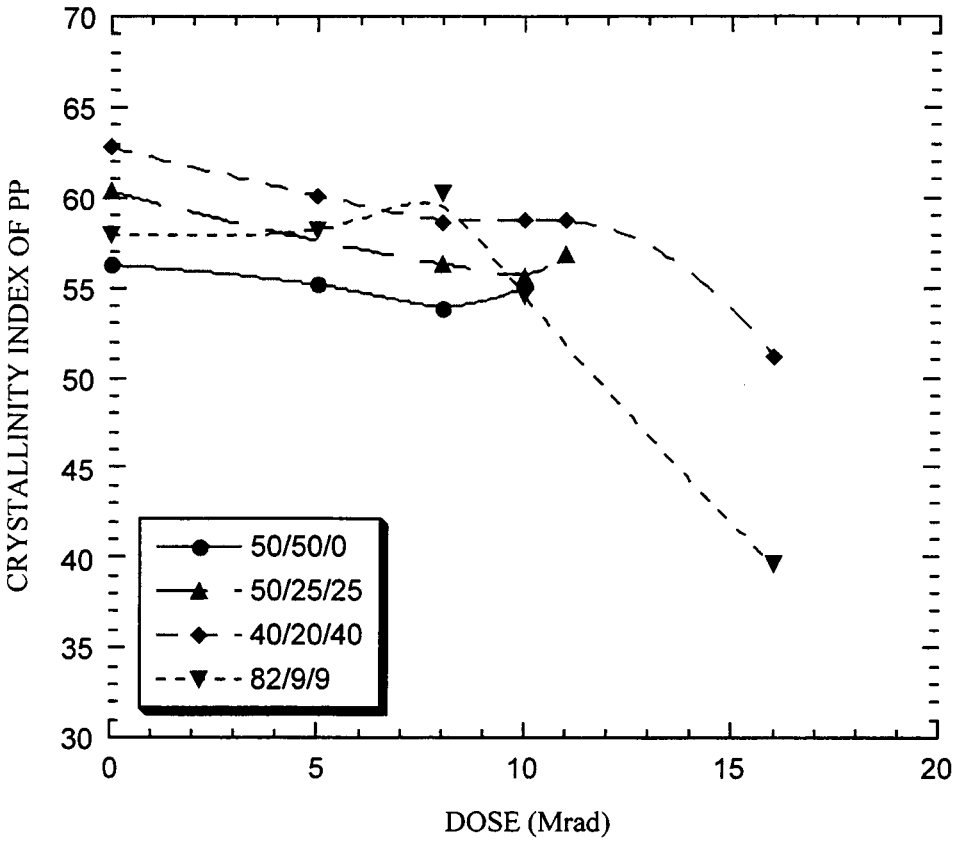

Figure 28. Variation in crystallinity index of PP component with radiation dose.

at 8 Mrad and then decreases. This may be due to the increase intermolecular interaction caused by formation more polar groups with radiation dose as explained by Datta *et al.* (1996a). A significant drop in crystallinity is seen for 82/9/9/16 and 40/20/40/16 samples suggesting high degree of crystal imperfection. There are several studies in literature, which report variation in crystallinity with dose. Krestev *et al.* (1988) reported a significant drop in crystallinity of irradiated iPP only after 50 Mrad. Busfield *et al.* (1981) observed change in crystallinity after 150 Mrad. Other studies on irradiated polyolefins report a drop in crystallinity only at high radiation doses. Another factor contributing to the very small change in crystallinity, is the solid state irradiation. Gielenz et al (1982) found that the crystallinity remained constant for solid state irradiated sample. Thus solid state irradiation and low radiation dose may have contributed to absence of a drastic drop in crystallinity.

4.3.2 Lattice parameter study

Lattice parameters define unit cell of crystals. The calculated lattice parameters for (040), (110) and (200) reflections in PP and EVA are listed in table 7. In the calculations, it is assumed that EVA has an orthorhombic unit cell (same as PE) and the α form of PP retains its monoclinic structure even after irradiation. The calculated lattice parameters for PP are close to the literature value of 20.96 Å for the monoclinic unit cell. The variation in lattice parameters with radiation dose and blend

Table 7 Lattice parameters of blend samples.

Sample ID	b_{PP} (Å)	b_{EVA} (Å)	a_{EVA} (Å)
50/50/0/0	20.6820	5.0423	7.5058
50/50/0/5	21.0312	5.0082	7.5176
50/50/0/8	20.9518	5.1093	7.3938
50/50/0/10	21.0914	5.1339	7.5262

Sample ID	b_{PP} (Å)	b_{EVA} (Å)	a_{EVA} (Å)
50/25/25/0	20.5496	4.9198	7.4272
50/25/25/5	20.9760	5.0832	7.5514
50/25/25/8	21.1812	5.0491	7.5304
50/25/25/10	21.0804	5.0198	7.3388
50/25/25/11	20.8096	5.0196	7.4222

Table 7 (continued)

Sample ID	b_{PP} (Å)	b_{EVA} (Å)	a_{EVA} (Å)
40/20/40/0	20.5936	4.9573	7.3822
40/20/40/5	21.0672	5.0227	7.5366
40/20/40/8	21.0052	4.9536	7.4874
40/20/40/11	21.1460	5.0476	7.5338
40/20/40/16	21.3776	5.0590	7.6924

Sample ID	b_{PP} (Å)	b_{EVA} (Å)	a_{EVA} (Å)
82/9/9/0	21.0512	4.9821	7.4570
82/9/9/5	20.8456	4.9461	7.4676
82/9/9/8	21.1124	5.0518	7.5280
82/9/9/10	21.4404	5.0585	7.5822
82/9/9/16	21.8724	5.1717	7.6992

composition does not follow any particular trend. In case of EVA, the calculated a and b values are close to the literature values of 7.4069Å and 4.9491Å respectively. There is an increase in the lattice parameters for samples irradiated with 16 Mrad. This may be due the imperfections induced by the crosslinks. Various authors have studied the variation in lattice parameters due to crosslinking. Studies by Krestev *et al.* (1988), Datta *et al.* (1996a), Gielenz *et al.*(1982) and Lambert *et al.* (1988) did not observe any drastic crystal distortion at lower radiation doses or peroxide loading. Most other studies dealing with the effect of radiation dose on crystal structure have been carried out for very high radiation doses which are not of commercial interest. Unger (1981) and Keller *et al.* (1983) observed that, at very high radiation doses of the order of 1000 Mrad, the crystal structure is greatly affected by radiation. The effect of radiation on crystal structure may have been extensive if the samples were irradiated in molten form. This suggests that the blending and crosslinking has not affected the crystal structure to an appreciable extent in these samples.

4.3.3 Line broadening study

When a perfect crystal diffracts x-rays, sharp diffraction peaks are produced according to Bragg's law. As imperfections increase in a crystal, the diffraction peaks are broadened. Broadening is a feature of diffraction pattern when the size of diffracting crystals is less than 1000 Ă. Broadening may be caused by crystal size, micro-strains, thermal vibrations etc. Either breadth of a diffraction peak at half the

height of the peak or integral breadth of a diffraction peak is used to measure the broadening. The integral breadth of a diffraction peak was calculated using the following formula

Peak half width (β) = area of the peak / height of the peak (Eq.18)

The line broadening was calculated for two crystalline peaks corresponding to (110) reflection in EVA and (040) reflection in PP. The results are tabulated in Table 8. No appreciable effect of blend composition or radiation dose is observed on line broadening although samples irradiated with 16 Mrad show more broadening as compared to other samples. This indicates no large-scale destruction of crystal lattice with radiation dose. Datta *et al.* (1996a) also reported similar behavior for irradiated EVA.

4.4 Dynamic mechanical analysis

Dynamic mechanical analysis was used for detecting various relaxation processes in blends. The dynamic storage modulus (E'), loss modulus (E'') and tan δ are calculated from the dynamic mechanical measurements. The most reliable estimates of relaxation are normally obtained from the loss modulus peak observed in DMA. The ASTM D4065 standard asserts that the temperature of the maximum loss modulus is the appropriate standard value. Thus variation in loss modulus with

Table 8 Line broadening data for blend samples.

Sample ID	Half Width$_{(040)}$	$\beta_{(040)}$	Half Width$_{(110)}$	$\beta_{(110)}$
50/50/0/0	0.3645	0.154	0.393	0.181
50/50/0/5	0.4595	0.176	0.367	0.2104
50/50/0/8	0.422	0.203	0.4265	0.200
50/50/0/10	0.4165	0.185	0.452	0.213

Sample ID	Half Width$_{(040)}$	$\beta_{(040)}$	Half Width$_{(110)}$	$\beta_{(110)}$
50/25/25/0	0.441	0.181	0.392	0.192
50/25/25/5	0.413	0.145	0.502	0.187
50/25/25/8	0.334	0.144	0.474	0.171
50/25/25/10	0.423	0.199	0.372	0.207
50/25/25/11	0.310	0.127	0.551	0.156

Table 8 (continued)

Sample ID	Half Width$_{(040)}$	$\beta_{(040)}$	Half Width$_{(110)}$	$\beta_{(110)}$
40/20/40/0	0.358	0.160	0.421	0.200
40/20/40/5	0.363	0.206	0.376	0.205
40/20/40/8	0.331	0.167	0.480	0.214
40/20/40/11	0.372	0.120	0.377	0.154
40/20/40/16	0.49	0.173	0.572	0.228

Sample ID	Half Width$_{(040)}$	$\beta_{(040)}$	Half Width$_{(110)}$	$\beta_{(110)}$
82/9/9/0	0.34	0.160	0.50	0.197
82/9/9/5	0.25	0.155	0.34	0.166
82/9/9/8	0.41	0.167	0.43	0.185
82/9/9/10	0.37	0.155	0.37	0.161
82/9/9/16	0.58	0.213	0.55	0.195

temperature may give an idea about transitions, relaxation processes, structural heterogeneity and the morphology of polymer blend systems. The nomenclature used to identify relaxation peaks is shown in Figure 29. Before analyzing results, it is worth considering an instrumental factor that may contribute to erroneous measurements. As the sample thermocouple is not in direct contact with the sample, it is actually measuring the temperature in side the oven in which the sample is placed. The actual sample temperature is a function of various factors such as thermal conductivity, mass of the sample, heating rate and uniformity of oven environment. Thus an inadvertent change in thermocouple position may affect the peak position temperature.

The variation in loss modulus, storage modulus and tan δ are shown in Figure 30 to Figure 41. The storage modulus curve for all the samples indicates a high material stiffness at very low temperatures. This high modulus value is in the range of 2-5 x 10^9 dynes/cm^2 for all the samples. There is no appreciable effect of radiation dose or blend composition on the low temperature modulus. In all the samples, a slight drop in E' is observed in –30°C to 10°C range. This may be attributed to the relaxation processes taking place in EVA and PP components. The presence of crystalline material and crosslinks may be resulting in the inconspicuous drop in E' in the relaxation temperature range of the polymers. Above the transition temperatures, a continuous but inconspicuous decrease in E' is observed for all the samples. A

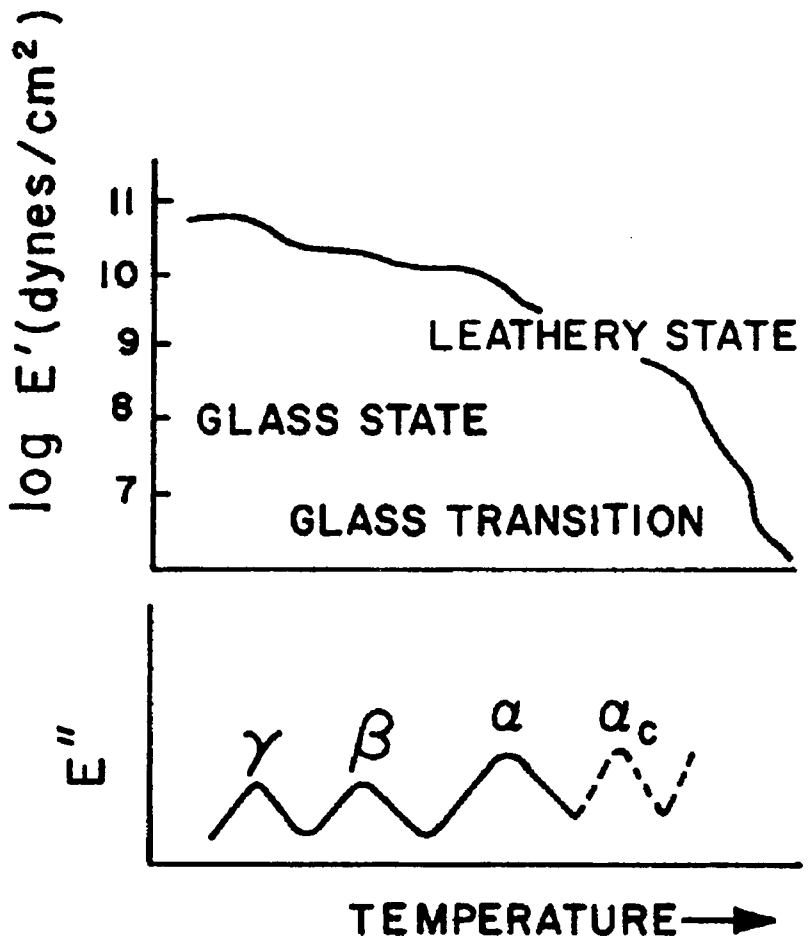

Figure 29. Typical dynamic mechanical properties of crystalline polymers

(Murayama 1978)

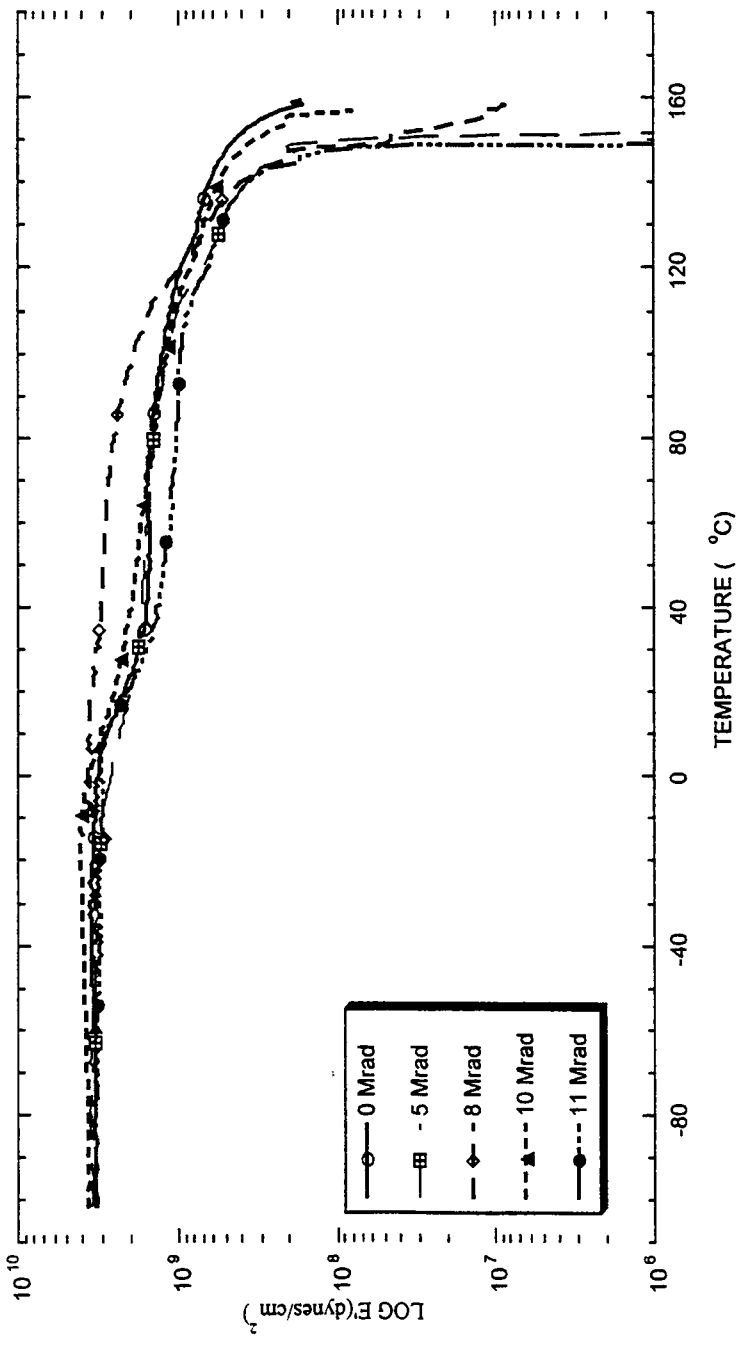

Figure 30.Storage Modulus for 50/50/0 Blend

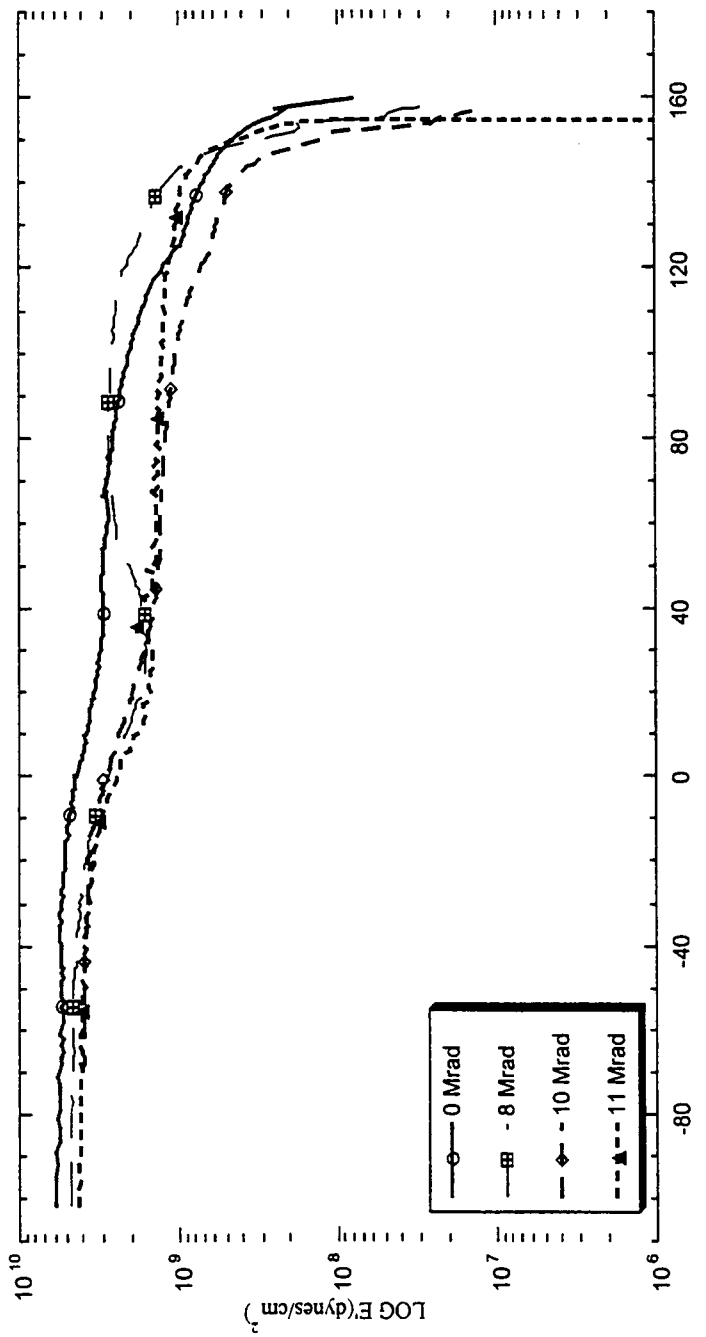

Figure 31.Storage Modulus for 50/25/25 Blend

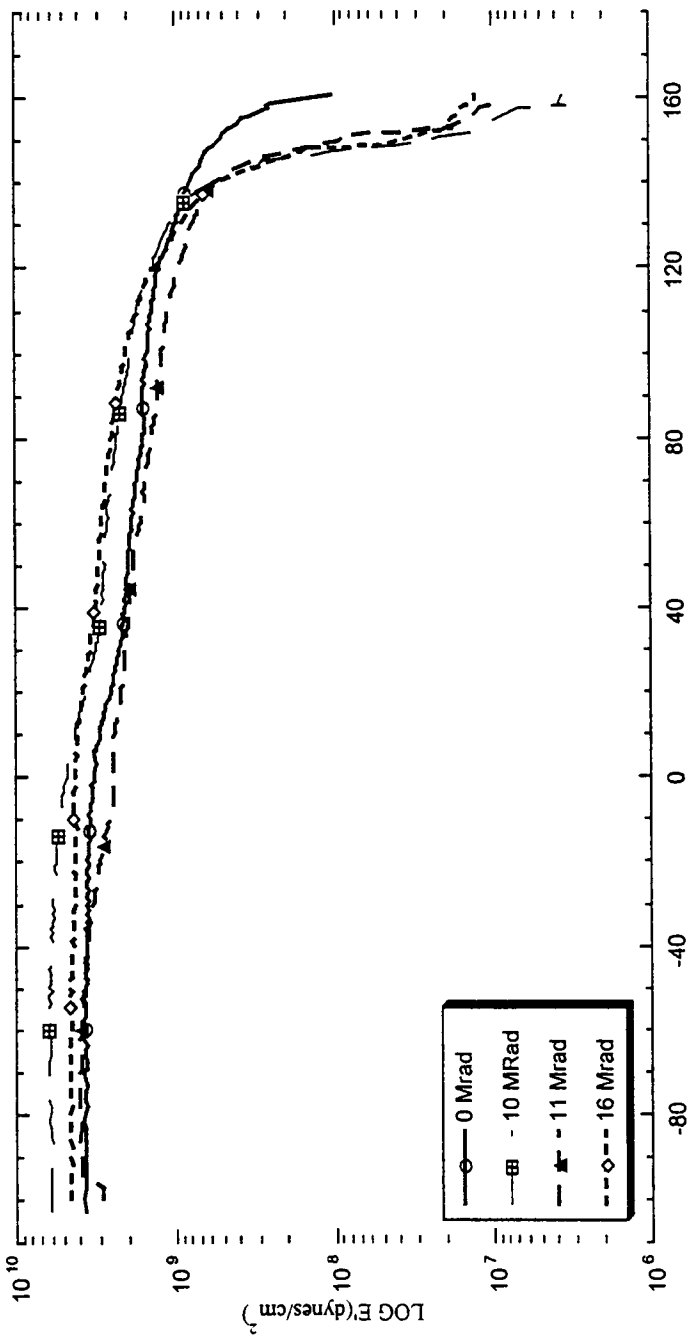

Figure 32.Storage Modulus for 40/20/40 Blend

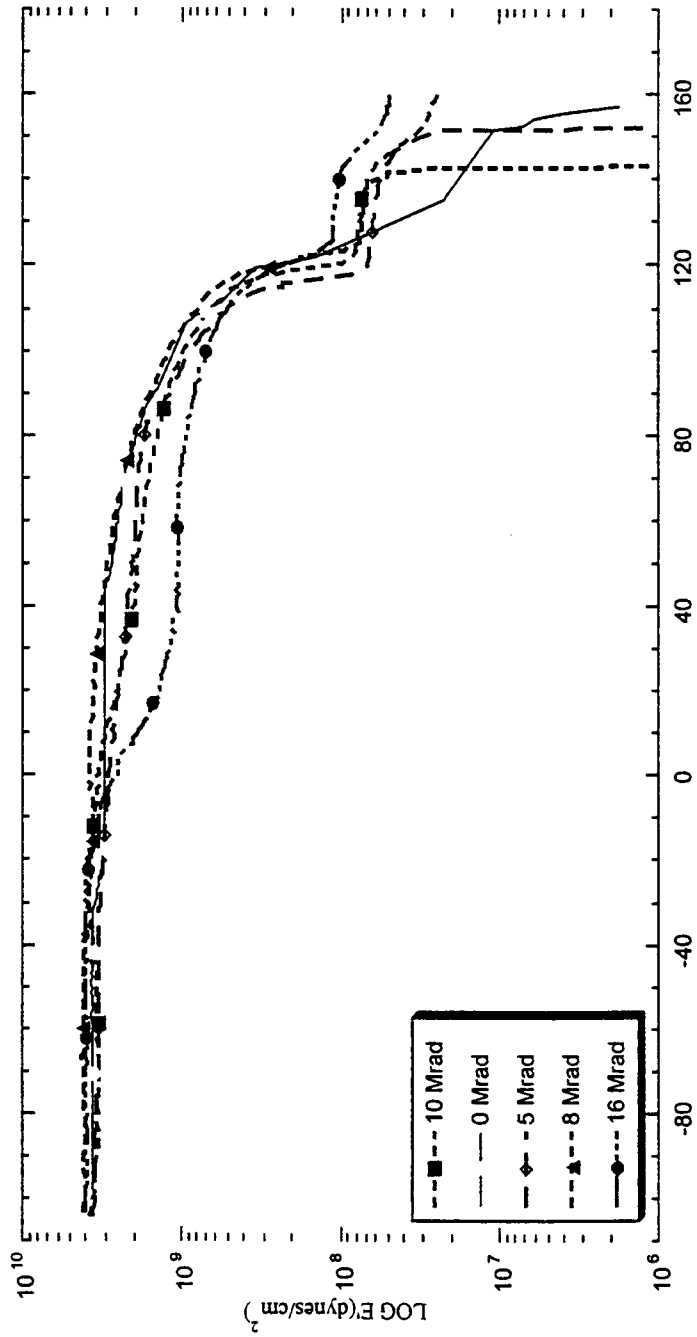

Figure 33. Storage Modulus for 82/9/9 Blend

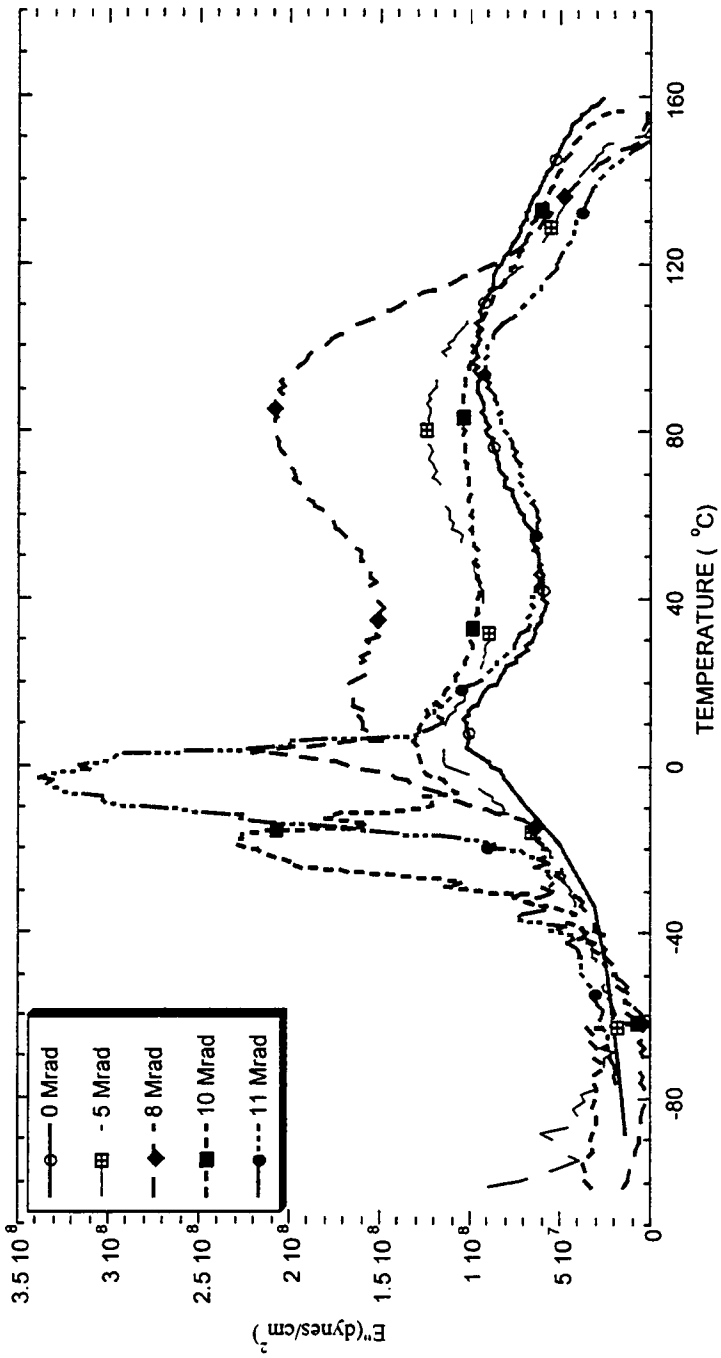

Figure 34. Loss Modulus for 50/50/0 Blend

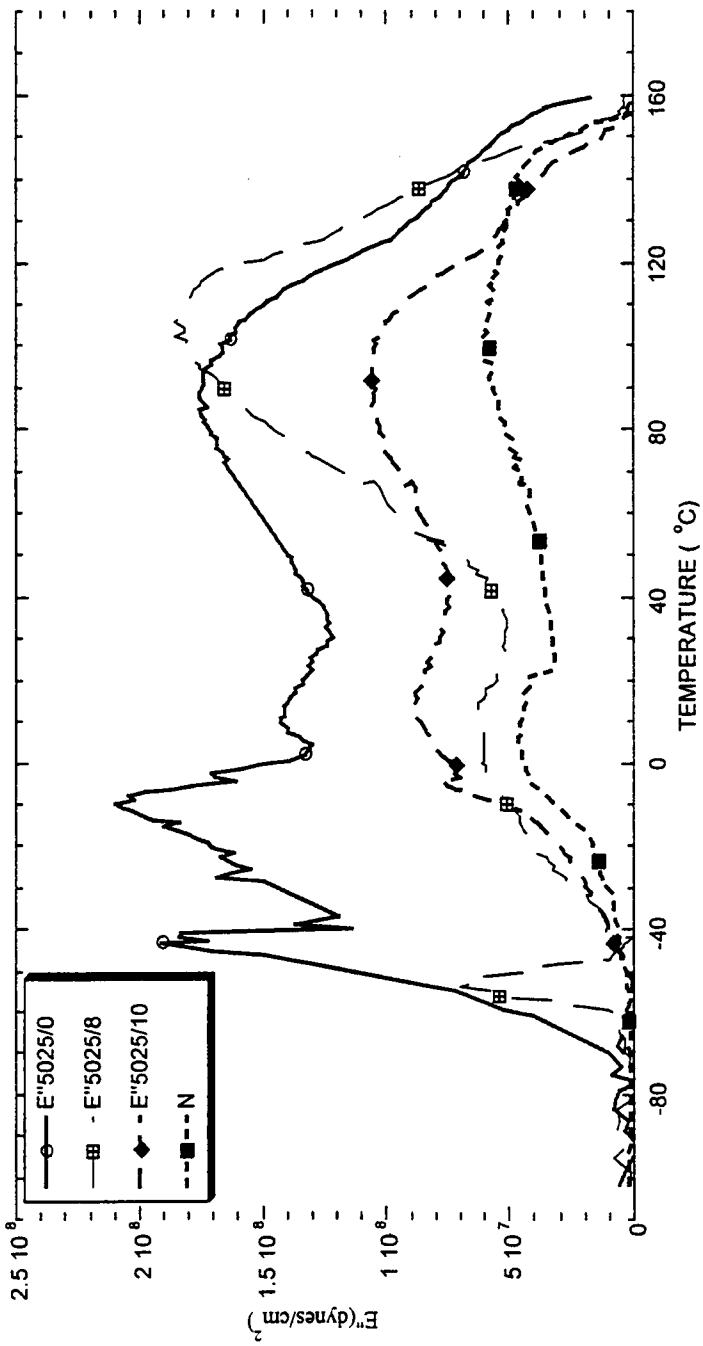

Figure 35. Loss Modulus for 50/25/25 Blend

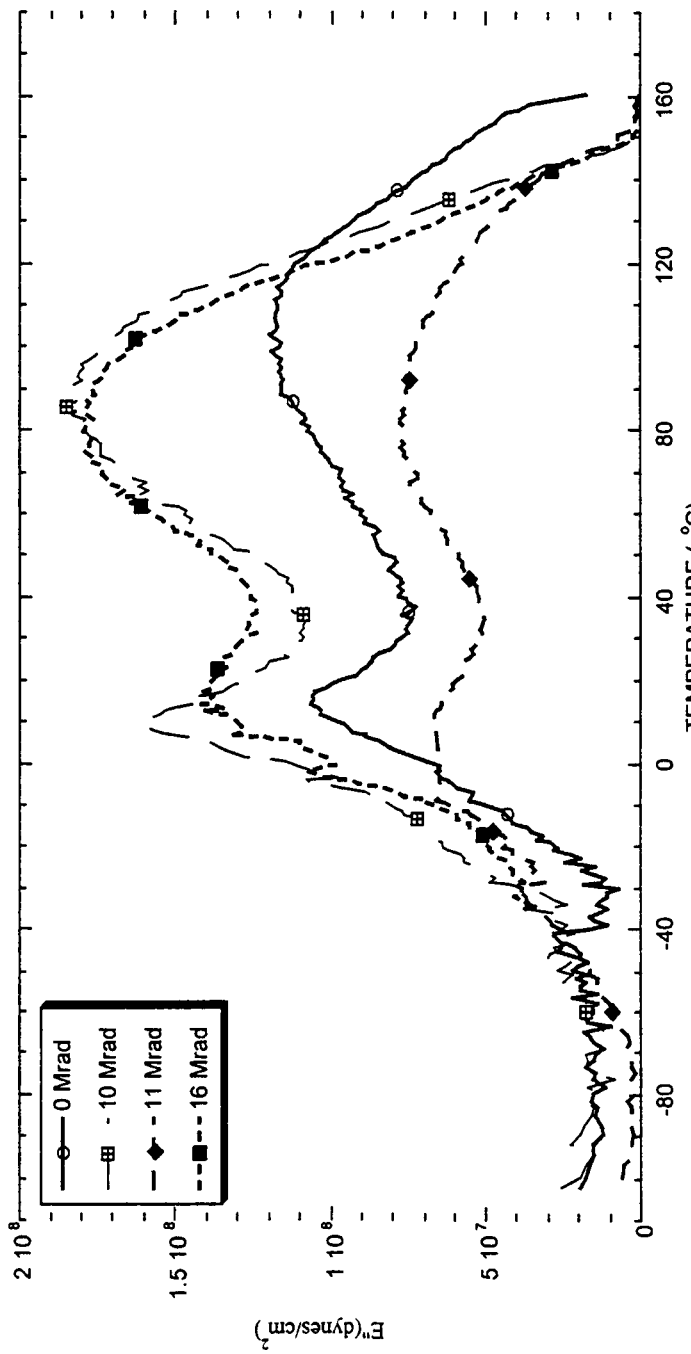

Figure 36. Loss Modulus for 40/20/40 Blend

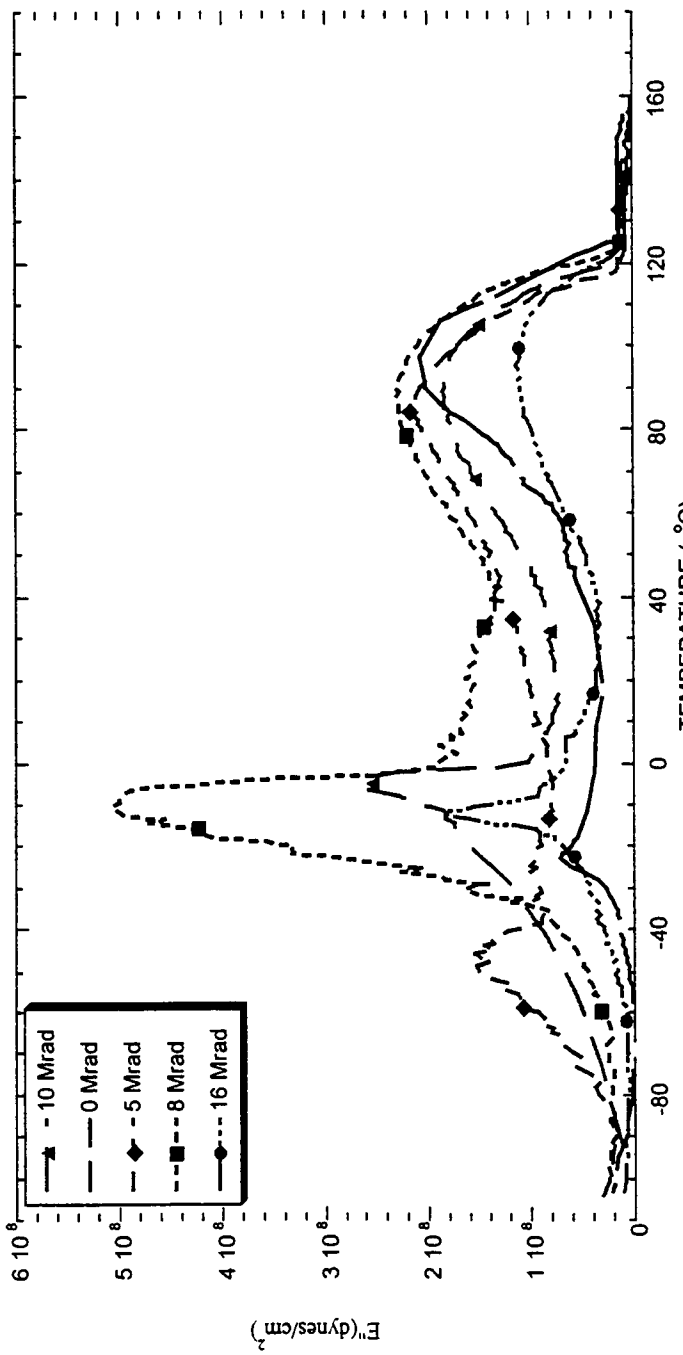

Figure 37. Loss Modulus for 82/9/9 Blend

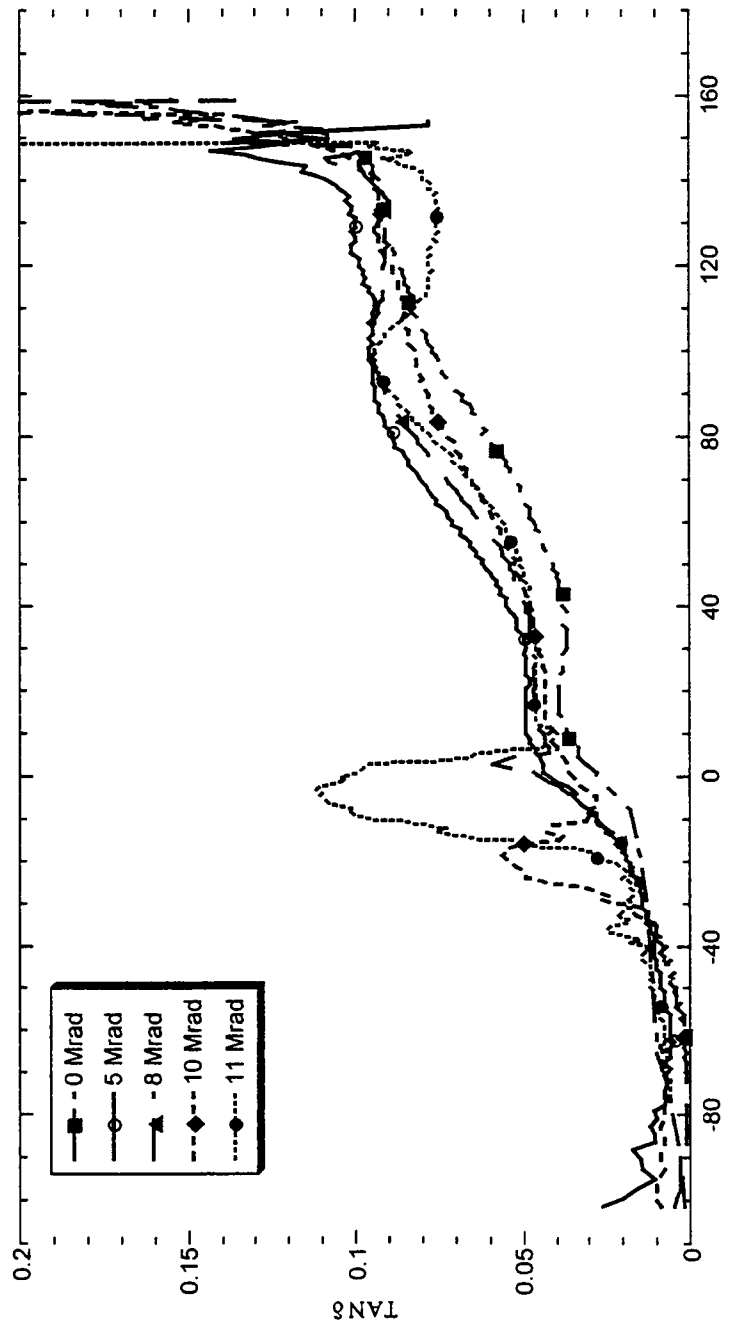

Figure 38. Tan δ for 50/50/0 Blend

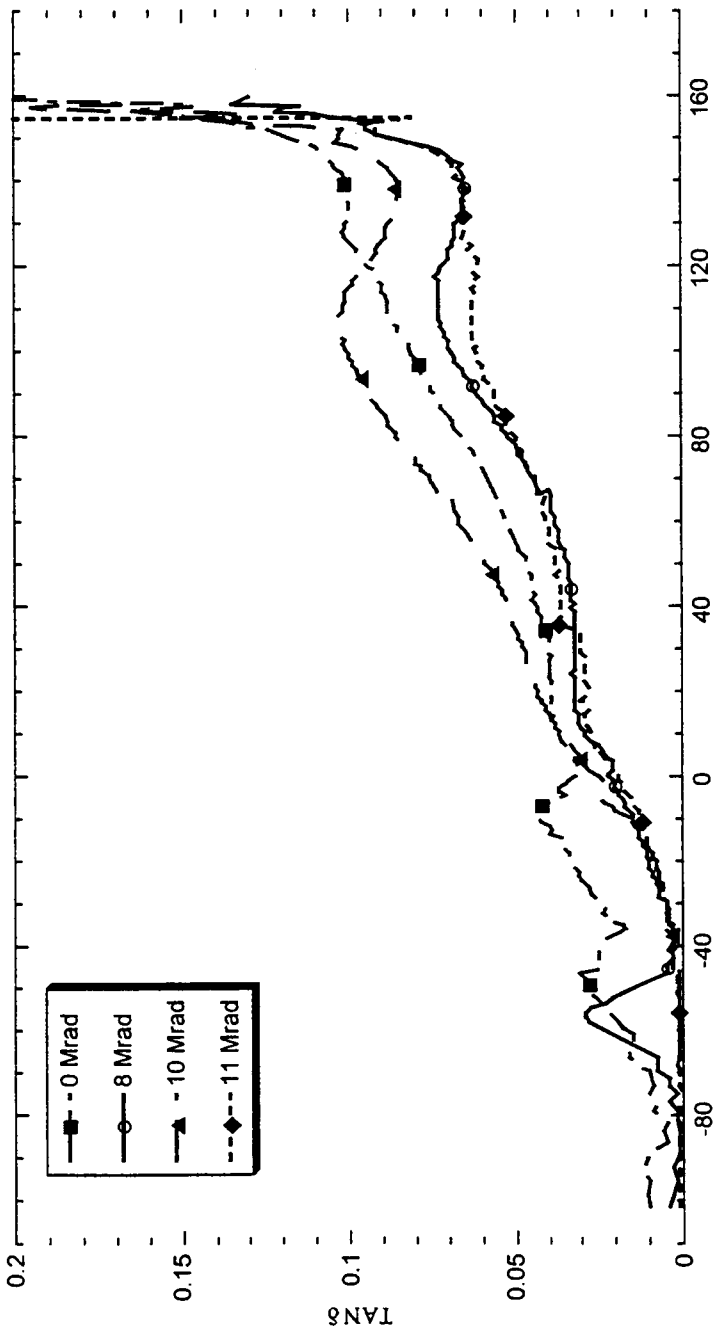

Figure 39. Tan δ for 50/25/25 Blend

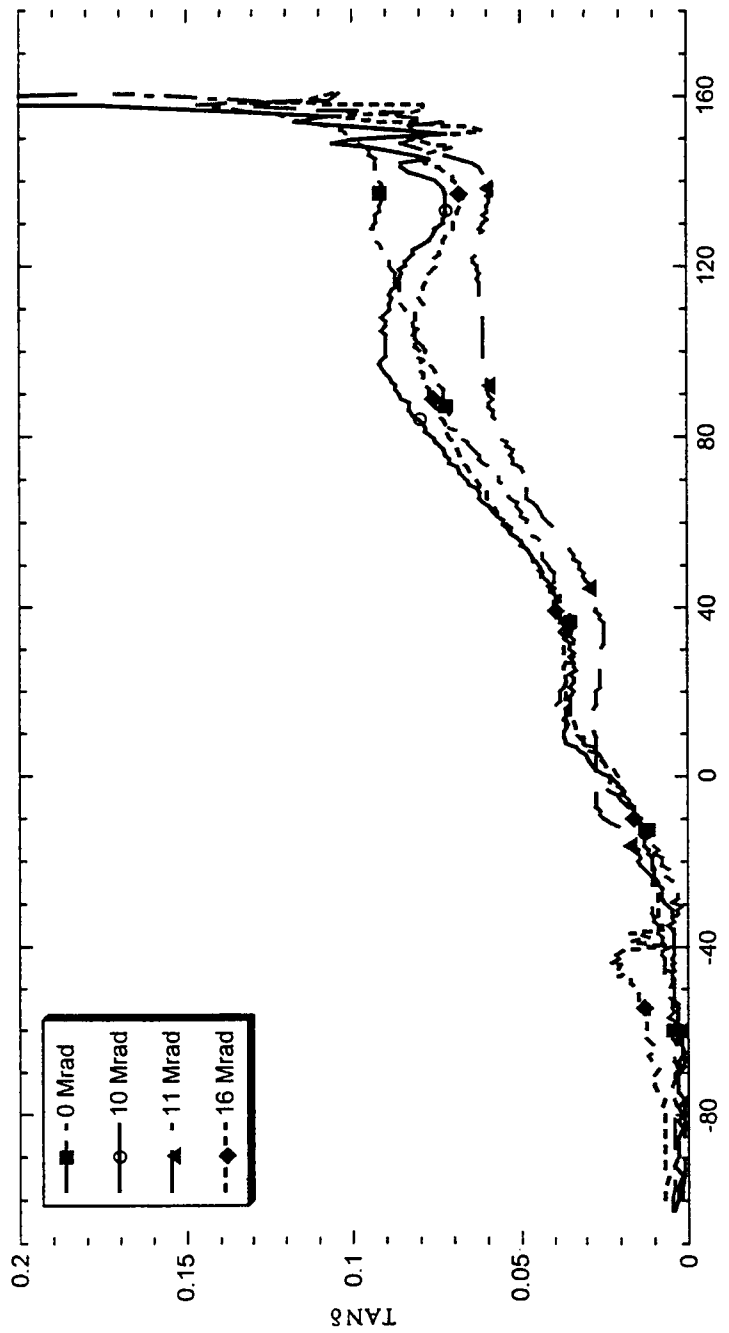

Figure 40. Tan δ for 40/20/40 Blend

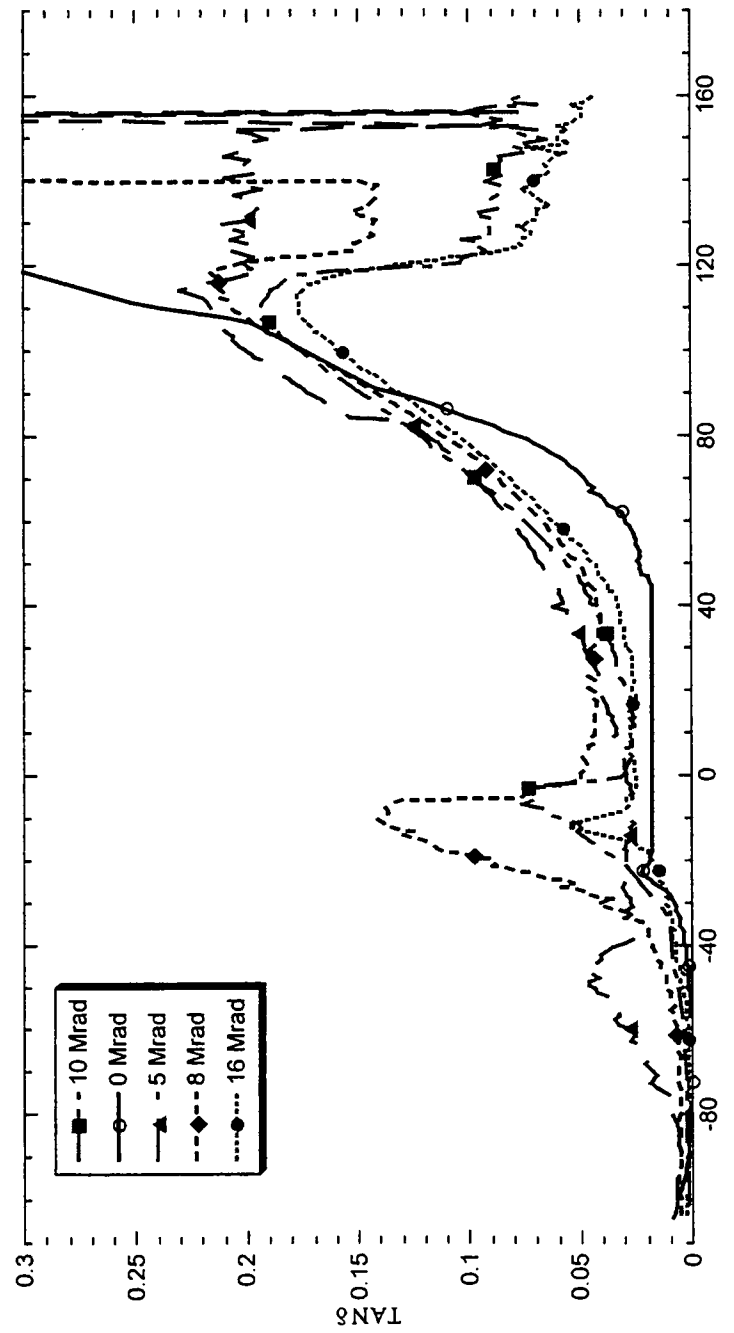

Figure 41. Tan δ for 82/9/9 Blend

significant drop in E' is observed as the melting of crystallites start. In case of 82/9/9 samples, moderate drop in E' is observed near 115°C and 140°C-155°C.

In case of 82/9/9/10 and 82/9/9/16 samples, a plateau in E' is seen at high temperatures after the two step drop in 110°C to 140°C range. A slight drop near 120°C followed by a drastic drop in the vicinity of 145°C is observed for 50/25/25 40/20/40 and 50/50/0 samples. No prominent effect of radiation dose on the high temperature modulus is seen in case of these samples. This is supported by a study on dynamically crosslinked EVA-PP blends by Thomas *et al.* (1989, 1992). Dynamically crosslinked sample showed a higher E' for blends containing higher amounts of EVA. For blends containing ≥50% PP, crosslinked samples exhibited lower modulus. They attributed this behavior to predominant crosslinking behavior of EVA and chain scissioning behavior of PP. A noticeable higher storage modulus is observed for 50/50/0/8, 50/25/25/8 and 40/20/40/8 samples.

In 50/50/0/0 sample, loss peaks are observed at –55°C and 10°C. In case of 50/50/0/10 and 50/50/0/11 samples, strong peaks are observed at -18°C and –4°C respectively. These may be the glass transition peaks of EVA. In all 50/50/0 samples, glass transition peak of polypropylene lie in 0°C to 10°C range. None of the 82/9/9 samples shows any peak that may be attributed to T_g of PP. Peaks observed in these samples may be attributed to relaxations in EVA. Most of the 50/25/25 and 40/20/40 samples show a relaxation peak in the vicinity of –50°C. The glass transition peak of polypropylene is observed in 5°C to 12°C range. A large peak is seen in all the

samples near the melting temperature of polymers. The position of this peak changes with radiation dose. This peak exhibited maximum intensity for samples irradiated with 8 Mrad dose. The differences in dynamic mechanical responses of samples may be attributed to crystallinity, perfection of crystallites, phase distribution, crosslinking and blend composition.

5 Discussion

5.1 Extraction study

In irradiated polymers, along with the usual radiation-induced chemical and physical events, two very important events take place. Because of the large number of monomer units composing the polymers, these events (namely scission of the polymer backbone and crosslinking of two or more polymer molecules) have great importance for the physical properties of polymers. It is generally accepted that during radiation, both scission and crosslinking events take place simultaneously. The predominance of one of these events depends on polymer chain structure, temperature, crystallinity and irradiation conditions. If scission dominates, then degradation of physical properties occurs. If crosslinking predominates, a three dimensional insoluble network called gel, forms at high doses. It is very important to know which event is dominating in a polymer and Charlesby-Pinner equation (Charlesby *et al.* 1959, Dawes *et al.* 1996) is widely used to determine this. The equation is written as

$$S + S^{1/2} = \frac{G(S)}{2 \cdot G(X)} + \frac{9.6 \times 10^6}{2 \cdot G(X) \cdot D \cdot M_n} \qquad \text{(Eq.19)}$$

where S is the sol fraction, D is the radiation dose, M_n is the molecular weight before irradiation, G (S) is the number of scissions occurred and G (X) is the number of crosslinks formed per 100eV of energy absorbed by the polymer. This equation permits the calculation of crosslinking efficiency from the slope of a plot of $S+S^{1/2}$

verses 1/D and the value of G (S)/ G (X) from the intercept at 1/D equal to zero. This equation is based on the assumptions that the polymer has the most probable molecular weight distribution before irradiation, crosslinking occurs by H-link mechanism, crosslinking and scission occur with random spatial distribution in the polymer without any clustering (Charlesby 1960, Dawes *et al.* 1996).

The Charlesby-Pinner plot for the blend samples is shown in Figure 42 and the crosslinking efficiency and G (S)/ G (X) for the blends are presented in Table 9. It can be determined from the value of G (S)/ G (X), whether a polymer is of crosslinking type or chain scission type. Polyethylene is known to be a polymer of crosslinking type with G (S)/ G (X) in 0.20 - 0.24 range (Charlesby *et al.* 1959). Polypropylene is known to be a polymer of chain scission type with G (S)/ G (X) ranging from 0.7 - 4 depending on tacticity and crystallinity (Charlesby *et al.* 1959, McGinniss 1986). EVA has shown predominantly crosslinking tendencies, hence it is considered as a polymer of crosslinking type in majority of studies (Datta *et al.* 1996a, Thomas *et al.* 1987 and Minkova *et al.* 1989). Although Matsui *et al.* (1992) has concluded that EVA is a polymer of chain scission type. From Table 9, it is seen that G (S)/ G (X) ratio is maximum in case of 40/20/40 blends and minimum in case of 82/9/9 blend As the amount of EVA increases, G (S)/G (X) ratio decreases and for 82/9/9 blend it approaches G (S)/ G (X) of polyethylene. This shows that EVA is a polymer of crosslinking type and PP is a polymer of chain scission type in the dose range considered. A theoretical examination suggests that hydrogens on tertiary

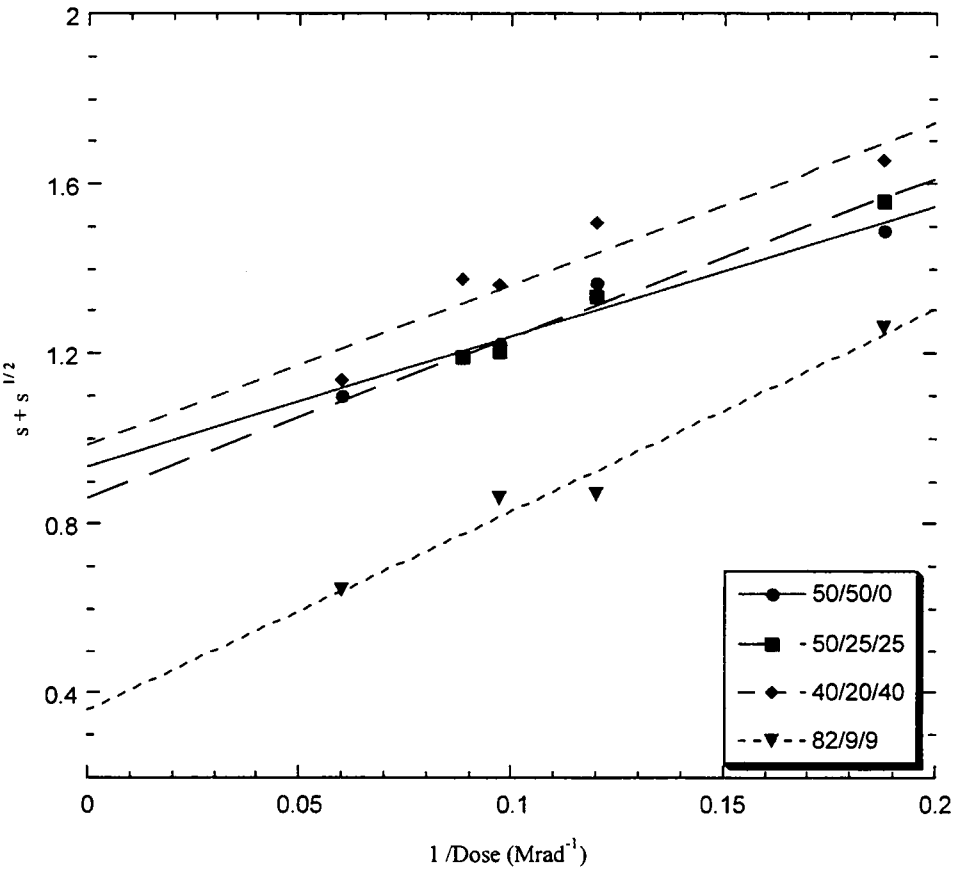

Figure 42. Charlesby-Pinner plot for the blend samples.

Table 9 Crosslinking efficiency and G (S)/ G (X) ratio for blend compositions.

Blend Composition	Crosslinking Efficiency	G(S)/ 2G(X)
50/50/0	2.996	0.943
50/25/25	3.761	0.860
40/20/40	3.817	0.986
82/9/9	4.716	0.361

carbons are much more reactive than hydrogens on primary carbons (Harpell *et al.* 1973). Another factor affecting the reactivity of radicals is the steric factor. As crosslinking is a bimolecular reaction while chain scission is an unimolecular reaction, the steric factor is much more important in case of crosslinking than in case of chain scission reaction. In case of primary carbon radicals, the steric factor favors coupling while in case of tertiary macroradicals, steric constraints lead to chain scission (Baldwin *et al.* 1972). As EVA is a copolymer of ethylene and vinyl acetate and the main chain being predominantly made of ethylene (primary carbon) steric factor favors crosslinking reaction, while in PP scission reaction is favored as the main chain is made of terttiary carbons. On this basis, the increase in scission probability with increasing PP content in the blends can be explained. The incorporation of ethylene in PPC should make it more prone to crosslinking, the scission to crosslinking ratio in case of 50/25/25 supports this hypothesis. The

50/25/25 blend has the same EVA content as 50/50/0 blend, but due to the incorporation of the copolymer it shows lower G (S)/ G (X) than 50/50/0. The incorporation of copolymer does not increase crosslinking in 40/20/40 sample. The higher proportion of PP component in this blend may be suppressing the crosslinking in EVA resulting in an overall lower gel fraction. It is possible that higher ratio is obtained due to higher scission tendency rather than lower crosslinking tendency. As the difference in G (S)/ G (X) values is very small, the assumption of linearity in plotting the data and experimental error in sol fraction measurements may also be responsible for this behavior. The crosslinking efficiency shows an interesting trend. As expected, 82/9/9 blend has the highest efficiency value but 40/20/40 blend shows higher efficiency value than 50/50/0 and 50/25/25 blends. The prominence of chain scission reaction in this blend may be offsetting the crosslinking efficiency.

5.2 Crystal Structure

The effect of radiation-induced crosslinking and chain scission reaction on the crystal structure of the blend components has been investigated with WAXD.

5.2.1 Crystallinity

The crystallinity indices obtained for EVA and PP components were presented in Table 6. It can be seen from the table that the crystallinity is almost unaffected by radiation dose up to 10 Mrad and the level of crystallinity is also high. It is possible

that in this dose range, a balance prevails between factors which may lead to increase in crystallinity such as reduction in molecular weight by scission reaction and factors, which may lead to reduction in crystallinity such as build-up of carbonyl and other impurity groups. Therefore, the introduction of crosslinks has not drastically lowered the crystallinity of the system. This also suggests that the crosslinks may have been incorporated in the crystals of EVA and PP and the crystal structure is only slightly distorted. The shape of melting endotherms obtained in the melting studies support this hypothesis. At higher radiation doses (≥ 11Mrad), a significant drop in crystallinity is seen. The loss of crystallinity indicates less perfect crystallites with increasingly distorted unit cell as seen from the lattice parameter studies. The melting studies indicate similar behavior. The melting peaks are broad and melting occurs at strikingly lower temperatures. The crosslinks are most probably excluded from the crystals of EVA and PP.

The incorporation of defects (crosslinks, comonomer) in crystals has been considered in the work by Sanchez and Eby (1973, 1975). Later, Lambert *et al.* (1994), on the basis of small angle x-ray scattering (SAXS) studies on crosslinked polyethylene showed that, it is possible to have incorporation of crosslinks in the crystal. They reported an increase in lamellar thickness with increasing defect content in lightly crosslinked samples. The defect content was calculated by taking reciprocal of chain length between crosslink junctions. In heavily crosslinked samples, they found a reduction in lamellar thickness with increasing defect content. They hypothesized a

solubility limit for the incorporation of crosslinks in the crystal. When the defect content was ≤ 0.2%, the crosslinks were incorporated in the crystal otherwise excluded from the crystal. In the present study, the defect content in samples with high gel fractions (82/9/9/10 and 82/9/9/16) has been calculated from DMA data. As gel fraction is an indication of the amount of crosslinks present, the defect content in these samples can be considered as the upper limits of defect content. The upper limits calculated from DMA data are 0.7% (for 82/9/9/10 sample) and 1.4% (for 82/9/9/16 sample). Thus, in samples with lower gel fractions the defect content must be low enough to satisfy the solubility limit. In these samples, crosslinks may be incorporated in the crystals with little distortion of the unit cell. In highly crosslinked samples, the defect content is above the solubility limit for incorporation of crosslinks in the crystal. The crosslinks may be excluded from the crystal, which may distort the crystal resulting in strikingly lower melting temperatures and broad melting peaks.

5.2.2 Crystal Perfection

The lattice parameter calculations show the absence of large-scale crystal distortion in samples irradiated with low radiation doses. A noticeable change in the lattice parameters is observed in case of samples irradiated with high radiation doses. The crystallinity index obtained for these samples is also significantly lower than the other samples. Therefore the most prominent crystal distortion must be occurring at high radiation doses in these samples. The melting studies also support this opinion. It is

speculated that for samples irradiated with low radiation doses, the crosslink density is not high enough to cause crystal distortion. As the crosslink density exceeds a critical value at high doses, the exclusion of crosslinks from the crystal affects crystal structure which is reflected in the lattice parameter calculations.

Line broadening data corroborates lattice parameter calculations. In low dose range, there is not appreciable increase in the half width of crystalline peaks but broadening is noticeable at high doses.

5.3 THERMAL BEHAVIOR

5.3.1 Melting behavior

The DSC thermograms show much greater effect of radiation on the samples than the x-ray diffraction study and dynamic mechanical analysis. The melting scans of blend samples are presented in Figure 11 to Figure 14. Two melting peaks are seen for the blends. The existence of two melting peaks eliminates the possibility of the intermiscibility of the crystalline phase of EVA and PP. Even if the polymers are intimately mixed in the melt, as the blends are cooled down from the melt, the crystallization of different component occurs separately leading to distinctly different crystalline phases.

All samples show a decrease in melting point with radiation dose. The decrease in melting point is seen in both EVA and PP components. The drop in the melting

temperature is more prominent in case of samples irradiated with high radiation doses. In case of 82/9/9 samples the melting temperature of EVA drops initially with dose, then remains almost constant while the melting temperature of PP drops continuously with dose. The lowering of melting temperatures may be due to formation of imperfect crystals formed by radiation-induced chain scission and crosslinking reactions. But the sharp natures of EVA melting peaks suggest absence of large-scale crystal distortion due to crosslinking at low doses. This interpretation is supported by WAXD data that shows high crystallinity indices and almost unchanged lattice parameters and line broadening. This lowering of melting point may be explained by two approaches.

The first approach (Kusy et al. 1971 and Minkova et al. 1989) is based on the thermodynamic parameters affected by electron-beam radiation. For a polymer, the melting temperature depends on the Gibb's free energy of the amorphous phase and the crystalline phase. Melting occurs when the Gibb's free energy of the amorphous phase (G_a) equals the Gibb's free energy of the crystalline phase (G_c). The crosslinking reaction mainly taking place in the amorphous phase decreases the Gibb's free energy of the amorphous phase. This results in decrease in the melting temperature as shown schematically in Figure 43. Hence, the lowering of melting temperature with radiation dose may be attributed to lowering of G_a.

The second approach considers that during heating in DSC, crystallites undergo continuous reorganization until they reach a maximum degree of perfection (Kamide

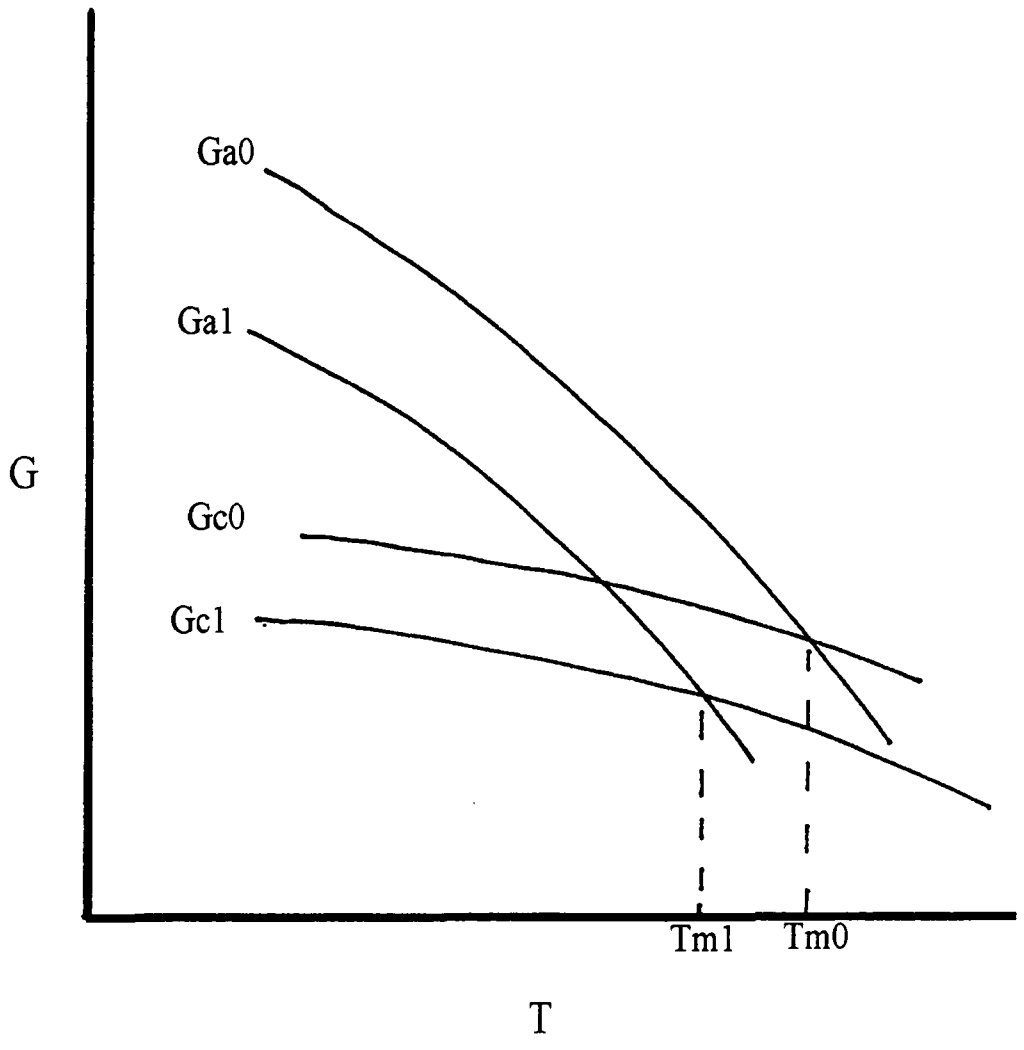

Figure 43. Effect of crosslinking on Gibb's energy. (Minkova *et al.* 1989)

Tm0 is the melting temperature of unirradiated polymer, Tm1 is the melting temperature of irradiated polymer, Gc0 is the free energy of unirradiated crystalline phase, Gc1 is the free energy of irradiated crystalline phase, Ga0 is the free energy of unirradiated amorphous phase and Ga1 is the free energy of irradiated amorphous phase.

et al. 1972) and the actual melting point is only slightly above the crystallization temperature. The maximum degree of perfection is controlled by structural factors such as chain ends, crosslinks, branch points, molecular weight and to a certain extent by kinetic factors such as polymer mobility and heating rate. It is this reorganized structure that determines the observed melting temperature in DSC scan. Due to radiation-induced reactions, crosslinks and chemical impurities are produced in the polymer, which reduces the degree of perfection relative to the unirradiated samples and a drop in melting temperature is obtained.

The drop in melting temperature depends upon blend composition for samples irradiated with same radiation dose. In case of 50/50/0, 40/20/40 and 50/25/25 samples, higher amounts of PP may be causing more destruction of EVA crystals over a period of time resulting in profound reduction in melting temperature. This is possible as the free radicals produced in PP have particularly long life times. Changes in properties of irradiated PP were observed even 6 months after irradiation (Wiesner 1991). In case of 82/9/9 blend samples, as a high gel fraction is obtained at a lower dose, the effect of dose on Ga and Gc at higher doses is less significant. Also the presence of PP in small amount and ability of sol fraction to influence the crystallization of unextracted material (Lambert 1988) may be resulting in higher melting temperatures.

With increase in radiation dose, multiple melting peaks are observed in EVA and PP components. There are numerous reports of the occurrence of double endotherms

during DSC experiments on polymers. The double melting peaks have been attributed to various possibilities such as presence of different crystal structure and/or morphologies (Kamide *et al.* 1972 and Shi *et al.* 1993), crystal transformation during heating (Rybnikar 1991 and O'Kane *et al.* 1994), reorganization during heating (Guerra *et al.* 1984, Janimak *et al.* 1992 and Rabello *et al.* 1997) and segregation of molecules with low molecular weight or with irregularities that form crystals with lower T_m (Duvall *et al.* 1994 and Cox *et al.* 1967). In the present study, it is speculated that the double melting peaks may be due to either melting of crystals with different melting points or reorganization during heating. In an attempt to explain the reason for the double melting peaks, an experiment was conducted. The experiment involved melting of a sample (which exhibited multiple melting) in DSC at heating rates of 5°C/min, 10°C/min and 20°C/min. At lower heating rates, there is sufficient time for reorganization to occur while reorganization is difficult at higher rates. If multiple melting is due to the reorganization during heating, then single peak should be obtained at higher heating rate and if it is due to melting of crystals with different melting points, then multiple peaks should persist at higher rate. The thermograms obtained during the experiment are shown in Figure 44. In case of PP component, multiple melting disappears at higher heating rate but in case of EVA, multiple peaks are seen even at higher heating rate. This suggests that multiple melting in PP results from reorganization during DSC run while in EVA, it is due to melting of crystals

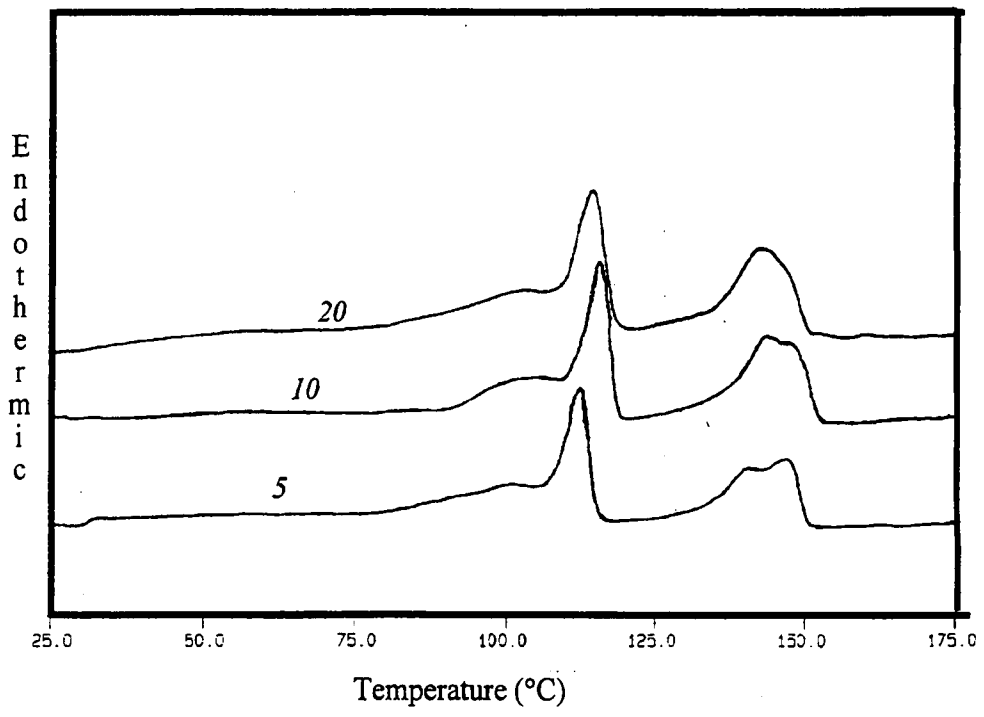

Figure 44. Endotherms for 50/50/0/10 samples (the numbers above the curves indicate heating rate in °C/min)

with different melting points. This may be explained on the basis of changes produced in the two polymers on irradiation. As PP degrades on irradiation the degraded PP molecules may be forming relatively unstable crystals, which may be melting and recrystallizing into more stable phase that melts at higher temperatures, giving rise to multiple melting. Radiation produces gel and sol fractions in EVA, which have different mobilities and during crystallization, the sol crystallizes first and gel crystallizes later, thus producing crystals with different melting points. Therefore, multiple melting in both components may be attributed to changes produced by irradiation.

5.3.2 Heat of fusion

The heat of fusion data for all blend samples is presented in Table 4. An interesting trend is observed in this data. In case of EVA component, the heat of fusion ΔHm_{EVA} increases with radiation dose up to 5 Mrad and then decreases with dose. This was observed in case of 50/50/0, 50/25/25 and 40/20/40 samples. The ΔHm_{EVA} decreases with dose in case of 82/9/9 blend. The heat of fusion of PP, ΔHm_{PP} remains almost constant or decreases slightly with radiation dose. This behavior is contrary to the melting temperature, which decreases continuously with radiation. This behavior may be explained on the basis of a rationale proposed by Minkova *et al.* (1989). The equation governing the heat of fusion of a homopolymer can be written as

$$\Delta H_m = X_C \cdot \Delta H_m^0 - X_C \cdot \Delta H_e + (1 - X_C) \cdot \Delta H_n \qquad \text{(Eq.20)}$$

where, Xc is the crystallinity, ΔH^0_m is the change in enthalpy of an ideal crystal, ΔH_e is the change in enthalpy of the crystal surface and ΔH_n is the change in the enthalpy of the amorphous areas. The enthalpy of an ideal crystal does not change while the enthalpy of crystalline phase and amorphous phase changes with radiation-induced scission and crosslinking reactions. Crosslinking in amorphous phase results in lowering of H_n due to decrease in chain mobility. This also affects H_e as crosslinking lowers the total number of conformations on the lamellar surface. This increases H_e. The scission reactions in amorphous phase have exactly opposite effect on H_e and H_n. Chain scission at the crystallite surface leads to an increase in the number of conformations and results in a decrease in H_e.

Upon irradiation, crosslinking and chain scission reactions take place in the blend. It has been shown that in EVA, radiation-induced scission is restricted to mainly crystalline regions (Matsui *et al.* 1992) while crosslinking prevails in amorphous regions. In PP chain scission prevails in both amorphous and crystalline regions.

In case of 82/9/9 blends, the greater proportion of crosslinking prone EVA results in predominance of crosslinking in these samples. The gel fraction data is corroborative to this interpretation. The crosslinking in the amorphous phase results in lowering of H_n and raising of H_e. As the amount of polypropylene in these blends is very small, the free radicals, which may cause destruction of EVA, are present in lesser quantities. Thus the decrease in He due to scission reaction is not large enough to

compensate for increase in H_e due to crosslinking. So the lowering of H_m with radiation dose may be explained on the basis of decrease in H_n and increase in H_e with radiation dose.

In case of 50/50/0, 50/25/25 and 40/20/40 blends, crosslinking in the amorphous EVA leads to decrease in H_n and increase in H_e. As the polypropylene content is high in these blends, more free radicals capable of initiating scission are generated. The resulting scission in EVA, which is predominant in the crystalline phase lowers H_e. At low radiation doses, the decrease in H_e is larger than decrease in H_n. This results in initial increase in H_m with dose. With increasing radiation dose the decrease in H_n exceeds the decrease in H_e, resulting in decrease in H_m with dose.

5.3.3 Non-isothermal crystallization behavior

The study of non-isothermal crystallization is very important from commercial aspect as most of the commercial processing involves crystallization under non-isothermal conditions. It can provide important qualitative information regarding crystallization process of the irradiated blend system. The non-isothermal crystallization behavior of the samples is shown in Figure 19 to Figure 22. It can be seen from the figures that samples show bimodal as well as monomodal crystallization peaks. The monomodal peaks suggest that PP and EVA are able to crystallize in the same temperature interval. The bimodal peaks indicate that PP and EVA are crystallizing in different

temperature intervals. In case of 50/50/0, 50/25/25 and 40/20/40 blends, the unirradiated blends show bimodal peaks. The 82/9/9 blend behave differently from the other blends as the unirradiated sample shows a monomodal peak while the irradiated samples show bimodal peaks. This may be attributed to the predominant crosslinking in these blends along with the high weight percentage of EVA in these blends. The gel fraction was found to crystallize at 90 - 94°C in these samples. Hence the low temperature peak can be attributed to crystallization of gel fraction.

The figures also show that the crystallization temperatures decrease with increase in radiation dose. The result indicates an increase in the level of impurity present in the crystallites. This increase may be attributed to the constraints imposed by radiation-induced crosslinks as well as large number of chemical irregularities present in the molecules of the irradiated material. An increase in the amount of crosslinks is accompanied by a decrease in the polymer chain mobility. The restrictions imposed by the crosslinks do not allow the polymer chains to crystallize in the same manner as in unirradiated polymer. It is also possible that with increasing radiation dose and crosslinking, the portion of a chain, which is able to crystallize, is shortened. This may lead to a decrease in the crystallization temperature.

5.4 DMA DISCUSSION

The dynamic mechanical properties of a material refer to the behavior of these materials when subjected to stresses or strains that change with time. The dynamic

mechanical analysis was performed on the blend samples to study behavior of storage modulus and loss modulus with respect to blend composition, radiation dose, crystallinity and temperature. The dynamic mechanical behavior of blend samples is shown in Figure 30 to Figure 41. The glass transition is an important criterion to determine polymer blend miscibility. A single glass transition temperature indicates blend miscibility while multiple glass transition temperatures suggest immiscibility. Peaks in the loss modulus have been used to identify relaxation temperatures. It can be seen from the figures that multiple peaks in loss modulus are observed for most of the samples. In case of 82/9/9/0 samples, a peak is seen in the vicinity of –28°C. This peak can be attributed to the glass transition temperature of EVA copolymer. This peak results from the initiation of micro-Brownian motion of the amorphous chains. The literature data (Thomas *et al.* 1995, Datta *et al.* 1996b) support the result. As the radiation dose increases, the position of this peak shifts to higher temperatures. At 10 Mrad dose level, the peak is observed at –4°C. The rise in the glass transition peak with radiation dose may be attributed to the radiation-induced crosslinking. When an uncrosslinked polymer is subjected to dynamic stresses, the polymer chains are able to slide past one another. With increasing radiation dose, the amount of crosslinking in the system increases as shown by the extraction data. The crosslinks restrain polymer chain motion. With increasing amount of crosslinking in the system, it becomes more and more difficult for the polymer chains to respond to temperature change and show viscoelastic flow. This raises the glass transition temperature. None

of the 82/9/9 samples show any glass transition peak corresponding to the polypropylene component. This may be due to the low proportion of polypropylene present in these blends. It is commonly observed that when the amount of one component in a polymer blend is very low, then the glass transition temperature of that component is hard to observe (Rostami 1992).

In case of 50/50/0 and 50/25/25 and 40/20/40 samples, a peak corresponding to the glass transition of polypropylene is observed in 0 °C to 12 °C range. A drop in the glass transition temperature is observed as the radiation dose is increased. The decrease in the glass transition temperature with radiation dose may be attributed to the increase in the chain mobility with radiation dose. As polypropylene is a polymer of scission type, the radiation-induced scission reaction lowers the molecular weight of the polymer. With lowering of molecular weight, there is an increase in the chain mobility that lowers the glass transition. In 50/50/0/10, 50/50/0/11 samples, a very prominent peak corresponding to the glass transition temperature of EVA copolymer is observed. As these samples do not exhibit substantially lower crystallinity and the gel fractions, the factors that may produce such high intensity peaks are instrumental error and different blend morphology. In some of the samples, a peak corresponding to the β transition temperature of EVA copolymer is observed. The beta transition is related to local molecular motion in the polymer chain. It is observed in the vicinity of –50°C. As all samples do not show this transition, no particular trend could be observed in case of this transition with respect to radiation dose or blend composition.

Another relaxation peak is observed in all samples, which occurs at a temperature between the glass transition and melting temperature. This relaxation may be attributed to the α_c relaxation. As only one peak is observed and this peak has a shoulder at high temperature, the peak seems to comprise of both EVA and PP. This relaxation is characteristic of crystalline phase. It is related to rotation about the chain axis of chain folded polymers to a second order expansion of lattice parameters perpendicular to the chain direction on crystalline phase. The magnitude of this relaxation is decreasing with increasing radiation dose except in case of samples irradiated with 8 Mrad dose. The decrease in magnitude may be attributed to change in crystalline structure with dose. In case of samples irradiated with 8 Mrad dose, the α_c peak has the highest intensity. The distinct dynamic mechanical behavior of samples irradiated with 8 Mrad is also evident from the storage modulus data. As intensity of the α_c peak is proportional to crystallinity, strain induced crystallization, which may be taking place during heating in the instrument may be increasing the sample crystallinity. The morphology of these samples may also be contributing to this behavior.

The storage modulus (E') represents the in phase component of modulus in dynamic mechanical experiment. In the temperature range of –100°C to –30°C, the storage modulus shows very high value characteristic of glassy state. The modulus is of the order of 10^9 dynes/cm^2 in this range. In the glassy region, thermal energy is insufficient to overcome the potential barriers for translational and rotational motions

of segments of the polymer molecules. The polymer chains are frozen in fixed position. Under applied stress, the polymer chains are unable to slide past one another. This results in high modulus value at these temperatures. As the temperature increases and approaches the glass transition temperature, the increase in free volume results in increased chain mobility. In case of amorphous polymers, the modulus drops by order of magnitudes in the region of glass transition. But as the blend samples are crystalline and the irradiated samples are crosslinked, the drop in the storage modulus even after crossing the glass transition is insignificant. The samples show a leathery region. The appearance of leathery state is caused by the micro-Brownian motion of the amorphous region under the structural constraints imposed by the crystallites. The reinforcing action of the crystallites enables the polymer to withstand applied stress at temperatures exceeding the glass transition temperature. The radiation-induced crosslinking adds to the reinforcing effect of the crystallites. The blend samples show a significant drop in the storage modulus only in the vicinity of melting of crystallites. Thus the presence of crystallinity and crosslinking raises the maximum service temperature of the blend from the glass transition temperature to the melting temperature and above. In case of 50/50/0, 50/25/25 and 82/9/9 samples, an interesting behavior is observed in case of samples irradiated with 8 Mrad. These samples exhibit higher storage modulus than all other samples. This behavior may be attributed to the strain-induced crystallization and morphology in these samples. It can be said that 8 Mrad is the optimum dose for getting better mechanical properties

till the softening temperature. As the melting temperatures of blend components approach, a drop in the storage modulus is seen. In case of 82/9/9 samples, a significant drop in E' is observed near 115°C coinciding with the melting of EVA crystals. The modulus shows a plateau, followed by a sharp drop near the melting temperature of EVA copolymer. In case of 82/9/9/10 and 82/9/9/16 samples, a plateau is observed even after melting of PPH crystallites. These samples have a higher proportion of crosslinks as shown by the gel fraction data. Crosslinking theory (Flory 1953) requires a high degree of crosslinking to result in a higher value of E' after the transition. Because of these crosslinks, the blend is able to show a modulus of the order of 10^7 dynes/cm^2 even after 155°C. The storage modulus after melting of crystallites is used to calculate the molecular weight between the crosslinks (Mc) using the following equation (Murayama 1978)

$$E' = \frac{3 \cdot \rho \cdot R \cdot T}{Mc} \qquad \text{(Eq.21)}$$

where, ρ is the blend density (0.93 g/cc), R is the gas constant, T is the temperature above melting temperature of crystallites (428°K). The values of Mc obtained using the above equation are 3973 g/mol and 1986 g/mol for 82/9/9/10 and 82/9/9/16 samples respectively. It can be concluded that for retaining superior mechanical properties at temperatures above the melting temperatures of the crystallites, the radiation dose should be high enough to produce Mc less than 4000 g/mol.

The plateau after melting of crystallites is not seen in any other sample, although in 40/20/40/16 sample, the elastic modulus seems to asymptotically approach a plateau. The higher proportion of chain scission prone PP in these samples must be causing more degradation as shown by G (S)/ G (X) value. The crosslinks produced in 50/25/25, 50/50/0 and 40/20/40 may not be sufficient to withstand loads at high temperatures. The decrease in the storage modulus at higher temperature with increase in the amount PP was also observed by Thomas *et al.* (1992) in case of dynamically crosslinked EVA-PP blend. It can be concluded that to obtain better properties at high temperatures, the amount of EVA should be higher in irradiated EVA-PP blends.

6 Conclusions

A study of the structural characteristics, thermal behavior and dynamic mechanical properties of electron-beam irradiated blend system; comprised of polypropylene homopolymer and copolymer and, ethylene vinyl acetate copolymer has been conducted as a function of radiation dose and blend composition. Several interesting features of this system have come forth in the course of this study.

6.1 Structural features

Extraction studies on the irradiated samples show that the gel fraction increases as a function of radiation dose and EVA content. Blends containing the highest weight percent of EVA show the highest crosslinking efficiency and lowest G (S)/ G (X) value. This suggests that in the dose range of study, EVA is a polymer of crosslinking type while PP is a polymer of scission type.

The wide-angle x-ray diffraction studies show high crystallinity values for all samples, except those irradiated at 16 Mrad. The introduction of radiation-induced crosslinking starts affecting the crystal structure only at high doses where crosslink density is high. It is speculated that at low dose level crosslinks may be incorporated into the crystal and their exclusion at high dose level may be distorting the crystal structure. The lattice parameter and line broadening calculations also suggest that distortion occur at high dose level when high crosslink density is obtained.

6.2 Thermal behavior

The non-isothermal crystallization studies show that the crystallization temperature decreases with increasing crosslink density. The crystallization range changes with radiation dose and blend composition. The restriction on molecular mobility and the chemical impurities produced by radiation-induced reactions may be causing the lowering of crystallization temperature with dose.

The heat of fusion of EVA shows an initial rise with dose in samples containing lower weight percent of EVA while in the samples containing high weight percent of EVA it decreases with dose. In case of PP, the heat of fusion remains unchanged with dose. The variation in the heat of fusion has been attributed to the changes in enthalpies of amorphous and crystalline regions of polymers produced by crosslinking and scission.

The melting endotherms show much greater changes after irradiation of the blends than the x-ray diffraction study and dynamic mechanical analysis. A drop in the melting temperatures of EVA and PP components is seen in all irradiated samples and it has been attributed to change in thermodynamic parameters and reduction in ability of irradiated polymer to achieve maximum degree of perfection during heating. The most prominent drop in the melting temperature of EVA is observed in samples with high weight percent of PP at high dose level. Multiple melting peaks are seen in the irradiated samples. The multiple melting peaks in PP have been attributed to

reorganization taking place during DSC scan. In EVA it has been attributed to the presence of crystals with different melting points.

6.3 Dynamic mechanical properties

The dynamic storage modulus at low temperatures is independent of blend composition and radiation dose. Below 100°C, samples irradiated with 8 Mrad show higher modulus than other samples and it is speculated that morphology and strain induced crystallization may be responsible for this behavior. At high temperatures the effect of crosslinks come into picture. Samples with high crosslinks densities show a plateau in the storage modulus. The critical value of molecular weight between crosslinks to retain good mechanical properties at high temperatures has been estimated to be 4000 g/mol.

The dynamic loss modulus shows various relaxation peaks. Existence of two glass transition peaks suggests immiscibility between the blend components. The temperature at which transition in EVA occurs increases with dose, while in case of PP it decreases with dose. This has been attributed to crosslinking in EVA and chain scission in PP component.

7 Further Work

7.1 Study of irradiated polypropylene copolymer

It is important to study properties of irradiated polypropylene copolymer for better understanding of behavior of the irradiated blends. The contribution of polypropylene copolymer to factors such as enthalpies of EVA can be estimated along with its effect on crystallinity and gel fractions.

7.2 Morphology study

As SEM studies on the blend samples could not provide information about phase size and distribution in these blends, morphology study using TEM may be useful. It may throw some light on different dynamic mechanical behavior of samples irradiated with 8 Mrad.

7.3 Lamellar details

Study of lamellar morphology using SAXS and TEM will be very helpful in verifying the hypothesis of incorporation of crosslinks inside the crystals at lower doses and exclusion at higher doses.

References

Alfonso G.C., Russell T., *Macromol.*, 19:1143 (1986)

Andrews E.H., Owen P.J., Singh A., *Proc. R. Soc. London*, A324:79 (1971)

Arakawa K., Seguchi T., Hayakawa N., Machi S., *J. Polym. Sci. Polym. Chem. ed.*, 21:1173 (1983)

Baldwin F.B., Ver Strate G., *Rubb. Chem. Tech.*, 45:709 (1972)

Bank M., Leffenguell G., Thies C., *Macromolecules*, 4:43 (1971)

Bartczak Z., Galeski A., Pracella M., *Polymer*, 27:537 (1986)

Bassett D.C., in "Principles of Polymer Morphology", Cambridge Univ. Press, London (1981)

Becker R.C., Bly J.H., Cleland M.R., Farell J.P., *Radiat. Phys. Chem.*, 14:353 (1979)

Blom H.P., Ten J.W., Rudin A., *J. Appl. Polym. Sci.*, 60:1405 (1996)

Bradley A., Fales J.D., *Chem. Technol.*, 232 (April 1971)

Brannock G.R., Paul D.R., *Macromol.*, 23:5240 (1990)

Brooks N.M., *J. Indust. Irradiation Tech.*, 1:237 (1983)

Bucknall C.B., "Toughned Plastics", Appl. Sci., London (1977)

Busfield W.K., O'Donnell J.H., *Europ. Polym. J.*, 15:379 (1979)

Busfield W.K., O'Donnell J.H., *Europ. Polym. J.*, 13:741 (1981)

Chapiro A., in "Radiation Chemistry of Polymeric Systems, High polymers". vol XV, Interscience, NY (1962)

Chappell S.E., Sauer J.A., Woodward A.E., *J. Polym. Sci.*, A1:2805 (1963)

Charlesby A., Hancock N., *Proc. R. Soc. London*, Ser. A, 218:245 (1953)

Charlesby A., in "Atomic Radiation and Polymers", Pergamon, London (1959)

Charlesby A., Pinner S.H., *Proc. R. Soc. London*, Ser. A, 249:369 (1959)

Charlesby A., *Proc. R. Soc. London*, Ser. A, 222:60 (1954)

Charlesby A., Ross M., *Proc. R. Soc. London*, Ser. A, 217:122 (1953)

Cizek E.P., US Patent 3383435 to General Electric Co. (1968)

Cox W.W., Duswalt A.A., *Polym. Eng. Sci.*, 7:309 (1967)

D'Orazio L., Mancarella C., Martuscelli E., Sticotti G., Ghisellini R., *J. Appl. Polym. Sci.*, 53:387 (1994)

Datta S., Lohse D.J., in "Polymeric Compatibilizers", Carl Hanser Verlag, NY (1996)

Datta S.K., Bhowmick A.K., Despande R.S., *Polymer*, 37(1):45 (1996)

Davidson W.L., Geib I.G., *J. Appl. Phys.*, 19:422 (1948)

Dawes , in "Physical Properties Of Polymer Handbook", Mark J.E. (Ed.), AIP Press, NY (1996)

Dole M., in "The radiation chemistry of macromolecules", Acd. Press, NY (1973)

Dole M., in Dole M. (Ed.), "The Radiation Chemistry of Macromolecules", Acad. Press, NY, 1:(265-286) (1972)

Dole M., *Radiat. Phys. Chem.*, 22(1-2):11 (1983)

Dunn T.S., Epperson B.J., Sugg H.W., Stannett V.T., Williams J.L., *Radiat. Phys. Chem.*, 14:625 (1979)

Duvall J., Selliti C., Myers C., Hiltner A., Baer E., *J. Appl. Polym. Sci.*, 52:207 (1994)

Fischer Z., *Nature*, 12A:173 (1957)

Flory P.J. in "Principles of Polymer Chemistry", Cornell Univ. Press, Ithaca, NY (1953)

Flory P.J., *J. Chem. Phys.*, 9:660 (1941)

Flory P.J., *Trans. Farad. Soc.*, 51:848 (1955)

Fox T.G., *Bull. Amer. Phys. Soc.*, 2, 123 (1956).

Gezovich D.M., Geil P.H., *Polym. Eng. Sci.*, 8:202 (1968)

Gielenz G., Jungnickel B.J., *Colloid Polym. Sci.*, 260:742 (1982)

Gordon M., Taylor J.S., *J. Appl. Chem.*, 2:493 (1952)

Greco R., Mancarella C., Martuscelli E., Ragosta G., Jinghua Y., *Polymer*, 28:1929 (1987)

Guerra G., Petraccone V., Corradini P., Rosa C., Napolitano R., Pirozzi B., Giunchi G., *J. Polym. Sci. Polym. Phys. Edn.*, 22:1029 (1984)

Harpell G.A., Walrod D.H., *Rubb. Chem. Technol.*, 46:1007 (1973)

Hendra P.J., Vile J., Willis H.A., Zichy V., Cudby M.E.A., *Polymer*, 25:785 (1984)

Hoffman J.D., Lauritzen J.I., *J. Res. NBS.*, A65:297 (1961)

Hoffman J.D., Miller R.L., *Macromol.*, 21:3038 (1988)

Huggins M.L., *J. Chem. Phys.*, 9:440 (1941)

Iriante M., Iribarren J., Etxeberria A., Iruis J., *Polymer* 30:1160 (1989)

Janimak J.J., Cheng S.Z., Zhang A., Hsieh E.T., *Polymer*, 33:728 (1992)

Kamide K., Yamaguchi K., *Makromol. Chem.*, 162:219 (1972)

Kao Y.H., Phillips P.J., *Polymer*, 27:1669 (1986)

Kao Y.H., Phillips P.J., *Polymer*, 27:1679 (1986)

Keller A., *Rep. Prog. Phys.*, 31:623 (1968)

Keller A., Ungar G., *Radiat. Phys. Chem.*, 22:155 (1983)

Kita H., Muraoka M., Tanaka K., Okamota K., *Polymer J.*, 20(6):485 (1988)

Krestev V., Dobreva B., Kresteva M., Minkova L., Nedkov E., *Bulg. J. Phys.*, 15:265 (1988)

Krestev V., Dobreva V., Kresteva M., Minkova L., Nedkov E., *Bulg. J. Phys.*, 15:265 (1988)

Kusy R.P., Turner D.T., *Macromol.*, 4:337 (1971)

Lambert W.S., M.S. Thesis, University of Tennessee, Knoxville (1988)

Lambert W.S., Phillips P.J., Lin J.S., *Polymer*, 35:1809 (1994)

Lovinger A.J., Meille S.V., Padden F.J., Bruckner S., Ferro D.R., *Macromolecules*, 27:2615 (1994)

Maciel A., Del-Real A., Garcia-Garduno M., Oliva E., Manero O., Castano V.M., *Polymer International*, 41:227 (1996)

Matsui T., Mizumoto S., Kotani A., Imakura H., Shimoda M., Osajima Y., *J. Sci. Food Agric.*, 50:507 (1990)

Matsui T., Shimoda M., Osajima Y., *Polym. Int.*, 29:85 (1992)

Matsui T., Shimoda M., Osajima Y., *Polym. Int.*, 29:91 (1992)

McGinniss V.D., in "EPSE", Kroschwitz J. (Chief Ed.), 2nd Ed., John Wiley & Sons, NY, 4:(418-449) (1986)

McGinniss V.D., in "Kirk-Othmer Encycl. Chem. Tech., Grayson M. (Ed.), 3rd Ed., 19:607 (1982)

Meille S.V., Bruckner, *Prog. in Polym. Sci.*, 16:361 (1991)

Meligi G., Yoshii F., Sasaki T., Makuuchi K., Rabie A.M., Nishimoto S., *Polym. Degrad. Stab.*, 49:323 (1995)

Mezghani K., Phillips P.J., *Polymer*, 36:2407 (1995)

Minkova L., Nikolova M., *Polym. Degrad. Stab.*, 25:49 (1989)

Minkova L., Sodeva D., *J. Elastomers and Plastics*, 27:168 (1995)

Modern Plastics. McGraw-Hill Co., p.55 (January 1998)

Morrow D., Newman B., *J. Appl. Phys.*, 39:4944 (1968)

Murayama T., in "Dynamic Mechanical Analysis Of Polymeric Materials", Elsevier Scientific Publ. Co., Amsterdam (1978)

Nadkarni V.M., Shingankuli V.L., Jog J.P., *J. Appl. Polym. Sci.*, 46:339 (1992)

Natta G., Corradini P., Cesari M., *Rend. Accad. Nazl. Lincei*, 21:365 (1956)

Natta G., Corradini P., *Nuovo Cimento*, 15:40 (1960)

Natta G., *Makromol. Chem.*, 35:93 (1960)

Natta G., Peraldo M., Corradini P., *Rend. Accad. Nazl. Lincei*, 26:14 (1959)

Nishi T., Wang T., *Macromol.*, 8:909 (1975)

Nishimoto S., *Biannual J. Jpn. Soc. Radiat. Chem.*, 52:2 (1991)

Nishimoto S., Kitamura K., Watanabe Y., Kagiya T., *Radiat. Phys. Chem.*, 37:71 (1991)

O'Kane W.J., Young R.J., Ryan A.J., Bras W., Derbyshire G.E., Mant G.R., *Polymer*, 35:1352 (1994)

Olabisi O., Robeson L.M., Shaw M.T., in "Polymer-Polymer Miscibility", p. 117, Acad. Press, NY (1979)

Paul D.R. in Paul D.R., Newman S. (Ed.), "Polymer Blends", Acad. Press, NY (1978)

Paul D.R., Barlow J.W., Keskkula H., in Mark H.F., Bikales M.M., Overberger C.G., Menges G., (Ed.), "Encycl. Polym. Sci.", 2nd edition, Wiley, NY, 12:399 (1988)

Phillips P.J., in "Handbook of Crystal Growth", Hurle D.T.J. (Ed.), 2:1169 (1994)

Phillips P.J., Lambert W.S., *Macromol.*, 23:2075 (1990)

Phillips P.J., *Rep. Prog. Phys.*, 53:549 (1990)

Rabello M.S., White J.R., *Polymer*, 38:6389 (1997)

Ransohoff J.A., *Radiat. Phys. Chem.*, 18:293 (1981)

Ray J., Khastgir D., *J. Polym. Eng.*, 13:29 (1994)

Rizzo G., Spadaro G., Acierno D., Calderaro E., *Radiat. Phys. Chem.*, 21:349 (1983)

Rostami S., in "Multicomponent Polymeric Systems", Miles I., Rostami S. (Ed.), Longman Scientific & Technical, London (1992)

Rybnikar F.J., *Macromol. Sci. Phys.*, B30:201 (1991)

Sanchez I.C., Eby R.K., *J. Res. NBS*, 77A:353 (1973)

Sanchez I.C., Eby R.K., *Macromol.*, 8:639 (1975)

Sanchez I.C., Lacombe R.H., J. Phys. Chem., 80:2352 (1976)

Sanchez I.C., Lacombe R.H., Macromol., 11:1145 (1978)

Sawyer L., Grubb D., in "Polymer microscopy", Chapman & Hall, 2nd ed., NY (1995)

Seguchi T., Arakawa K., Hayakawa N., Watanabe Y., Kuriyama I., *Radiat. Phys. Chem.*, 19:495 (1982)

Seguchi T., Arakawa K., Ito M., Hayakawa N., Machi S., *Radiat. Phys. Chem.*, 21:495 (1983)

Seguchi T., Hashimoto S., Arakawa K., Hayakawa N., Kawakami W., Kuriyama I., *Radiat. Phys. Chem.*, 17:195 (1981)

Shi G., Zhang X., Cao Y., Hong J., *Makromol. Chem.*, 194:269 (1993)

Singh V.B., Walsh D.J., *J. Macromol. Sci.-Phys.*, B25:65 (1986)

Snyder C.E., *Radiat. Phys. Chem.*, 22(1-2):3 (1983)

Spadaro G., Rizzo G., Acierno D., Calderaro E., *Radiat. Phys. Chem.*, 23:445 (1984)

Spinks J.W.T., Woods R.J., in "An Introduction to Radiation Chemistry", John Wiley & Sons Inc., NY (1964)

Sweet G.C., in "Developments in Rubber Technology", Whelan A., Lee K.S. (Ed.), Appl. Sci. Publishers, London (1979)

Thomas S., George A., *Europ. Polym. J.*, 28:1451 (1992)

Thomas S., George A., *Europ. Polym. J.*, 28:1451 (1992)

Thomas S., Gupta B.R., De S.K., *Polym. Degrad. Stab.*, 18:189 (1987)

Tidjani A., Watanabe Y., *J. Appl. Polym. Sci.*, 60:1839 (1996)

Tomlison J.N., Kline D.E., J. Appl. Polym. Sci., 11:1931 (1967)

Ungar G., *J. Mat. Sci.*, 16:2635 (1981)

Van Gisbergen J.G.M., Meijer H.E.N., Lemstra P.J., *Polymer*, 30:2153 (1989)

Van Gisbergen J.G.M., Meijerink J.I., Overbergh N., "Integration of Fundamental Polymer Science and Technology: Part 3", p. 128, Elsevier Appl. Sci. Publication, London (1989).

Walsh D.J., Rostami S., *Adv. Polym. Sci.*, 70:121 (1985).

Walsh D.J., Rostami S., Singh V.B., *Makromol. Chem.*, 186:145 (1985)

Wiesner L., *Radiat. Phys. Chem.*, 37:77 (1991)

Williams J.L., Dunn T.S., Sugg H., Preprints IUPAC International Symp. on Macromolecules, p.657 (1977)

Wunderlich B., in "Macromolecular Physics" Acad. Press, (1976)

Yurkevich V.G., Karpov V.L., Zverev B.I., Aleksandrova L.B., *J. Polym. Sci.*, C42:859 (1973)

VITA

Dattatreya (Ketan) Panse was born in Pune, India on October 19, 1973. He joined Maharashtra Institute of Technology, Pune to study Polymer Engineering in 1991. He received Bachelor of Engineering with a major in Polymer Engineering in June 1995. He began his studies at the University of Tennessee, Knoxville in August 1996 and received his Master of Science degree in Polymer Engineering in December of 1998.